Characterization of *Sod1* knockout mouse embryonic fibroblasts

Long Truong-Ong

Department of Biology

McGill University, Montreal

August 2024

A thesis submitted to McGill University in partial fulfillment of the requirements of the degree of Master of Science in Biology

Table of Contents

Abstract

Sod1 encodes a superoxide dismutase, the only type of enzyme that directly converts superoxide into hydrogen peroxide, both of which are reactive oxygen species. In humans, the dysregulation of this enzyme has been associated with many diseases such as amyotrophic lateral sclerosis, heart failure, cancer, diabetes, Down's syndrome, and Parkinson's disease. Although germline *Sod1* knockout mice (*Sod1*$^{-/-}$) displayed an accelerated muscle atrophy with age, a ~30% reduction in lifespan, and an increased incidence of liver cancer, their phenotype is milder than what would have been expected from the central roles played by SOD1. *Sod1* is highly conserved between species from bacteria to mammals and its levels of expression are particularly high. Thus, the viability of *Sod1*$^{-/-}$ mice is surprising. However, the same cannot be said for mouse embryonic fibroblasts (MEFs) obtained from *Sod1*$^{-/-}$ embryos. Previous studies have shown that *Sod1*$^{-/-}$ MEFs die after only a few days in cell culture. This contradiction between the viability of *Sod1*$^{-/-}$ mice and the poor survival of *Sod1*$^{-/-}$ MEFs is not understood. To solve this question, one possible approach is to generate *Sod1*$^{-/-}$ MEFs and search for interventions that could restore their viability. Our first attempt used a mouse strain carrying floxed *Sod1* alleles and *Sod1* was excised *in vitro* by expressing recombinase Cre. Although the deletion of *Sod1* appeared to be validated by western blotting, *Sod1* was not excised in a few cells and these cells gradually overgrew Cre-mediated *Sod1* knockout MEFs (*Sod1*$^{\Delta/\Delta}$-Cre). As an alternative, MEFs used were instead isolated from germline knockout *Sod1*$^{-/-}$ mice. The next objective is finding compounds that can rescue *Sod1* knockout MEFs from cell death or senescence or both. Vitamin C increased the survival of *Sod1*$^{\Delta/\Delta}$-Cre MEFs, but L-NAME did not. The reasoning

behind the use of L-NAME, which inhibits the synthesis of nitric oxide, is to reduce the formation of peroxynitrite that results from the reaction of superoxide with nitric oxide. Vitamin C also increased the survival of *Sod1*$^{-/-}$ MEFs, but proliferation eventually stopped after ~39 treatment days. A library of redox-active compounds was screened in combination with vitamin C to observe a possible synergistic effect that could completely rescue the survival of *Sod1*$^{-/-}$ MEFs. Unfortunately, this was unsuccessful. The SOD1 protein is involved in numerous processes, which are reviewed in the thesis's literature review and discussion. The finding that vitamin C is capable of partially rescuing the survival and proliferation of *Sod1* knockout MEFs suggests that their poor viability is partially linked to an alteration in redox metabolism. However, since their rescue with vitamin C is incomplete, this suggests that another non-redox or non-enzymatic function of SOD1 might be involved as well.

Résumé

Sod1 encode une superoxyde dismutase, le seul type d'enzyme qui convertit directement les anions superoxydes en peroxyde d'hydrogène, les deux étant des espèces réactives de l'oxygène. Chez les humains, la dérégulation de cette enzyme a été associée à plusieurs maladies telles que la sclérose latérale amyotrophique, l'insuffisance cardiaque, le cancer, le diabète, le syndrome de Down et la maladie de Parkinson. Bien que les souris *Sod1* knock-out depuis la lignée germinale (*Sod1*$^{-/-}$) démontrent une accélération de l'atrophie musculaire avec l'âge, une durée de vie réduite de ~30% et une incidence plus élevée du cancer du foie, leur phénotype est moins sévère que ce à quoi on aurait pu s'attendre vu les rôles centraux que SOD1 joue. *Sod1* est hautement conservé parmi les espèces, à partir des bactéries jusqu'aux mammifères, et possède un niveau d'expression particulièrement élevé. Donc, la viabilité des souris *Sod1*$^{-/-}$ est surprenante. Cependant, ceci n'est pas le cas pour les fibroblastes embryonnaires de souris (MEFs) isolés à partir d'embryons *Sod1*$^{-/-}$. Des études précédentes ont démontré que les MEFs *Sod1*$^{-/-}$ meurent après seulement quelques jours en culture cellulaire. Cette contradiction entre la viabilité des souris *Sod1*$^{-/-}$ et la faible survie des MEFs *Sod1*$^{-/-}$ demeure incomprise. Pour résoudre cette question, une approche possible est de produire des MEFs *Sod1*$^{-/-}$ et de chercher des interventions qui pourraient restaurer leur viabilité. Notre première tentative a utilisé une lignée de souris possédant des allèles *Sod1 floxed* et *Sod1* a été excisé *in vitro* en exprimant la recombinase Cre. Bien que la délétion de *Sod1* apparût validée par le buvardage de western, *Sod1* n'était pas excisé dans quelques cellules qui ont graduellement envahi les MEFs *Sod1* knock-out médié par Cre (*Sod1*$^{\Delta/\Delta}$-Cre). En tant qu'alternative, les MEFs utilisés ont été générés à partir de souris *Sod1*$^{-/-}$

homozygotes classiques (*Sod1*$^{-/-}$). Le prochain objectif est de trouver des traitements qui pourraient prévenir la mort ou la sénescence des MEFs *Sod1* knock-out. La vitamine C a amélioré la survie des MEFs *Sod1*$^{\Delta/\Delta}$-Cre, mais pas le composé L-NAME. Le raisonnement derrière l'utilisation de L-NAME, qui inhibe la synthèse de l'oxyde nitrique, est de réduire la formation du peroxynitrite qui résulte de la réaction du superoxyde avec l'oxyde nitrique. La vitamine C avait aussi amélioré la survie des MEFs *Sod1*$^{-/-}$, mais leur prolifération s'est arrêtée après ~39 jours de traitement. Une librairie de composés rédox-actifs a été criblée en combinaison avec la vitamine C afin d'observer un effet synergique possible qui pourrait complètement restaurer la survie des MEFs *Sod1*$^{-/-}$. Malheureusement, cela a été en vain. La protéine SOD1 est impliquée dans plusieurs processus, qui sont passés en revue dans la revue de littérature et la discussion de la thèse. La trouvaille que la vitamine C est capable de partiellement restaurer la survie et la prolifération des MEFs *Sod1* knock-out suggère que leur mort est partiellement liée à une altération du métabolisme rédox. Cependant, puisque l'effet de la vitamine C résulte à un secours incomplet, ceci suggère qu'une fonction autre que l'activité rédox ou enzymatique de SOD1 soit aussi impliquée.

Acknowledgements

I would like to express my deepest gratitude to Professor Siegfried Hekimi for his guidance in the direction of my experiments, his editorial help for the thesis, and especially his patience and witty humor.

I also wish to thank the members of my supervisory committee, Dr. Alanna Watt and Dr. Arnold Hayer, for providing valuable constructive feedback for my research.

I am also extremely grateful to Dr. Ying Wang for being patient with me, teaching me how to do most experiments, assisting me in various things such as using laboratory equipment, experimental troubleshooting, data interpretation, experimental planning, and editorial help for the thesis.

I would like to also thank Dr. Robyn Sara Branicky for helping me in the laboratory's onboarding process and for ordering reagents, laboratory equipment, and especially the new cuffed laboratory coat that I needed.

Special thanks to Samaneh Kamyabiazar, who taught me how to analyze BCA assay's protein concentration results, performed HPLC analysis on my MEFs samples, and assisted me in experimental troubleshooting.

Many thanks to Noah Lilienfeldt in helping me find laboratory equipment, assisting me when I thought I accidentally splashed a drop of the SDS-PAGE gel mix on my eyes, and helping me in reading published papers from Professor Siegfried Hekimi's laboratory.

I must also thank Dr. Tzu-Yu Lin for being very supportive during my graduate studies. You were like sunshine during my rainy days, and I always looked forward to doing cell culture work whenever you were present. You're a gift to those around you and I will definitely miss your great sense of humor and our interesting discussions.

Finally, I cannot begin to express my thanks to my dad for his tireless efforts in supporting the family, his perseverance, kindness, empathy, and humor. Of course, I would not be who I am without my mom's love and care, and I sincerely appreciate her indefatigable efforts in cleaning, cooking, organizing, and maintaining the house every day. To both, thank you for providing me with the opportunity and freedom to choose what I want to do with my life.

Contribution of Authors

Long Truong-Ong: Performed all experiments, reviewed relevant literature, created all figures, wrote all chapters of the initial drafts and revised the thesis multiple times.

List of Figures

List of Abbreviations

Abbreviation	Full name
$^{\bullet}NO$	Nitric oxide
$^{\bullet}NO_2$	Nitrogen dioxide
8-oxo-dG	8-oxo-2-deoxyguanosine
ADP	Adenosine diphosphate
ALS	Amyotrophic lateral sclerosis
Apo-SOD1	Metal-free SOD1
APPS	L-ascorbyl 2-phosphate 6-palmitate
BHT	2,6-di-tert-butyl-4-methylphenol
Bp	Base pairs
CCS	Copper chaperone of SOD1
CDK	Cyclin-dependent kinase
CDKI	Cyclin-dependent kinase inhibitor
$CO_3^{\bullet -}$	Carbonate radical
Complex I	NADH-Q oxidoreductase
Complex II	Succinate-Q oxidoreductase
Complex III	Q-cytochrome c oxidoreductase
Complex IV	Cytochrome c oxidase
Complex V	ATP synthase
Cu,Zn-SOD	Copper-zinc superoxide dismutase
ER	Endoplasmic reticulum
ERO1	Endoplasmic reticulum oxidoreductin-1
FACS	Fluorescence-activated cell sorter
FAD	Flavin adenine dinucleotide
fALS	Familial amyotrophic lateral sclerosis
Fe^{2+}	Ferrous iron
Fe^{3+}	Ferric iron
G1	Gap 1
G2	Gap 2

GPX	Glutathione peroxidase
GSH	Reduced glutathione
GSSG	Oxidized glutathione
H_2O	Water
H_2O_2	Hydrogen peroxide
HCO_3^-	Bicarbonate
$HO^\bullet$	Hydroxyl radical
Holo-SOD1	Fully metalated SOD1
$HOO^\bullet$	Hydroperoxyl radical
HRP	Horseradish peroxidase
KO	Knockout
KRAS	Kirsten rat sarcoma virus
$L^\bullet$	Lipid radical
L-NAME	L-NG-nitroarginine methyl ester
$LO^\bullet$	Lipid alkoxyl radical
$LOO^\bullet$	Lipid peroxyl radical
LOOH	Lipid hydroperoxide
MEFs	Mouse embryonic fibroblasts
MMO	Microsomal monooxygenase system
Mn-SOD	Manganese superoxide dismutase
MnTBAP	Mn(III) tetrakis (4-benzoic acid) porphyrin chloride
mTOR	Mammalian target of rapamycin
NAC	N-acetylcysteine
NAD^+	Oxidized nicotinamide adenine dinucleotide
NADPH	Reduced nicotinamide adenine dinucleotide phosphate
NOS	Nitric oxide synthase
NOX	NADPH oxidase
NSCLC	Non-small-cell lung cancer
O_2	Oxygen
$O_2^{\bullet-}$	Superoxide

$ONOO^-$	Peroxynitrite
p16	$p16^{INK4a}$
p19	$p19^{INK4d}$
p21	$p21^{Cip1}$
PBS	Phosphate-buffered saline
PBS-T	PBS containing 0.5% Tween 20
PCR	Polymerase chain reaction
PDI	Protein disulfide isomerase
PeBoW	PES1-BOP1-WDR12
PRDX	Peroxiredoxin
Q	Ubiquinone
QH_2	Ubiquinol
RNS	Reactive nitrogen species
$RO^{\bullet}$	Alkoxyl radical
$ROO^{\bullet}$	Peroxyl radical
ROS	Reactive oxygen species
$RS^{\bullet}$	Thiyl radical
S phase	DNA synthesis phase
SOD	Superoxide dismutase
Sod1$^{-/-}$	Germline *Sod1* knockout
Sod1	Superoxide dismutase 1
Sod1$^{fl/fl}$	Homozygous floxed *Sod1* alleles
Sod1$^{\Delta/\Delta}$-Cre	Cre-mediated *Sod1* knockout
TRX	Thioredoxin
UPR	Unfolded protein response
XDH	Xanthine dehydrogenase
XO	Xanthine oxidase
XOR	Xanthine oxidoreductase

Introduction

Considering how highly *Sod1* is conserved between species, the importance of its function, and its high levels of expression, the viability of *Sod1*$^{-/-}$ mice is surprising (Fridovich, 1995; Miao & St. Clair, 2009; Okado-Matsumoto & Fridovich, 2001; Sturtz et al., 2001). In contrast, *Sod1*$^{-/-}$ mouse embryonic fibroblasts (MEFs) undergo increased cell death, and quickly die after only a few days in cell culture (Huang et al., 1997; Tsunoda et al., 2013). However, it is unknown why *Sod1*$^{-/-}$ mice are viable and yet *Sod1*$^{-/-}$ MEFs are not. One way to answer this is by treating *Sod1*$^{-/-}$ MEFs with specific compounds and observing their effects. The effectiveness of one compound or intervention over the other could reveal *Sod1*'s role in different pathways leading to cell viability or death. A good starting point would be to test if the death of *Sod1*$^{-/-}$ MEFs is caused by increased levels of $O_2^{\bullet-}$ resulting from the lack of SOD1. The first objective is inactivating *Sod1* in MEFs and characterizing their phenotype in detail. To remove *Sod1*, viral infections were performed to introduce Cre recombinase in MEFs carrying a floxed *Sod1* gene (*Sod1*$^{fl/fl}$). These *Sod1*$^{fl/fl}$ MEFs were isolated from an in-house mouse strain. The Cre-*loxP* recombination system was first tested on *Mclk1*$^{fl/fl}$ MEFs to test the protocol's effectiveness in gene knockout (KO). Validation of Cre-mediated *Sod1* deletion was ascertained by analyzing the presence or absence of the SOD1 protein through western blotting. The rationale behind the use of Cre-mediated *Sod1* KO in MEFs (*Sod1*$^{\Delta/\Delta}$-Cre) was to avoid unknown compensatory properties that may have been gained during the development of embryos originating from germline *Sod1* KO mice (*Sod1*$^{-/-}$). However, due to the gradual reappearance of *Sod1* expression in Cre-infected *Sod1*$^{fl/fl}$ cells, the wild-type phenotype could be confused with the rescue of *Sod1*$^{\Delta/\Delta}$-Cre MEFs. Therefore, germline *Sod1*

KO mice had to be used instead. For *Sod1*$^{-/-}$ MEFs, genotyping was performed through polymerase chain reaction (PCR). The next objective is identifying treatments or molecular manipulations that could rescue *Sod1*$^{-/-}$ MEFs from cell death or senescence or both. In summary, highly effective *Sod1* KO in MEFs was achieved using the Cre-*loxP* system, but *Sod1* expression gradually reappeared in Cre-infected *Sod1*$^{fl/fl}$ cells over time, suggesting that *Sod1* expression remained in a few cells which gradually overgrew *Sod1*$^{\Delta/\Delta}$-Cre MEFs. Vitamin C increased *Sod1*$^{\Delta/\Delta}$-Cre MEFs' survival, but not L-NAME. Vitamin C also increased *Sod1*$^{-/-}$ MEFs' survival, but proliferation eventually stopped after ~39 days. After screening a library containing 84 compounds with defined prooxidant and antioxidant properties, 2,6-Di-*tert*-butyl-4-methylphenol (BHT) was initially identified as a potentiator of vitamin C's rescue effect in *Sod1*$^{-/-}$ MEFs, but further testing has shown that it was a false positive. By understanding more about *Sod1*'s role in cell viability and death, the findings of this study will potentially further our understanding of *Sod1*'s role in maintaining cellular functions, reactive oxygen species homeostasis, diseases and possibly aging.

Literature Review

Reactive oxygen species and reactive nitrogen species

Mitochondria generate large amounts of adenosine triphosphate (ATP) through cellular respiration, especially through oxidative phosphorylation, to support the energy requirements of many organisms. Using the energy resulting from metabolic oxidations during cellular respiration, coenzymes nicotinamide adenine dinucleotide (NAD^+) and flavin adenine dinucleotide (FAD) are reduced to NADH and $FADH_2$ respectively. NADH is a substrate for mitochondrial NADH-Q oxidoreductase (complex I) and FAD is contained in FAD-dependent enzymes such as mitochondrial succinate-Q oxidoreductase (complex II) (Hernansanz-Agustín & Enríquez, 2021). Complex I catalyzes the two-electron oxidation of NADH by ubiquinone (Q), resulting in ubiquinol (QH_2). For complex II, electrons from succinate are used to reduce FAD^+ to $FADH_2$ which subsequently transfers its electrons to Q, resulting in QH_2. Q–cytochrome c oxidoreductase (complex III) oxidizes QH_2 to reduce cytochrome c which subsequently transfers its electrons to cytochrome c oxidase (complex IV). Complex IV reduces oxygen (O_2) to water (H_2O). Additionally, during the electron transport, complex I, III and IV also pump protons from the matrix, across the inner mitochondrial membrane, and into the mitochondrial intermembrane space. This creates an electrochemical gradient: the proton motive force. Those protons are transferred back into the matrix through ATP synthase (complex V), releasing energy. This energy is used to phosphorylate adenosine diphosphate (ADP) to ATP. Complexes I, II, III, and IV are part of the electron transport chain. For more details, this has been recently reviewed in Hernansanz-Agustín & Enríquez (2021) and countless other reviews.

Under normal circumstances, electron leakage from electron transport chains, such as the ones present in mitochondria and the endoplasmic reticulum, represents a major source of reactive oxygen species (ROS) (Valko et al., 2004). ROS are highly reactive chemicals mainly resulting from the reduction of O_2 by electrons. Around 1–3% of electrons flowing through the electron transport chain prematurely react with O_2, mostly at complex I and complex III, instead of reducing O_2 at complex IV, resulting in the formation of superoxide ($O_2^{\bullet -}$) (Balaban et al., 2005; Hernansanz-Agustín & Enríquez, 2021; Murphy, 2008; Nolfi-Donegan et al., 2020; Valko et al., 2004). To be more specific, $O_2^{\bullet -}$ results from one-electron transfers to O_2. (Valko et al., 2004). Two-electron, three-electron, and four-electron transfers to O_2 can also occur, resulting in hydrogen peroxide (H_2O_2), hydroxyl radical ($HO^{\bullet}$), and H_2O respectively (Valko et al., 2004). Since uncontrolled levels of $O_2^{\bullet -}$ are harmful, the cell uses superoxide dismutases such as SOD1 to convert $O_2^{\bullet -}$ to H_2O_2 (McCord & Fridovich, 1969). H_2O_2 can then be enzymatically converted to O_2 and H_2O by catalase, or to H_2O by glutathione peroxidase (GPX) and peroxiredoxins (PRDX) (Cox et al., 2009; Jomova et al., 2023; Mondola et al., 2016).

While ROS can be deleterious by reacting to other biomolecules and contribute to oxidative stress under pathological conditions, they are necessary for cell signalling since cellular redox status regulates various transcription factors and activators (D'Autréaux & Toledano, 2007; Jomova et al., 2023; Miao & St. Clair, 2009; Sies & Jones, 2020; Sun & Oberley, 1996). Within a healthy and physiological range, ROS such as H_2O_2 can promote cellular differentiation and proliferation (Reczek & Chandel, 2015; Sies & Jones, 2020). H_2O_2 is a major redox signalling molecule that can cross biological membranes, reversibly oxidize thiols groups on proteins, and has slow reaction kinetics with the surrounding biomolecules,

allowing its accumulation in cells and tissues at high concentrations (Andrés et al., 2022; Reczek & Chandel, 2015; Sies & Jones, 2020). These properties confer plenty of favorable characteristics for H_2O_2 to act as a second messenger (Colavitti et al., 2002; Sundaresan et al., 1995). An example illustrating the beneficial effects of ROS is found in yeast and human cells where mammalian target of rapamycin (mTOR) complex 1 inhibits SOD1's activity in response to nutrients, but activates SOD1 in response to starvation (Tsang et al., 2018). SOD1 will be discussed in detail later, but as mentioned previously, SOD1 catalyzes the conversion of $O_2^{\bullet-}$ to H_2O_2, allowing other enzymes to subsequently convert H_2O_2 to non-reactive products. The controlled inhibition of SOD1 allows the cell to carefully increase ROS production for optimal cell proliferation when nutrients are abundant, while limiting oxidative stress during starvation.

Through the Fenton reaction, H_2O_2 can be further reduced by labile ferrous iron (Fe^{2+}), generating $HO^{\bullet}$, which is one of the most reactive ROS (Ayala et al., 2014; Valko et al., 2007; Valko et al., 2005). However, at low or physiological concentrations of bicarbonate (HCO_3^-), $HO^{\bullet}$ is not the main product from the reaction of H_2O_2 with Fe^{2+}, but instead it is the carbonate radical ($CO_3^{\bullet-}$) according to this final equation: $Fe^{2+}(CO_3)(OOH)(H_2O)_2 \rightarrow Fe^{3+}(OH)_3(H_2O) + CO_3^{\bullet-}$ (Fleming & Burrows, 2020; Illés et al., 2019; Kornweitz et al., 2015). The formation of $CO_3^{\bullet-}$ was also confirmed in the Fenton reaction of HCO_3^- with Fe^{2+}(citrate), which is one of the main species from the mobile pool of non-transferring bound iron present in biological systems at physiological concentrations (Illés et al., 2020). The other main species in this pool is ferric (Fe^{3+}) citrate. $CO_3^{\bullet-}$ is a one-electron oxidant that mainly damages DNA through the formation of a guanine radical cation, leading to the formation of C8 or C5 oxidation products (Fleming & Burrows, 2020; Rokhlenko et al., 2012). Additionally, due to the high

reactivity and extremely short *in vivo* half-life of HO•, HO• can only react near its site of formation (Di Meo et al., 2016; Donaghy et al., 2015). The resulting Fe^{3+} from the Fenton reaction can then be reduced back to Fe^{2+} by another H_2O_2, generating a hydroperoxyl radical (HOO•) (Gaschler & Stockwell, 2017). Under physiological conditions, 0.6% of $O_2^{\bullet-}$ also exists in the form of HOO• (Jomova et al., 2023). In this case, HOO• results from the reaction of $O_2^{\bullet-}$ with a proton. $O_2^{\bullet-}$ can also react with nitric oxide (•NO) to generate peroxynitrite ($ONOO^-$), a highly reactive nitrogen species (RNS) (Huie & Padmaja, 1993). •NO is synthesized by nitric oxide synthase (NOS) (Palmer & Moncada, 1989). $ONOO^-$ can also act as a signaling and regulatory molecule (Abalenikhina et al., 2020; Pacher et al., 2007), but unregulated levels of $ONOO^-$ are even more toxic to cells than H_2O_2 or $O_2^{\bullet-}$ because $ONOO^-$ is a much more powerful oxidant, can cross cell membranes, and induce damage far from its initial site of synthesis (Murphy et al., 1998; Pacher et al., 2007; Szabó et al., 2007). $ONOO^-$ causes damage through the oxidation or nitrosylation of lipids, proteins, and nucleic acids (Abalenikhina et al., 2020; Pacher et al., 2007). Additionally, $ONOO^-$ can also react with CO_2, resulting in one-electron oxidants $CO_3^{\bullet-}$ and nitrogen dioxide ($^{\bullet}NO_2$) (Jomova et al., 2023; Pacher et al., 2007; Szabó et al., 2007).

In the case of lipid peroxidation, prooxidants abstract a hydrogen from lipids containing more than one carbon double bond, resulting in a resonance-stabilized, carbon-centered lipid radical (L•) (Ayala et al., 2014; Gaschler & Stockwell, 2017; Jomova et al., 2023). More specifically, lipid peroxidation occurs preferentially on polyunsaturated fatty acids by strong radicals such as HO• or HOO• (Ayala et al., 2014; Yin et al., 2011). The resulting L• reacts with O_2 to form a lipid peroxyl radical (LOO•) that can react with another lipid, leaving behind a lipid hydroperoxide (LOOH) and generating a new L• that continues the chain

reaction. LOOH is vulnerable to one-electron reduction by traces of redox metals, decomposing LOOH into LOO• or a lipid alkoxyl radical (LO•) and further propagating lipid peroxidation (Ayala et al., 2014; Jomova et al., 2023). The LOO• radical will continue to propagate to new lipids until it either reacts with another radical to form a new bond between both molecules, or receives a hydrogen atom from antioxidants such as vitamin E (Gaschler & Stockwell, 2017; Niki, 2014; Yin et al., 2011). The resulting vitamin E radical can be reduced by vitamin C or QH_2, regenerating vitamin E (Niki, 2014). Lipid peroxidation significantly affects membrane fluidity and permeability (Jomova et al., 2023), and its by-products are involved in many pathological processes (Ayala et al., 2014; Yin et al., 2011).

Intracellular sources of ROS include the cytoplasm, mitochondria, plasma membrane, endoplasmic reticulum, peroxisomes, and chloroplasts (Di Meo et al., 2016; Donaghy et al., 2015; Jomova et al., 2023; Snezhkina et al., 2019). ROS production is also present in lysosomes where the existence of a lysosomal redox chain has previously been reported (Arai et al., 1991; Gille & Nohl, 2000). Additionally, other cytosolic soluble cell components such as thiols, hydroquinones, catecholamines, and flavins can undergo redox reactions and also contribute to intracellular ROS (Di Meo et al., 2016). It is generally assumed that mitochondria are the main source of ROS in cells, where oxidative phosphorylation generates most of the produced cellular ROS, ~90% according to one source (Balaban et al., 2005). However, certain authors dispute this claim (Brown & Borutaite, 2012). Major sites of mitochondrial ROS production include complex I and complex III (Balaban et al., 2005; Hernansanz-Agustín & Enríquez, 2021; Murphy, 2008; Nolfi-Donegan et al., 2020). Under specific experimental conditions where complex I and complex III are inhibited, complex II can also become an important source of mitochondrial ROS (Hernansanz-Agustín & Enríquez,

2021; Kausar et al., 2018; Quinlan et al., 2012; Quinlan et al., 2013). A study by Quinlan et al. (2013) quantified the combined production of $O_2^{\bullet-}$ and H_2O_2 by different mitochondrial sites using different substrates and found that when palmitoylcarnitine and carnitine were used as a substrate, complex II's flavin site became a major contributor of $O_2^{\bullet-}$ and H_2O_2. This sheds light on the physiological relevance of complex II's ROS production since changes in substrates can determine rates of mitochondrial ROS production. Excluding the mitochondrial respiratory chain, ROS production in other mitochondrial locations have also been reported, but whether this contribution is significant to total mitochondrial ROS production is unknown (Di Meo et al., 2016; Murphy, 2008).

NADPH oxidases (NOXs) are another well-recognized source of ROS. As reviewed in Bedard and Krause (2007), NOX are transmembrane proteins that transfer an electron across the membrane from reduced nicotinamide adenine dinucleotide phosphate (NADPH) to FAD, then to the inner and outer hemes, and lastly to O_2, reducing it to $O_2^{\bullet-}$. The main function of NOX is the generation of $O_2^{\bullet-}$ for purposes such as host defense, posttranslational processing of proteins, cellular signaling, regulation of gene expression, and cell differentiation (Bedard & Krause, 2007). $O_2^{\bullet-}$ generation can occur either in the intraorganellar or extracellular space and can subsequently pass through anion channels to penetrate membranes (Fisher, 2009). The mammalian NOX family includes NOX1, NOX2, NOX3, NOX4, NOX5, dual oxidase 1, and dual oxidase 2. Early studies of NOX2 found it to be highly expressed in phagocytes, but when the other NOX are included, they are found in virtually every tissue. This is by no means an exhaustive list, but possible tissues they may be expressed in are the colon epithelium (NOX1), cochlear, vestibular sensory epithelia and the spiral ganglion (NOX3), kidney and fibroblasts (NOX4), testis, spleen, lymph nodes (NOX5), etc. (Bedard & Krause, 2007). The

NOX isoform most commonly associated with the endoplasmic reticulum (ER) is NOX4 (Zeeshan et al., 2016).

The ER is another source of ROS and is involved in the synthesis, transport and folding of proteins, lipid biogenesis, and calcium storage (Görlach et al., 2006; Schwarz & Blower, 2015). To promote proper protein folding and disulfide bond formation, the lumen of the ER contains an oxidizing environment (Cao & Kaufman, 2014; Görlach et al., 2006; Malhotra & Kaufman, 2007). Protein disulfide isomerase (PDI) can oxidize, isomerize, and reduce thiols during protein folding to ensure the formation of appropriate disulfide bonds (Cao & Kaufman, 2014; Malhotra & Kaufman, 2007; Tu & Weissman, 2004). The ER also contains a ratio of reduced to oxidized glutathione (GSH/GSSG) between 1:1 and 3:1, necessary to maintain optimal ER redox homeostasis (Cao & Kaufman, 2014; Görlach et al., 2006; Malhotra & Kaufman, 2007). GSH acts as a redox buffer and assists in reducing non-native disulfide bonds in misfolded proteins (Malhotra & Kaufman, 2007; Zeeshan et al., 2016). To restore PDI's oxidative ability, endoplasmic reticulum oxidoreductin-1 (ERO1) oxidizes the reduced PDI and subsequently transfers the electrons to O_2, generating H_2O_2. Mammals have two genes that are homologs of yeast *ERO1*: *ERO1A* and *ERO1B* (Zito et al., 2010). During oxidative protein folding, the formation of disulfide bonds can result in ~25% of total cellular ROS production, at least in yeast (Cao & Kaufman, 2014; Malhotra & Kaufman, 2007; Tu & Weissman, 2004). Proteins that do not fold properly after a certain period of time are retrotranslocated to the cytosol and targeted for ER-associated degradation (Görlach et al., 2006; Zeeshan et al., 2016). Excessive accumulation of unfolded or misfolded proteins initiates the unfolded protein response (UPR) in an attempt to restore the ER lumen back to an optimal protein-folding environment (Cao & Kaufman, 2014). Severe or chronic ER stress

activates apoptosis but also increases Ca^{2+} leakage from the ER lumen, increasing mitochondrial ROS generation and resulting in a positive feedback loop where increased ROS exacerbates ER stress further (Cao & Kaufman, 2014; Malhotra & Kaufman, 2007). This guarantees cell death through multiple pathways.

The microsomal monooxygenase system (MMO) is another important source of ROS in the ER. This has been reviewed in Davydov (2016). This membrane-bound multienzyme system is composed of multiple cytochrome P450 species, NADPH-P450 reductase, and cytochrome b_5 (Davydov, 2011). NADPH-P450 reductase is the main electron donor for cytochrome P450 in the MMO. Cytochrome b_5 increases catalytic efficiency and can also act as an alternate electron donor. In eukaryotes, most cytochromes P450 are localized in the ER membrane, but some are also localized in the mitochondria. In animals tissues, the MMO is highly present in the ER of liver cells, but also in the lung, kidney, brain, vascular smooth muscle, intestinal epithelium, nasal mucosa, mammary gland, lymphocytes, etc. (Başaran & Can Eke, 2017; Davydov, 2016). The MMO detoxifies the cell by catalyzing the oxidation of exogenous compounds and endogenous substrates into hydrophilic, oxygenated, and readily excreted metabolites. Cytochrome P450 enzymes also participate in the biosynthesis of alkaloids, amino acids, bile acids, bilirubin, cholesterol, eicosanoids, fatty acids, indole, melatonin, steroid hormones, terpenes, and vitamins (Hrycay & Bandiera, 2012, 2015). The monooxygenase reaction uses two electrons from NADPH to proceed with the four-electron reduction of O_2 and the two-electron oxidation of the substrate, resulting in a monooxygenated substrate and H_2O (Hrycay & Bandiera, 2012, 2015). This reaction is often highly inefficient and uncoupling sometimes occurs, resulting in the generation of $O_2^{\bullet-}$ or H_2O_2 instead of the monooxygenated substrate (Hrycay & Bandiera, 2012, 2015). The MMO

continues producing ROS even in the absence of substrates, suggesting a possible role in cellular ROS signalling such as cytochrome c–dependent apoptosis (Davydov, 2016). The main feature of all eukaryotic MMO is the high ratio of cytochrome P450 to NADPH reductase, leading to competition between various cytochrome P450 isoforms for NADPH reductase. The central mechanism regulating the coordination of different cytochrome P450 isoforms has been hypothesized to originate from the interactions existing between the different cytochrome P450 isoforms. For further details, this has been extensively reviewed by Davydov (2016). According to the author, the main physiological role of this mechanism is the maintenance of an optimal balance between P450-dependent substrate oxidation and P450-dependent ROS generation.

Xanthine oxidoreductase (XOR) exists in two forms, xanthine dehydrogenase (XDH) and xanthine oxidase (XO). XDH can be reversibly converted to XO by the formation of a disulfide bond between Cys535 and Cys992, or irreversibly converted to XO by the proteolysis of the inter-domain linker peptide (Nishino et al., 2008). XOR is mainly involved in the breakdown of purine nucleotides, catalyzing the oxidation of hypoxanthine to xanthine and xanthine to uric acid (Jomova et al., 2023). During the catalysis of xanthine to uric acid, XDH preferentially uses NAD^+ as an electron acceptor to generate NADH but it can also use O_2 (Berry & Hare, 2004; Nishino et al., 2008; Saito & Nishino, 1989). In contrast, XO only uses O_2 as an electron acceptor, generating $O_2^{\bullet-}$ and H_2O_2. In the past, XO was reportedly found in the cytosol (Ichikawa et al., 1992) and peroxisomes (Angermüller et al., 1987) of rat liver cells. However, these studies could not differentiate between an active or inactive protein, nor between XDH or XO activity (Frederiks & Vreeling-Sindelárová, 2002). Using electron microscopy, a study by Frederiks and Vreeling-Sindelárová (2002) has also detected XOR

activity in the cytosol, but XO activity was confined to peroxisomes. This suggests that in rat liver cells, cytoplasmic XOR has XDH activity, and its major function is not the production of $O_2^{\bullet-}$ but of uric acid. Although, XDH can still produce some $O_2^{\bullet-}$, albeit at a slower rate (Berry & Hare, 2004). Additionally, in Kupffer cells and sinusoidal endothelial cells, XOR activity was also detected in vesicles and sometimes on the granular ER, but XO activity was not detected in those cells (Frederiks & Vreeling-Sindelárová, 2002).

As reviewed in Antonenkov et al. (2010), mammalian peroxisomes perform many important metabolic functions, mainly the oxidative degradation of long-chain fatty acids, but also the oxidation of purines, L-α-hydroxy acids, polyamines, and the synthesis of plasmalogenes, waxes, and ketone bodies. Peroxisomes are also one of the main intracellular sources of H_2O_2. Palmitoyl-CoA oxidase and urate oxidase are the main enzymes involved in the production of peroxisomal H_2O_2. As for the decomposition of peroxisomal H_2O_2, catalase is the main enzyme. Mammalian peroxisomes contain many enzymes that produce ROS such as acyl-CoA oxidase, urate oxidase, 2-hydroxyacid oxidase, N^1-acetyl polyamine oxidase, L-pipecolic acid oxidase, sarcosine oxidase, D-amino oxidase, D-aspartate oxidase, XO, and NOS (Antonenkov et al., 2010). Most of them are FAD or FMN-dependent oxidases generating H_2O_2. The presence of both XO and NOS in peroxisomes is potentially damaging since they produce $O_2^{\bullet-}$ and $^{\bullet}NO$ respectively, which can react together to form $ONOO^-$ (Di Meo et al., 2016; Snezhkina et al., 2019).

Sod1 and other superoxide dismutases

In mammals, three SOD isoforms are expressed: SOD1, (McCord & Fridovich, 1969), SOD2 (Weisiger & Fridovich, 1973), and SOD3 (Marklund, 1982). SOD1 is a copper-zinc superoxide

dismutase (Cu,Zn-SOD) that is mainly found in the cytosol, but also in the nucleus, mitochondrial intermembrane space, lysosomes, and peroxisomes (Chang et al., 1988; Crapo et al., 1992; Geller & Winge, 1982; Keller et al., 1991; Kira et al., 2002; Liou et al., 1993; Okado-Matsumoto & Fridovich, 2001; Sturtz et al., 2001). Protein extracts from mouse spinal cords also show SOD1's localization in the endoplasmic reticulum (Kikuchi et al., 2006). In rat liver hepatocytes, 73.1% of Cu,Zn-SODs were in the cytoplasmic matrix, 11.9% in the nucleus, 8.6% in mitochondria, 5.4% in lysosomes, and the remaining 1% were in peroxisomes and the smooth endoplasmic reticulum (Chang et al., 1988). In the same study, the highest concentration of Cu,Zn-SOD was found in lysosomes (5.81 mg/cm^3), followed by the cytoplasm (1.36 mg/cm^3), nucleus (0.71 mg/cm^3), peroxisomes (0.27 mg/cm^3), mitochondria (0.21 mg/cm^3), and smooth endoplasmic reticulum (0.02 mg/cm^3). Depending on the metabolic state of the rat, 8.4% of total cellular Cu,Zn-SODs are lysosomal in fasted rats, compared to 2.3% in fed rats (Geller & Winge, 1982). Starvation can stimulate autophagy and during autophagy, there is enhanced protein degradation of cytosolic enzymes (Goldberg & St. John, 1976). Their observations of increased lysosomal Cu,Zn-SOD during fasting is consistent with autophagy (Geller & Winge, 1982).

The metalation of SOD1 is mainly done by the copper chaperone of SOD1 (CCS), a homolog of *Saccharomyces cerevisiae* LYS7 (Culotta et al., 1997). This mainly occurs on the cytosolic side of the plasma membrane by shuttling copper from integral membrane transporter CTR1 to SOD1 (Ge et al., 2019; Markossian & Kurganov, 2003; Pope et al., 2013; Skopp et al., 2019). However, SOD1 can also acquire copper in a CCS-independent manner using GSH (Carroll et al., 2004; Leitch et al., 2009; Wong et al., 2000). Despite its name, CCS can also bind zinc (Ge et al., 2019) and zinc acquisition by metal-free SOD1 (apo-SOD1) is

promoted through CCS interaction (Trist et al., 2021). In humans, CCS is ubiquitously expressed in a variety of tissues which includes the kidney, liver, and brain (Ge et al., 2019). Using immunoelectron microscopy on rat liver cells, CCS was mainly localized in the cytosol (6.86 gold particles/μm^2) and peroxisomes (3.62 gold particles/μm^2), but also faintly in mitochondria (1.92 gold particles/μm^2), rough ER (1.87 gold particles/μm^2), and nucleus (1.85 gold particles/μm^2) (Islinger et al., 2009). In HepG2 cells, CCS is localized in the cytoplasm and nucleus (Casareno et al., 1998). In yeast, CCS is largely cytosolic, but is also found in the mitochondrial intermembrane space (Sturtz et al., 2001). Apo-SOD1 is able to cross into the mitochondria (Field et al., 2003; Kawamata & Manfredi, 2010), which could explain why SOD1 is found in various subcellular compartments despite lacking obvious localization signals such as the nuclear localization sequence. In the mitochondria, the maturation of apo-SOD1 to a fully metalated SOD1 (holo-SOD1) by CCS traps it in the intermembrane space (Field et al., 2003; Kawamata & Manfredi, 2010). This is also the case in rat liver peroxisomes (Islinger et al., 2009). Palmitoylation is likely another mechanism used to anchor SOD1 to specific subcellular compartments since the palmitoylation of SOD1's Cys6 plays a significant role in its nuclear localization (Marin et al., 2012).

The human *SOD1* gene is located on chromosome 21's region 21q22.11 (Levanon et al., 1985), with a genomic size of 9307 base pairs (bp) and consists of five exons interrupted by four introns (Milani et al., 2011). Significant similarities in *SOD1*'s gene sequence have been found between mice, rats, bovines, and humans (Miao & St. Clair, 2009). The promoter of human *SOD1* contains regulatory elements for constitutive expression such as a TATA box, a CCAAT box and a GC-rich region, but also binding sequences for early growth response 1, aryl hydrocarbon receptor, nuclear factor erythroid 2-related factor 2, nuclear factor-kappa

B, activating protein 1, and thyroid hormone receptor (Trist et al., 2021). These transcription factors regulate the expression of *SOD1* throughout multiple intracellular molecular events such as increased $O_2^{\bullet-}$ or H_2O_2, the exposure to cytokines, radiation, growth factors and thyroid hormones, increased neuronal NOS, and the presence of synthetic halogenated and nonhalogenated aromatic hydrocarbons (Trist et al., 2021). The human SOD1 enzyme is a 32-kDa homodimer containing, within each monomer, a copper binding site composed of four histidine residues, a zinc binding site composed of three histidine and one aspartic acid residues, an electrostatic loop, a conserved disulfide bond, and an eight-stranded Greek-key β-barrel motif (Trist et al., 2021; Valentine et al., 2005). The copper site contains the enzymatic active site that catalyzes the disproportionation of $O_2^{\bullet-}$ and cycles between Cu^{2+} and Cu^{+}. $O_2^{\bullet-}$ is oxidized by Cu^{2+}, resulting in O_2, and another $O_2^{\bullet-}$ is reduced by Cu^{+} in the presence of two protons, resulting in H_2O_2 (Trist et al., 2021). The zinc ion is important for SOD1's structural stability and function (Boyd et al., 2020). The electrostatic loop is composed of charged and polar residues that creates a positive electric field, which guides $O_2^{\bullet-}$ to the active site containing Cu^{2+} (Polticelli et al., 1998). The binding of copper and zinc and the presence of an oxidized disulfide bond are important for the structural stability of the enzyme, but also to avoid aberrant folding and interactions (Trist et al., 2021). SOD1 is sensitive to cyanide, a property that helps in distinguishing SOD1 from SOD2 which is, in contrast, relatively resistant to cyanide (Fukai & Ushio-Fukai, 2011). Additionally, bicarbonate-mediated inactivation of SOD1 by H_2O_2 can happen due to SOD1's peroxidative activity (Liochev & Fridovich, 2004; Valentine et al., 2005). This is possibly an additional mechanism regulating the inactivation of SOD1.

Other than the dismutation of $O_2^{\bullet-}$ to H_2O_2 and O_2, additional functions of SOD1 have also been reported such as the regulation of $O_2^{\bullet-}$ and H_2O_2 levels. In a reduced environment, SOD1 is bound to Rac1-GTP to inhibit its GTPase activity, stabilizing GTP-Rac and leading to the activation of Rac1-dependent NOX such as NOX2 (Harraz et al., 2008). This increases NOX-dependent $O_2^{\bullet-}$ production. In an oxidized environment, increased H_2O_2 concentrations lead to the uncoupling of SOD1 from Rac1, accelerating its hydrolysis to Rac-GDP and leading to the inactivation of NOX2. This decreases NOX-dependent $O_2^{\bullet-}$ production. Interestingly, the authors also hypothesized that SOD1 activated Rac1-NOX2 complexes in MEFs' endosomes and observed that adding purified bovine or human SOD1 to these endosomes rapidly increased NOX-dependent $O_2^{\bullet-}$ production. Using 1 μM of wild-type human SOD1 in isolated MEFs' endosomes, $O_2^{\bullet-}$ production peaked at 15 minutes but gradually lowered afterwards until it reached baseline levels at 60 minutes.

Another function of SOD1 has been observed in yeast and human fibroblasts where in response to elevated cellular ROS, ATM/Mec1's effector Cds1/Dun1 phosphorylates SOD1, which relocates to the nucleus and acts as a transcription factor, promoting the expression of oxidative resistance and DNA repair genes (Tsang et al., 2014). The response to elevated cellular ROS does not seem to be limited to $O_2^{\bullet-}$ since nuclear localization was also observed after treatment with H_2O_2, ROS-generating agents such as paraquat or menadione, or by mutating glutathione reductase and catalase.

In many human cancers such as non-small-cell lung cancer (NSCLC), nasopharyngeal carcinoma, and breast cancer, SOD1 is overexpressed and highly expressed in the nuclei of 20 types of human tumors (Xu et al., 2022). However, $O_2^{\bullet-}$ is not produced in the nucleus and

$O_2^{\bullet-}$ does not readily permeate through membranes such as the nuclear membrane. Therefore, if only SOD1's main function in the dismutation of $O_2^{\bullet-}$ is considered, the accumulation of nuclear SOD1 seems unusual. To understand this phenomenon, previous studies have shown that SOD1 stabilized the PES1-BOP1-WDR12 (PeBoW) complex (Wang et al., 2021). This complex is necessary for the production of 60S ribosome subunits by processing 41S pre-rRNA (Hölzel et al., 2005). In cancer cells, hyperactive ribosome biogenesis contributes to oncogenic growth, supported by observations where ribosome biogenesis is upregulated in proliferating cells such as cancer cells (Montanaro et al., 2008). This is also supported by observations from Wang et al. (2021), where nuclear SOD1 was essential for the proliferation of Kirsten rat sarcoma virus (KRAS) mutant NSCLC cells after *Sod1* KO, not cytoplasmic SOD1. Other than the dismutation of $O_2^{\bullet-}$, these observations reinforce the idea that SOD1 fulfills other functions such as the regulation of $O_2^{\bullet-}$ and H_2O_2 levels, the regulation of oxidative stress resistance and repair genes, and the stabilization of the PeBoW complex.

Another isoform of superoxide dismutases is SOD2, an 88-kDa homotetramer exclusively located in mitochondria, mainly in the matrix and the inner membrane (Okado-Matsumoto & Fridovich, 2001; Slot et al., 1986; Weisiger & Fridovich, 1973). SOD2 is also named manganese superoxide dismutase (Mn-SOD). SOD2 contains one manganese cofactor per subunit (Dhar & St. Clair, 2012; Zelko et al., 2002) and is relatively resistant to cyanide, unlike SOD1 (Fukai & Ushio-Fukai, 2011). Lastly, SOD3 is a 135-kDa homotetrameric glycoprotein that also has Cu and Zn as its catalytic center, but is located in the extracellular matrix (Miao & St. Clair, 2009; Zelko et al., 2002).

Role of *SOD1* in human diseases

The *SOD1* gene is implicated in many diseases such as amyotrophic lateral sclerosis (ALS), heart failure, cancer, diabetes, Down's syndrome, and Parkinson's disease (Lewandowski et al., 2019; Miao & St. Clair, 2009; Trist et al., 2021). ALS is a neurodegenerative disorder resulting in the progressive loss of both upper and lower motor neurons in the brain and spinal cord, eventually leading to fatal respiratory paralysis, typically in 3 to 5 years (Brown & Al-Chalabi, 2017). 10–15% of ALS cases are hereditary, also known as familial ALS (fALS). In 1993, the first mutated gene discovered to cause fALS was the *SOD1* gene (Rosen et al., 1993). Since 1993, approximately 200 *SOD1* mutations associated with the risk of ALS have been found (Abel et al., 2012). Depending on the population sampled, *SOD1* mutations accounted for 12.0–23.5% of all fALS cases (Andersen, 2006). A pathological hallmark of ALS-linked *SOD1* mutations is the accumulation of misfolded or aggregated SOD1 proteins, causing selective motor neuron degeneration (Broom et al., 2014; Bruijn et al., 1998). Mature, holo-SOD1 is extremely stable (Forman & Fridovich, 1973) due to the presence of the disulfide bond and the binding of the copper and zinc ion, therefore misfolding and aggregation most likely involves the unstable apo-SOD1 protein instead (Trist et al., 2021). ALS-linked *SOD1* mutations can disrupt the incorporation of the copper and zinc ion or the formation of the disulfide bond, contributing to the misfolding of SOD1 and leading to aggregation (Furukawa, 2022). Mouse models are useful to study the pathophysiology of ALS and possible treatments. The $Sod1^{G93A}$ transgenic mouse model is the first and most studied ALS animal model (Gurney et al., 1994), replicating most pathological mechanisms of ALS (Lutz, 2018). Even though humans rarely possess the $Sod1^{G93A}$ mutation, rodents with the $Sod1^{G93A}$ mutation are often used in the study of fALS, since the accumulation and aggregation

of insoluble Cu,Zn-SODs is present in the motor neurons of both fALS patients and *Sod1*^{G93A} mutant rodents (Miao & St. Clair, 2009).

Mutant superoxide dismutases in KO and transgenic mice

Studies done on SOD KO mice and SOD transgenic mice have been summarized in several excellent reviews (Deepa et al., 2019; Lutz, 2018; Pérez et al., 2009; Pouyet & Carrier, 2010; Salmon et al., 2010; Tsan, 2001; Wang et al., 2018). *Sod1*-deficient mice (*Sod1*$^{-/-}$ and *Sod1*$^{+/-}$) develop normally into adulthood (Reaume et al., 1996). Considering how highly *Sod1* is conserved between species, the importance of its function, and its high levels of expression, the viability of *Sod1*$^{-/-}$ mice is surprising (Fridovich, 1995; Miao & St. Clair, 2009; Okado-Matsumoto & Fridovich, 2001; Sturtz et al., 2001). Although viable, *Sod1*$^{-/-}$ mice display phenotypic abnormalities such as decreased female fertility (Ho et al., 1998; Matzuk et al., 1998), increased oxidative stress sensitivity (Huang et al., 1999), 30% decreased lifespan (Elchuri et al., 2005), increased incidence of liver cancer (Elchuri et al., 2005), increased mutation frequency and apoptosis in the liver (Busuttil et al., 2005), fatty liver (Uchiyama et al., 2006), accelerated age-related muscle atrophy (Muller et al., 2006), macular degeneration (Hashizume et al., 2008; Imamura et al., 2006), anemia (Iuchi et al., 2007), increased expression of collagenase MMP-13 (Dasgupta et al., 2009), osteopenia (Morikawa et al., 2013; Nojiri et al., 2011), skin atrophy (Shibuya et al., 2012), and denervation of fast twitch muscle (Fischer et al., 2012). Double *Sod1* and *Sod3* KO in mice did not decrease lifespan further than a single KO of *Sod1* (Sentman et al., 2006). Additionally, *Sod1* deficiency led to the accumulation of carbonylated proteins, lipid peroxidants, oxidized nucleic acids, and advanced glycation end products in tissues (Watanabe et al., 2014). As for heterozygous

Sod1$^{+/-}$ mice, they had 50% of wild-type SOD1's activity, and were also more sensitive to acute oxidative stress (Huang et al., 1999).

Multiple studies were also done to verify if there was a mechanism compensating for a deficiency in *Sod1*. Decreased Cu,Zn-SOD activity had no effect on the activity of other antioxidant enzymes such as Mn-SOD, catalase, GPX, glutathione reductase, and glucose-6-phosphate dehydrogenase in *Sod1*$^{+/-}$ and *Sod1*$^{-/-}$ mice (Ho et al., 1998). Compared to *Sod1*$^{+/+}$ mice, *Sod1*$^{-/-}$ mice also did not have a significantly different expression of GPX1, glutathione reductase, aldose reductase, aldehyde reductase, PRDX1 and PRDX4 (Yamanobe et al., 2007). However, other studies have found that GPX1 levels were decreased in *Sod1*$^{-/-}$ mice (Iuchi et al., 2008; Sentman et al., 2006). Additionally, one study has looked into the possibility of glutathione compensating for the loss of SOD1 through the cystine/glutamate exchange transport system but this is unlikely, since the double KO of *Sod1* and *xCT*, the cystine transporter gene, did not exacerbate phenotypic consequences already present in *Sod1*$^{-/-}$ mice (Iuchi et al., 2008).

Homozygous *Sod2*$^{-/-}$ mice are unable to develop into adulthood, dying within days or weeks after birth from cardiomyopathy or neurodegeneration depending on the genetic background (Huang et al., 2001; Huang et al., 1999; Lebovitz et al., 1996; Li et al., 1995). They also displayed abnormalities in enzymes involved in the citric acid cycle and electron transport chain, increased oxidative DNA damage, increased lipid accumulation in the liver and skeletal muscle, and metabolic acidosis (Li et al., 1995; Melov et al., 1999; Melov et al., 1998). A study has used superoxide dismutase mimetics such as Mn(III) tetrakis (4-benzoic acid) porphyrin chloride (MnTBAP) to extend the mean lifespan of small and large litters

from 8.3 days to about 16.4 days (Melov et al., 1998). Subsequently, they also used SOD-catalase mimetics such as salen manganese complexes to extend the mean lifespan of *Sod2*$^{-/-}$ mice from 9 days to 28 days at most (Melov et al., 2001). This suggests that SOD2 is essential for the viability of mitochondria and ATP production, especially for tissues with demanding energy requirements (Marecki et al., 2014). Since *Sod2*$^{-/-}$ is embryonic or neonatal lethal, studies have been done on tissue-specific *Sod2* KO using Cre-*loxP* (Bhaskaran et al., 2023; Ikegami et al., 2002; Lustgarten et al., 2009; Marecki et al., 2014; Nojiri et al., 2006; Oh et al., 2012; Parajuli et al., 2011; Sasaki et al., 2011; Treiber et al., 2011). Ordered from the greatest to smallest reduction in lifespan, total *Sod2* KO reduced the lifespan of mice when performed in the brain (Sasaki et al., 2011), heart/muscle (Nojiri et al., 2006), liver (Ikegami et al., 2002), or connective tissue (Treiber et al., 2011). Other than the ~43% reduced lifespan, performing a *Sod2* KO in connective tissues resulted in weight loss, skin atrophy, kyphosis, osteoporosis, and muscle degeneration (Treiber et al., 2011). Double *Sod2* and *p53* KO did not improve the dilated cardiomyopathy observed in *Sod2*$^{-/-}$ mice (Watanabe et al., 2021). As for heterozygous *Sod2*$^{+/-}$ mice, they had 50% of wild-type SOD2's activity and increased tumor incidence, but the same lifespan as *Sod2*$^{+/+}$ mice and no significant differences for certain biomarkers of aging (Van Remmen et al., 2003). Heterozygous *Sod2*$^{+/-}$ mice also had increased oxidative damage to mitochondrial DNA and impaired functions of the electron transport chain (Van Remmen et al., 2003; Williams et al., 1998). It was previously reported that nuclear DNA from livers of *Sod2*$^{+/-}$ mice at 2 to 4 months of age had no significant oxidative damage by measuring 8-oxo-2-deoxyguanosine (8-oxo-dG) (Williams et al., 1998), but at 26 months of age they had 60% higher 8-oxo-dG (Van Remmen et al., 2003). Cytosolic proteins from *Sod2*$^{+/-}$ mouse livers also had no significant differences in oxidative damage

(Williams et al., 1998). These observations are consistent with SOD2's localization in the mitochondria. As for compensatory changes, no significant change in the activity of GPX or Cu,Zn-SOD was observed, but the total level of glutathione was decreased by 30% in the liver (Williams et al., 1998).

In *Sod3*-deficient mice, homozygous *Sod3*$^{-/-}$ mice were able to develop into adulthood, were healthy for at least 14 months (Carlsson et al., 1995), and had a similar lifespan as wild-type mice (Sentman et al., 2006). However, they had increased sensitivity to hyperoxia (Carlsson et al., 1995), increased sensitivity to ischemia-reperfusion injury in skeletal muscle (Park et al., 2005), slightly increased systemic lipid peroxidation (Sentman et al., 2006), increased lung oxidative stress and injury in response to asbestos (Fattman et al., 2006), and an impaired neovascularization after ischemia and reperfusion (Kim et al., 2007).

The use of mouse embryonic fibroblasts in the study of superoxide dismutases

Mouse embryonic fibroblasts are often used due to their relative ease of collection and maintenance, rapid growth rates, physiological relevance, and the possibility to perform numerous large-scale experiments (Garfield, 2010; Hansen & Piorczynski, 2019; Tan & Lei, 2019). Fibroblasts possess an elongated and branched morphology but are often spindle-shaped when crowded. They are mesenchymal-derived, are found in every animal organ, are the most common cell type in animal connective tissues, are involved in self-renewal, tissue remodeling and repair, and the synthesis of extracellular matrix and collagen (Bozkurt, 2021; Yusuf et al., 2013). Additionally, they are involved in the regulation of self-tolerance, organ development, wound healing, inflammation, and fibrosis (Yusuf et al., 2013). They are an useful *in vitro* model to study cell cycle regulation, immortalization, transformation,

senescence, apoptosis, and differentiation (Yusuf et al., 2013). However, they present certain limitations since MEFs are highly heterogeneous and can contain many distinct cell subtypes, complicating the interpretation of experimental results (Garfield, 2010; Singhal et al., 2016).

The oldest study on *Sod1* KO MEFs observed a ~75% reduction in the proliferation rate of *Sod1*$^{-/-}$ MEFs (Huang et al., 1997). Since their experiments are closely related to ours, their observations will be summarized in this paragraph. Using terminal transferase *in situ* labeling, the authors determined the number of apoptotic cells and observed increased cell death: the number of *Sod1*$^{-/-}$ MEFs that underwent apoptosis was four to ten times the number of apoptotic *Sod1*$^{+/+}$ MEFs. The highest number of apoptotic cells was detected six hours after the second passage, which is six days after initially isolating *Sod1*$^{-/-}$ MEFs from embryos. 48 hours after the second passage, most *Sod1*$^{-/-}$ MEFs were dead, with some sparsely scattered healthy cells. *Sod1*$^{-/-}$ MEFs were also 80 times more sensitive to paraquat compared to *Sod1*$^{+/+}$ MEFs. In comparison, *Sod2*$^{-/-}$ MEFs only had a ~40% reduction in growth rate and were only 12 times more sensitive to paraquat compared to *Sod2*$^{+/+}$ MEFs. Additionally, heterozygous *Sod1*$^{+/-}$ MEFs were only around two times more sensitive to paraquat than *Sod1*$^{+/+}$.

The most recent study on *Sod1* KO MEFs found that *Sod1*$^{-/-}$ MEFs quickly died *in vitro* after a few days under normoxic conditions (20% O_2), but were alive under hypoxic conditions (2% O_2) for up to 2 weeks, albeit with a senescent morphology (Tsunoda et al., 2013). Their observations will also be summarized in this paragraph, with some additional interpretation. *Sod1*$^{-/-}$ MEFs had the same levels of SOD2, PRDX1, and PRDX2 compared to wild-type MEFs, but decreased levels of catalase and increased levels of hyperoxidized PRDX.

Levels of ROS and lipid peroxidation were significantly higher. Additionally, under 20% O_2 conditions, fluorescence-activated cell sorter (FACS) analyses of *Sod1*$^{-/-}$ MEFs' cell cycles showed that ~37.5% of *Sod1*$^{-/-}$ MEFs were aneuploid, which corresponds to dead cells, and ~12.5% of *Sod1*$^{-/-}$ MEFs were tetraploid. The remaining ~50% of cells were diploid. These tetraploid cells were most likely senescent MEFs due to acute and severe DNA damage, resulting in Gap 2 (G2) exit and permanent growth arrest at the next Gap 1 (G1) phase (Aylon & Oren, 2011; Margolis et al., 2003; Roger et al., 2021). This is also supported by observations from Tsunoda et al. (2013) where, under 2% O_2 conditions, ~50% of *Sod1*$^{-/-}$ MEFs were tetraploid and clearly looked senescent in microscopy pictures. This contrasts to the ~12.5% tetraploid cells observed under 20% O_2 conditions. The increased $O_2^{\bullet-}$ generation and apoptotic cell death were also observed by a previous study using *Sod1*$^{-/-}$ primary dermal fibroblasts, except hypoxic conditions (1% O_2) only increased cell viability on incubation day 3, but eventually all *Sod1*$^{-/-}$ fibroblasts died by day 8 (Shibuya et al., 2012).

Levels of cyclin A2 and cyclin B1 were downregulated in *Sod1*$^{-/-}$ MEFs (Tsunoda et al., 2013). Since the authors did not expand further into the significance of the cyclin results, additional interpretation will be done here to discuss the possible causes explaining *Sod1*$^{-/-}$ MEFs' cell cycle arrest at 2% O_2 and death at 20% O_2, which in turn could provide useful insights. While cyclin A1 is expressed during meiosis and embryogenesis, cyclin A2 is expressed during the mitotic division of somatic cells (Martínez-Alonso & Malumbres, 2020). Cyclin A control certain aspects of DNA replication and entry to mitosis from the G2 phase. In mutant mice, reduced levels of cyclin A led to impaired resolution of stalled replication forks, insufficient repair of double-stranded DNA breaks, and improper segregation of sister chromosomes (Kanakkanthara et al., 2016). Cyclin-dependent kinase 2 (CDK2) can bind to

cyclin A, and these cyclin A–CDK2 complexes are necessary for the activation of cyclin B, an important regulator for mitotic entry (Martínez-Alonso & Malumbres, 2020). Downregulation of cyclin B1 impairs cell proliferation (Fang et al., 2014; Müssnich et al., 2015). Therefore, *Sod1*$^{-/-}$ MEFs likely downregulate cyclins A2 and B1 to prevent mitosis due to increased oxidative DNA damage.

Tsunoda et al. (2013) also found that *Sod1*$^{-/-}$ MEFs' upregulated cyclins were cyclin D1 and cyclin E1. Cyclin D, alongside cyclin C, control cell cycle entry from quiescence and G1 phase progression (Martínez-Alonso & Malumbres, 2020). Cyclin D–CDK4/6 complexes phosphorylate Rb1-family proteins which are major repressors of genes involved in DNA replication and chromosome segregation (Martínez-Alonso & Malumbres, 2020). Phosphorylation inactivates Rb1 proteins, leading to the transcription of genes involved in the DNA synthesis phase (S phase) and in chromosome segregation for mitosis. In the event of DNA damage, one of the mechanisms proliferating cells use to arrest cell cycle progression is by downregulating cyclin D1 (Jirawatnotai et al., 2012). Cyclin D1 is also involved in DNA repair, independently of CDK4/CDK6 (Jirawatnotai et al., 2012). As for cyclin E, it controls DNA replication and completes the entry into S phase. After the phosphorylation of Rb1 by cyclin D–CDK complexes, cyclin E genes are expressed and cyclin E–CDK complexes can further phosphorylate Rb1 to completely inactivate it (Martínez-Alonso & Malumbres, 2020). Cyclin E–CDK complexes are inhibited by cyclin-dependent kinase inhibitors (CDKI) $p21^{Cip1}$ (p21), $p27^{Kip1}$ and $p57^{Kip2}$. Paradoxically, cyclin D1 and E were overexpressed in senescent MEFs (Leontieva et al., 2012) and *Sod1*$^{-/-}$ MEFs (Tsunoda et al., 2013). Since *Sod1*$^{-/-}$ MEFs cultured *in vitro* are undergoing increased oxidative stress and DNA damage, the upregulation of cyclin D1 seems contradictory since it should be downregulated to prevent

cell cycle progression. This is explained by the conversion of cell cycle arrest into senescence, also called geroconversion (Blagosklonny, 2012). After cell cycle arrest by p21 and $p16^{INK4a}$ (p16), growth-promoting pathways such as mTOR remain active and converts the cell cycle arrest into irreversible senescence, accompanied by a growth in size and a large accumulation of cyclin D1 and cyclin E (Leontieva et al., 2012). Cyclin D1 is involved in metabolic switch and cell growth, while cyclin E induces hypoxia- inducible factor 1 which may contribute to the hyper-secretory phenotype of senescent cells (Leontieva et al., 2012). This is supported by observations where inhibitors of mTOR such as rapamycin can decelerate the accumulation of cyclins D1 and E and slow down senescence in cell cycle–arrested cells which remain quiescent and retain their proliferative potential for longer (Demidenko et al., 2009; Leontieva et al., 2012).

Tsunoda et al. (2013) observed the upregulation of p21 and the downregulation of $p19^{INK4d}$ (p19) in *Sod1*$^{-/-}$ MEFs. p53-p21 is one of the two main molecular pathways involved in senescence (Rufini et al., 2013). p53 is a transcription factor involved in cell cycle control, DNA repair, cellular stress response, energy metabolism, apoptosis, and senescence (Rufini et al., 2013). p21 is a CDKI, a downstream target of p53, and is involved in cell cycle arrest, DNA replication and repair, cell differentiation, senescence, and apoptosis (Vurusaner et al., 2012). In the event of DNA damage, p53 activates p21 and the latter initiates cell cycle arrest to allow the cell some time for DNA repair (Vurusaner et al., 2012). Evidence show *p21*$^{-/-}$ MEFs were unable to undergo p53-dependent G1 arrest following DNA damage (Brugarolas et al., 1995). Characteristics of senescent cells are typically a large and flat morphology, senescence-associated-beta-galactosidase staining, hyper-secretory phenotype, permanent loss of regenerative or replicative potential, and increased expression of p53, p21 and p16

(Leontieva et al., 2012; Rufini et al., 2013). Under physiological conditions, p53 has an antioxidant function, but excessively high levels of active p53 increase the transcription of proapoptotic genes and ROS generation instead, leading to apoptosis (Kang et al., 2013; Macip et al., 2003; Vurusaner et al., 2012). For example, severe stress, such as excessive DNA damage in cells, activates p53 which enhances the transcription of proapoptotic genes and inhibits catalase, subsequently leading to an unbalanced intracellular ROS composition and resulting in cell death (Kang et al., 2013; Vurusaner et al., 2012). This function is central to the tumor-suppressive activity of p53. As for p19, it is a CDK4 and CDK6 inhibitor (Chan et al., 1995). Knowing that cyclin D1 is part of the cyclin D–CDK4/6 complex, p19's downregulation would increase the formation of cyclin D–CDK4/6 complexes and may assist in geroconversion (Datar et al., 2000; Leontieva et al., 2012; Nelsen et al., 2003). In summary, this analysis allows us to understand that hypoxic *Sod1*$^{-/-}$ MEFs experience increased oxidative stress and DNA damage, leading to the downregulation of cyclins A2 and B1 to prevent DNA synthesis and mitotic entry, the upregulation of p21 for cell cycle arrest, and the upregulation of cyclin D1 and E1 due to geroconversion. However, in the case of normoxic *Sod1*$^{-/-}$ MEFs, excessive oxidative stress causes severe DNA damage and leads to the upregulation of p53, further increasing intracellular ROS to guarantee cell death.

Another study on *Sod1* mouse cells was done by Watanabe et al. (2013) to study the cellular phenotypes of *Sod1*$^{-/-}$ primary dermal fibroblasts. Those studies did not use MEFs since they isolated dermal fibroblasts from 5-day-old mice neonates' skin tissues instead of ~13.5-day-old mouse embryos. Nevertheless, their observations can provide additional insights and might be relevant to MEFs since primary dermal fibroblasts are also fibroblasts and originate from mice. In *Sod1*$^{-/-}$ primary dermal fibroblasts, the authors observed a 2.7-

fold increase in cytoplasmic $O_2^{\bullet-}$, but also a 4-fold increase in mitochondrial $O_2^{\bullet-}$ compared to the wild-type counterpart (Watanabe et al., 2013). This was most likely due to how SOD1 is localized not only in the cytosol, but also in the mitochondrial intermembrane space (Okado-Matsumoto & Fridovich, 2001). Due to the negative charge of $O_2^{\bullet-}$ in the intermembrane space, $O_2^{\bullet-}$ decreases the mitochondrial membrane potential and destabilizes the mitochondria, leading to apoptosis (Brenner & Moulin, 2012). Watanabe et al. (2013) confirmed this by observing a 2.2-fold increase in the number of low–membrane potential mitochondria and an increase in apoptotic cell death as indicated by the increased expression of cleaved caspase 3 and annexin V–positive cells. A previous study has also observed a 56.0% increase of Annexin V–positive cells in *Sod1*$^{-/-}$ primary dermal fibroblasts (Shibuya et al., 2012). Additionally, Watanabe et al. (2013) also observed increased phosphorylation of the DNA damage marker H2AX, increased expression and phosphorylation of p53, and upregulation of p21. As explained earlier, oxidative stress activates the DNA damage response, resulting in the upregulation and phosphorylation of p53 and the subsequent activation of p21 (Rufini et al., 2013; Vurusaner et al., 2012). The loss of SOD1 did not induce a compensatory increase of other antioxidant enzymes such as SOD2, GPX1, and catalase (Watanabe et al., 2013). Other than increased apoptosis, Watanabe et al. (2013) observed other cellular phenotypes such as impaired cell proliferation and a significant decrease in the number of *Sod1*$^{-/-}$ primary dermal fibroblasts after only three days under 20% O_2 cell culture conditions. A subsequent study by Watanabe et al. demonstrated that double *Sod1* and *p53* KO in primary dermal fibroblasts led to fewer apoptotic cells and suppressed the cell number decline observed in *Sod1* KO cells, but they still had lowered proliferation and similar levels of $O_2^{\bullet-}$ as *Sod1*$^{-/-}$ MEFs (Watanabe et al.,

2021). As mentioned previously, this is likely due to p53's role as a tumor suppressor after severe DNA damage, guaranteeing apoptosis by expressing proapoptotic genes and increasing ROS. Without p53, cells with a *Sod1* and *p53* double KO had an improved survival rate, likely because ROS levels cannot reach the threshold required for apoptosis anymore and the cell now needed to trigger another apoptotic mechanism.

Homozygous *Sod2*$^{-/-}$ MEFs also have an impaired growth in cell culture. *Sod2*$^{-/-}$ MEFs had a ~40% reduction in their proliferation rate, compared to the ~75% reduction in *Sod1*$^{-/-}$ MEFs (Huang et al., 1997). *Sod2*$^{-/-}$ MEFs were also 12 times more sensitive to paraquat compared to *Sod2*$^{+/+}$ MEFs (Huang et al., 1997). *Sod2*$^{-/-}$ MEFs had increased cell death, increased $O_2^{\bullet-}$ production, and chromosomal instability (Samper et al., 2003). But even with the initial poor cell growth, *Sod2*$^{-/-}$ MEFs were still able to be cultured (Huang et al., 1997). In another study, 40% of *Sod2*$^{-/-}$ MEFs cultures were able to eventually immortalize (Samper et al., 2003). Another more recent study has also found that *Sod2*$^{-/-}$ MEFs had significantly increased $O_2^{\bullet-}$ production and decreased proliferation, but also reduced cellular ATP and impaired O_2 consumption (Zhang et al., 2010). Zhang et al. (2010) also looked at possible compensatory mechanisms in *Sod2*$^{-/-}$ MEFs and saw no significant changes in the protein levels of antioxidative enzymes such as catalase, GPX1, GPX4, thioredoxin 1 (TRX1), TRX2, PRDX1, and SOD1, except PRDX3 which was dramatically decreased. In SOD2-depleted DT40 chicken cells, no significant change was detected in the frequency of sister chromatid exchange, showing that increased mitochondrial $O_2^{\bullet-}$ from the lack of SOD2 seems to have little impact on the integrity of nuclear DNA (Inoue et al., 2010).

Heterozygous *Sod2*$^{+/-}$ MEFs had 50% of Mn-SOD activity and were not more sensitive to paraquat toxicity than the wild type (Huang et al., 1997). Another study observed increased mitochondrial DNA glycation in *Sod2*$^{+/-}$ MEFs, but no significant nuclear DNA glycation (Breyer et al., 2012). Similarly, cytosolic proteins had no significant differences in levels of advanced glycation end-products or protein carbonyl contents (Breyer et al., 2012). To quantify the formation of advanced glycation end-products, Breyer et al. (2012) measured N^2-carboxyethyl-2'-deoxyguanosine, a major DNA-bound advanced glycation end-product that compromises DNA integrity and gene functions. Since 50% reduced SOD2 in *Sod2*$^{+/-}$ MEFs did not increase paraquat sensitivity, measurements were performed to quantify levels of Mn-SOD, Cu,Zn-SOD, catalase, and GPX in paraquat-treated *Sod2*$^{+/-}$ MEFs, but no compensatory changes were detected compared to untreated *Sod2*$^{+/-}$ MEFs (Huang et al., 1997).

Rescue attempts of *Sod1* KO MEFs with treatments

Due to the observations where certain antioxidant treatments can improve SOD1-deficient phenotypes *in vivo*, *Sod1*$^{-/-}$ mice are useful to study age-related tissue dysregulation and possible treatments (Watanabe et al., 2021). *In vitro*, multiple antioxidants such as 2-Mercaptoethanol, N-acetylcysteine (NAC), catalase, α-phenyl-N-tert-butylnitrone, disodium 4,5-dihydroxybenzene-1,3-benzenedisulfonate, 4-hydroxy-2,2,6,6-tetramethylpiperidine-1-oxyl, and SOD2 mimetic MnTBAP were tested on *Sod1*$^{-/-}$ MEFs at 20% O_2 and all showed no beneficial effects (Tsunoda et al., 2013). In another study treating mice with skin atrophy caused by a *Sod1* deficiency, multiple antioxidants such as vitamin C and vitamin C derivative L-ascorbyl 2-phosphate 6-palmitate (APPS) were also tested (Murakami et al., 2009). They

found that administering vitamin C to drinking water did not induce a significant rescue effect for skin atrophy, likely due to insufficient drug delivery to the skin. Afterwards, they instead performed a transdermal treatment using APPS because it is stabilized by its phosphate group and conjugated to a long hydrophobic chain that enhances its permeability through the cell membrane. APPS treatment completely rescued *Sod1*$^{-/-}$ mice's skin thinning. Subsequent studies by the same team found similar results (Shibuya et al., 2012; Shibuya et al., 2014).

In *Sod1*$^{-/-}$ primary dermal fibroblasts, 10 μM APPS suppressed 70.1% of the increased $O_2^{\bullet-}$ generation caused by a deficiency in *Sod1*, and 100 μM APPS suppressed it by 90% instead (Shibuya et al., 2012). 10 μM APPS significantly increased cell count and partially rescued cell viability but 100 μM did not rescue viability further (Shibuya et al., 2012). In another study by the same team, 10 μM APPS also partially rescued *Sod1*$^{-/-}$ primary dermal fibroblasts' proliferation, suppressed the increased $O_2^{\bullet-}$ levels, and inhibited p53 upregulation and phosphorylation down to nearly wild-type levels (Watanabe et al., 2013). NAC treatment was also tested and suppressed the increased intracellular $O_2^{\bullet-}$ levels, but only increased cell viability slightly (Watanabe et al., 2013).

Material & Methods

Chemicals and reagents

All chemicals were obtained from Sigma-Aldrich, and cell culture reagents were supplied by Wisent, Inc. unless otherwise specified.

Plasmid preparation and validation by restriction enzymes

Retroviral vectors pBABE-puro and pBABE-puro-Cre (Cre recombinase cDNA subcloned into the EcoRI and SalI sites of pBABE-puro) were constructed previously by Dr. Ying Wang (Wang & Hekimi, 2013). To prepare the plasmids for retrovirus-mediated expression in MEFs, these plasmids were first transformed into *E. coli* OneShot™ Stbl3™ cells from which they were purified using the PureYield Plasmid Miniprep/Midiprep System (Promega) and following the manufacturer's instructions. To validate the plasmid's identity, samples of the plasmids were digested by restriction enzymes (EcoRI and SalI) and the resulting fragments were analyzed by agarose gel electrophoresis and compared to their theoretical sizes.

Preparation of MEFs for cell culture

MEFs were isolated from 12.5 or 13.5-day-old *Sod1*$^{fl/fl}$ or *Sod1*$^{-/-}$ mouse embryos (Noë, 2021). The head of each embryo was removed and kept for genotyping. After removing the embryos' heart and liver, the remaining part of the embryo was finely minced and treated with 1 ml of 0.25% Trypsin/0.1% EDTA (Thermo Fisher Scientific Inc.) for 20 minutes under standard cell culture conditions (37°C, 5% CO_2). Each embryo was then individually dispersed to their own 10 cm cell culture plate containing 10 ml of cell culture medium. The cell culture medium's composition is described under the "Cell culture and treatments" section. The cell

culture medium was renewed the next day. When cells reached full confluence, usually in ~2-3 days, they were passaged and used for experiments. If more time was needed to determine their genotype, cells were passaged one more time. For *Sod1*$^{-/-}$ MEFs, they received vitamin C (200 μM) after isolation. Without it, they were unable to reach full confluence.

Retroviral infection

Phoenix™-Eco cells were seeded on 10 cm cell culture plates coated with poly-D-lysine (0.05 mg/ml). At ~80% confluence, Phoenix™-Eco cells were transfected with 15 μg of plasmid DNA (pBABE-puro or pBABE-puro-Cre) using Lipofectamine™ 2000 Transfection Reagent (Thermo Fisher Scientific Inc.) and following the manufacturer's instructions. 24 hours after transfection, Phoenix™-Eco cells' cell culture medium was renewed. The infection procedure was done three times: 48, 54 and 72 hours after transfection. For each infection, the viral supernatant was harvested, filtered with a PVDF syringe filter (0.45 μm pore size), and added with polybrene (final concentration: 5 μg/ml). Total virus from one 10 cm cell culture plate of transfected Phoenix™-Eco cells was used to infect two wells (6-well plates) of *Mclk1*/*Coq7*$^{fl/fl}$ or *Sod1*$^{fl/fl}$ MEFs when they were within ~50–70% confluence. After the infected MEFs were fully confluent, puromycin (final concentration: 2.5 μg/ml) was added and incubated for two days to select MEFs that stably expressed the inserted sequences.

Western blot

The cell culture medium was vacuumed out of each well containing cells, 5 ml of ice-cold PBS was added to each well, then cells were scraped off the plate. Cells were collected in a tube, centrifuged (400 RCF, 3 minutes, 4°C) and the PBS was vacuumed out. Subsequently, cells were resuspended and lysed in RIPA Lysis Buffer (Cell Signaling Technology) in the presence

of protease inhibitors (Sigma-Aldrich) at 4°C for 20 minutes. After centrifugation (21 300 RCF, 5 minutes, 4°C), supernatants were collected and their protein concentrations were measured using the Pierce™ BCA Protein Assay Kit. Western blot samples were prepared with a 4X Laemmli buffer and boiled at 95°C for 5 min. Using the measured protein concentrations, samples were loaded at an equal amount of protein into 12% SDS-PAGE gels, electrophoresed at 120 V and transferred to 0.22 µm nitrocellulose membranes. Membranes were blocked in 5% milk diluted in PBS-T (phosphate-buffered saline containing 0.5% Tween 20) for one hour and blotted overnight or over 2 days at 4°C with the appropriate antibodies: anti-MCLK1/COQ7 (Proteintech, 15083-1-AP), anti-SOD1 (Proteintech, 10269-1-AP), anti-VDAC1/Porin (Abcam, ab15895), or anti-GAPDH (Cell Signaling Technology, #2118). After three washes with PBS-T, membranes were incubated with 1:2000 HRP-conjugated anti-rabbit secondary antibody (Cell Signaling Technology, #7074) at room temperature for two hours, washed three more times with PBS-T, and visualized using an enhanced chemiluminescence detection kit (Froggabio Inc.) and autoradiography films (Diamed).

Cell culture and treatments

MEFs and Phoenix™-Eco cells were cultured in cell culture medium under standard cell culture conditions. The cell culture medium consisted of Dulbecco's modification Eagle's medium (Wisent Inc.) containing 10% v/v fetal bovine serum (Thermo Fisher Scientific Inc.) and 1% v/v antibiotic-antimycotic 100X solution (Wisent Inc., 450-115 EL). The antibiotic-antimycotic solution contains penicillin G, streptomycin, amphotericin B, and sodium chloride. To passage cells, the cell culture medium was removed, then cells were washed with PBS (Wisent Inc.), treated for 3 minutes using ¼ of total cell culture medium volume

(volumes are specified further below for each different plates used) as 0.05% trypsin (with 0.53mM EDTA) (Wisent Inc.), followed by the addition of fresh cell culture medium at ¾ of total cell culture medium volume, and this cell suspension is transferred at the specified dilution. Vitamin C–treated MEFs required a stronger trypsin concentration and longer treatment time. To passage vitamin C–treated MEFs, trypsin treatment was instead performed for 20 minutes at 37°C using 0.25% Trypsin (with 0.1% EDTA) (Thermo Fisher Scientific Inc.). Total cell culture medium volumes used: 10 ml for a 10 cm plate, 6 ml for a 60 mm plate, 2 ml per well in a 6-well plate, and 0.8 ml per well in a 12-well plate. To treat cells with compounds, they were added to the MEFs' cell culture medium at the specified concentration. Compounds used include ascorbic acid (Vitamin C), L-NG-nitroarginine methyl ester (L-NAME), and 2,6-di-tert-butyl-4-methylphenol (BHT).

For compound library screening, the SCREEN-WELL® REDOX Library (Enzo Life Sciences Inc., BML-2835) was used. From fully confluent plates, *Sod1*$^{-/-}$ MEFs were passaged to 12-well plates at a 1/4 dilution and incubated in the presence of vitamin C (100 μM) and a library's compound (10 μM). Each well contained a final volume of 0.8 ml. Two vitamin C–only wells and one untreated well were also prepared for each 12-well plate. During the initial seeding of MEFs onto plates, treatments were added at the specified concentrations; this is considered treatment day 0. MEFs had to be passaged every 3 or 4 days in order to renew treatments. This frequency was chosen due to these considerations: MEFs used were usually fully confluent every ~3 days, quantities of the library's compounds were limited, and treatments had to be renewed frequently enough to see an effect. Since *Sod1*$^{-/-}$ MEFs treated with vitamin C alone could not reach full confluence due to the frequency of vitamin C's renewal, vitamin C's concentration was increased from 100 to 200 μM at treatment day 5.

Additionally, cell culture media and vitamin C was renewed every 4 days for all vitamin C–treated MEFs even if they did not reach full confluence. Cell culture media was also renewed every 4 days for untreated MEFs, but vitamin C was not added. Library compounds were still only renewed after a cell passage.

Cell observation was done using the Leica DM IL inverted light microscope. Photographs were taken by placing a camera on the eyepiece. Total magnification was 100x, with objective magnification at 10x (Objective type: C Plan, Semi-Planachromat. Numerical Aperture: 0.22. Ph1 phase contrast condenser annulus. Leica Article Number 506078) and eyepiece magnification at 10x (Field of view: 18. Leica Article Number 527001). To enhance the visibility of cells in figures containing microscopy images of cells, these variables were modified: brightness, contrast, and sharpness. Each modified variable was applied equally throughout the figure.

Genotyping and PCR

DNA extraction was performed on heads from 12.5 or 13.5-day-old *Sod1*$^{-/-}$ mouse embryos using a DNA Isolation Kit (EZ BioResearch) and following the manufacturer's instructions. PCR was then performed on the eluted DNA. Each PCR reaction was done in 25 µl final volume using OneTaq® DNA Polymerase (New England BioLabs), ~120–800 ng of template DNA, and forward and reverse primers (final concentration: 0.4 µM) that were designed to specifically detect either the mutant or the wild-type allele of the *Sod1* gene. Primer sequences were as follows: *Sod1*-MUTANT forward sequence: 5'-CCG TCT TTT GGC AAT GTG AGG-3'; *Sod1*-MUTANT reverse sequence: 5'-TGG GGT ACC TTC TGG GCA TCC-3'; *Sod1*-WILDTYPE forward sequence: 5'-GGC GGA TGA AGA GAG GTG AGC-3'; *Sod1*-WILDTYPE

reverse sequence: 5'-ATT GGC CAC ACC GTC CTT TCC-3'. The PCR cycles used these settings: initial denaturation at 94°C for 30 seconds, 30–35 cycles of denaturation at 94°C for 30 seconds, annealing at 55°C for 30 seconds, and extension at 68°C for 1 minute. Lastly, final extension was set at 68°C for 5 minutes. The amplified products were 350 bp for the mutant allele and 786 bp for the wild-type allele.

Crystal violet staining

After the removal of cell culture media, cells were washed once with PBS before adding enough crystal violet solution (0.05% w/v crystal violet, 1% formaldehyde, and 1% methanol in 1X PBS) to cover the surface of each plate or well. The plates were then incubated at room temperature overnight with gentle agitation. Afterwards, all traces of dye were removed, then each well or plate was washed with distilled water, and cells were left to dry overnight. The next day, plates were photographed.

Research Findings

Successful validation of the Cre-*loxP* protocol using *Mclk1*$^{fl/fl}$ MEFs

Previous work from our lab indicated that after the complete loss of SOD1, MEFs had a decreased growth rate and eventually died *in vitro*. For the inactivation of *Sod1* floxed alleles, if the efficiency of Cre-mediated recombination is not close to 100%, Cre-mediated *Sod1* KO MEFs (*Sod1*$^{\Delta/\Delta}$-Cre) will eventually be overrun by the incompletely recombined *Sod1*$^{fl/fl}$-Cre or *Sod1*$^{fl/\Delta}$-Cre MEFs. Therefore, it is crucial to validate and optimize the efficiency of the Cre-*loxP* recombination system before using it to generate *Sod1* KO cells. For this purpose, *Mclk1*$^{fl/fl}$ MEFs were used. Previous work from our lab has shown that *Mclk1*/*Coq7* KO MEFs were able to grow and divide under standard cell culture conditions, at a rate comparable to that of unrecombined wild-type controls. Therefore, it is preferable to use *Mclk1*$^{fl/fl}$ MEFs to verify if the Cre-mediated KO protocol performs acceptably or not.

No detectable MCLK1 was found 41 days postinfection (22 days after puromycin selection) in *Mclk1*$^{fl/fl}$ MEFs infected with pBABE-puro-Cre retroviruses, indicating a prolonged and highly efficient Cre-mediated gene KO (Figure 1). For the controls, the same *Mclk1*$^{fl/fl}$ MEFs were used, but they were infected with retroviruses containing the empty vector pBABE-puro instead. Since the Cre-mediated gene KO protocol was able to produce a highly pure cell population of *Mclk1* KO MEFs and maintained the *Mclk1* KO even after an extended period, the experiments proceeded with *Sod1*$^{fl/fl}$ MEFs.

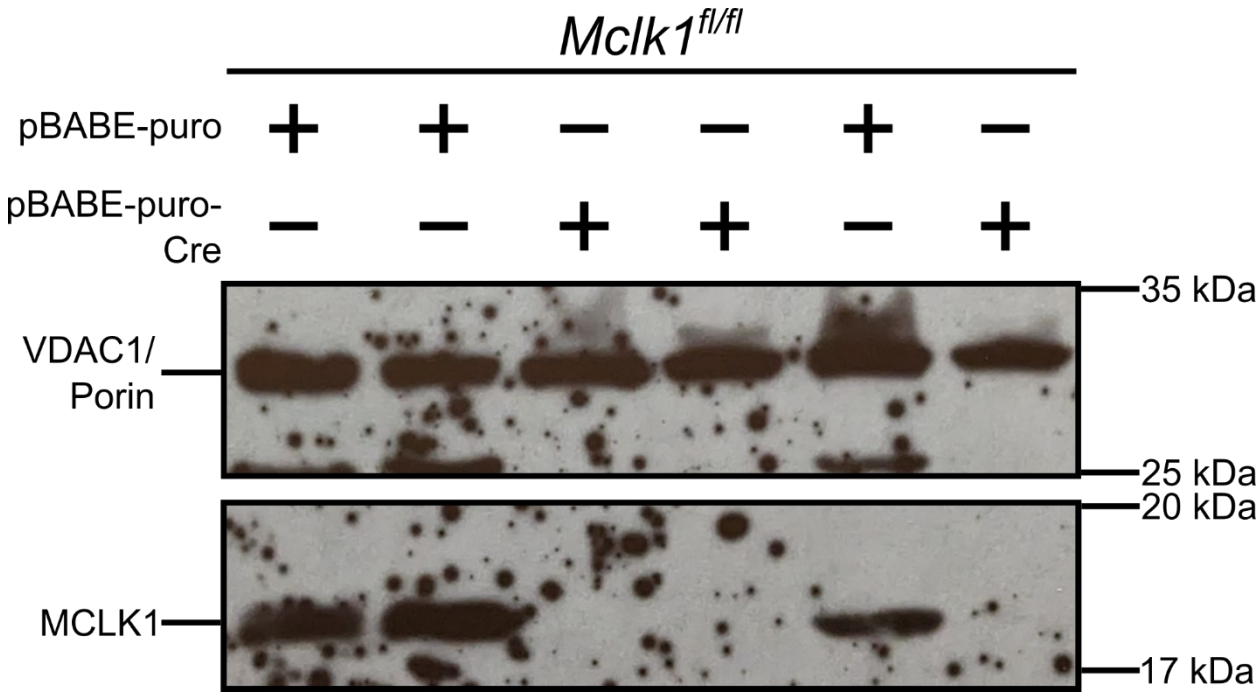

Figure 1. Undetectable MCLK1 levels after Cre-mediated *Mclk1* KO in *Mclk1*$^{fl/fl}$ MEFs. Immunoblot analysis of MCLK1 in *Mclk1*$^{fl/fl}$ MEFs infected with pBABE-puro or pBABE-puro-Cre retroviruses. MEFs were sampled 41 days postinfection (22 days after puromycin selection). Lanes #1, #2, and #5 are technical replicates of *Mclk1*$^{fl/fl}$ MEFs infected with pBABE-puro retroviruses, and lanes #3, #4, and #6 are technical replicates of *Mclk1*$^{fl/fl}$ MEFs infected with pBABE-puro-Cre retroviruses. In other words, each sample of *Mclk1*$^{fl/fl}$ MEFs originated from the same embryo, but cells were then distributed to different wells and subsequently infected. Each lane was loaded with 75 μg of the sample's total protein. Mitochondrial outer membrane porin VDAC1 was used as a loading control. VDAC1 primary antibody dilution: 1/1000. MCLK1 primary antibody dilution: 1/1500. Primary antibodies were incubated over 1 day. Horseradish peroxidase (HRP)–conjugated anti-rabbit secondary antibody dilution: 1/2000. These cells were also collected 25 days postinfection (6 days after puromycin selection) and showed similar results.

Generation of *Sod1* KO MEFs by Cre-*loxP* recombination

Sod1$^{\Delta/\Delta}$-Cre MEFs were generated by infecting *Sod1*$^{fl/fl}$ MEFs with pBABE-puro-Cre retroviruses. For the controls, the same *Sod1*$^{fl/fl}$ MEFs were used, but they were infected with

retroviruses containing the empty vector pBABE-puro instead. Inactivation of *Sod1* in *Sod1*$^{fl/fl}$ MEFs upon infection with Cre retroviruses was confirmed by immunoblot analysis (Figure 2). Complete loss of SOD1 was observed 9 days postinfection (4 days after puromycin selection), confirming that the conversion of *Sod1*$^{fl/fl}$ MEFs' floxed alleles into their null form *Sod1*$^{\Delta/\Delta}$ was virtually complete. Of note, there is a very faint ~17 kDa band in lane #4.

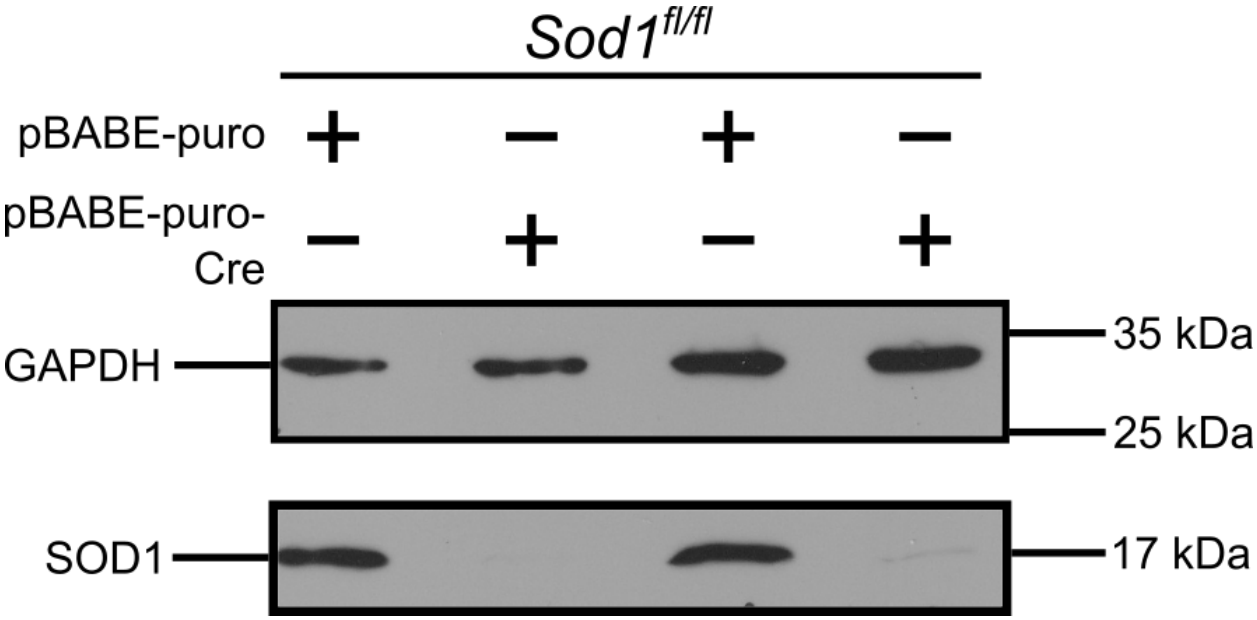

Figure 2. Undetectable SOD1 levels after Cre-mediated *Sod1* KO in *Sod1*$^{fl/fl}$ MEFs. Immunoblot analysis of SOD1 in *Sod1*$^{fl/fl}$ MEFs infected with pBABE-puro or pBABE-puro-Cre retroviruses. MEFs were sampled 9 days postinfection (4 days after puromycin selection). Each lane was loaded with 75 μg of the sample's total protein. Cytosolic protein GAPDH was used as a loading control. GAPDH primary antibody dilution: 1/4000. SOD1 primary antibody dilution: 1/2000. Primary antibodies were incubated over 2 days. HRP-conjugated anti-rabbit secondary antibody dilution: 1/2000. Including this representative result, this result was observed 2 times: 2 were technical replicates using the same uninfected *Sod1*$^{fl/fl}$ MEFs, but the infection protocol was performed at different days. Each replicate had 2 repeats: from the same infection protocol, *Sod1*$^{fl/fl}$ MEFs were passaged to 4 wells, then 2 wells were infected with pBABE-puro retroviruses, and 2 wells were infected with pBABE-puro-Cre retroviruses. These are represented by the different lanes: lanes #1 and #3 are repeats of

Sod1$^{fl/fl}$ MEFs' infection with pBABE-puro retroviruses, and lanes #2 and #4 are repeats of *Sod1*$^{fl/fl}$ MEFs' infection with pBABE-puro-Cre retroviruses.

Sod1$^{\Delta/\Delta}$-Cre MEFs experienced decreased growth, decreased confluence, were more sparsely populated, and some cells looked enlarged and flatter (Figure 3). Unexpectedly, continued maintenance of *Sod1*$^{\Delta/\Delta}$-Cre MEFs in cell culture appeared to result in a significantly improved growth rate, similar to wild-type MEFs' growth rate (data not shown). The suspected cause of this recovery was likely due to *Sod1*$^{\Delta/\Delta}$-Cre MEFs being overtaken by the incompletely recombined MEFs, since Cre-mediated recombination likely did not happen in 100% of the targeted *Sod1*$^{fl/fl}$ cell population. In that case, the incompletely recombined MEFs survived puromycin selection and their survival and proliferation advantage allowed them to rapidly overgrow the *Sod1*$^{\Delta/\Delta}$-Cre MEFs. Although puromycin was used to select for Cre-infected cells, it is possible that it did not entirely eliminate the incompletely recombined MEFs since pBABE-puro-Cre retroviruses can incorporate enough puromycin resistance but insufficient Cre expression to completely inactivate *Sod1* in *Sod1*$^{fl/fl}$ MEFs, resulting in the survival of *Sod1*$^{fl/fl}$-Cre and *Sod1*$^{fl/\Delta}$-Cre MEFs.

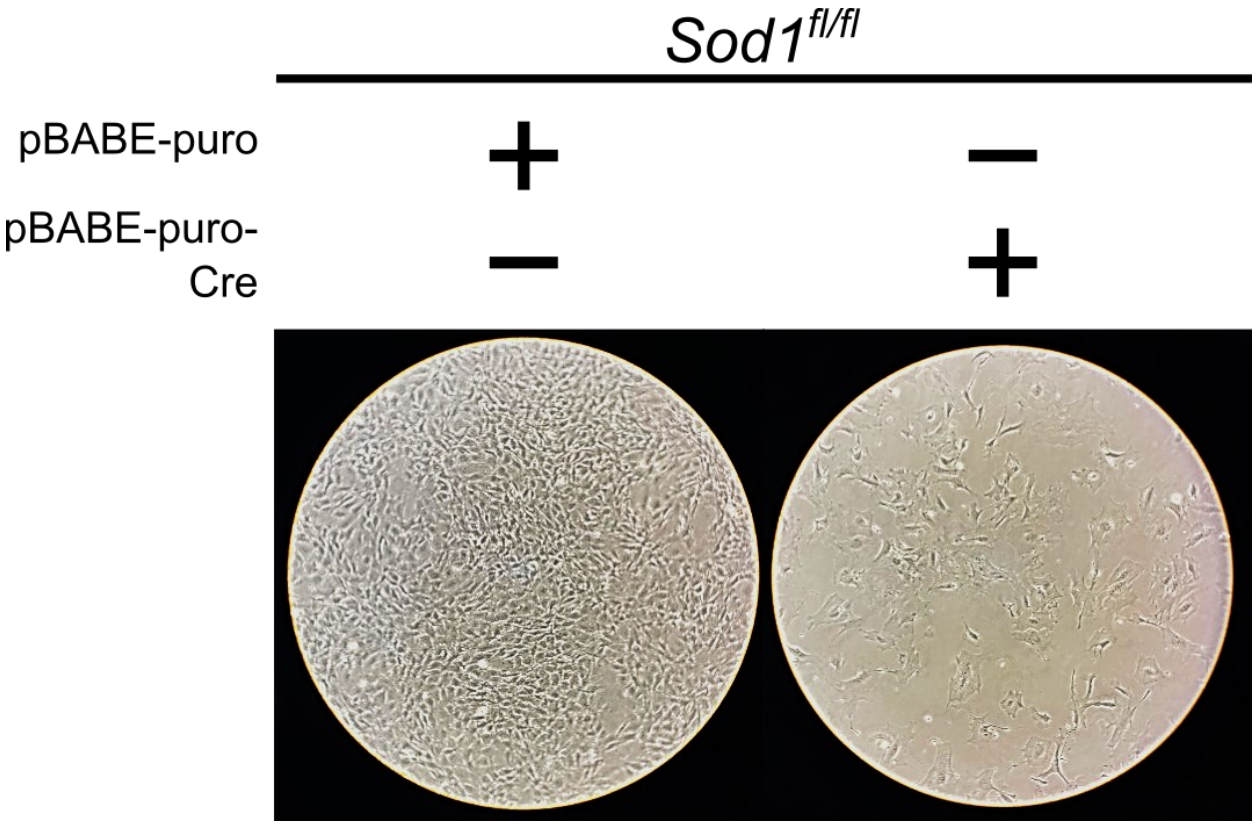

Figure 3. Decreased confluence and enlarged phenotype after Cre-mediated *Sod1* KO in *Sod1*$^{fl/fl}$ MEFs. Microscopy pictures of *Sod1*$^{fl/fl}$ MEFs infected with pBABE-puro or pBABE-puro-Cre retroviruses. 7 days postinfection, MEFs were 80–90% confluent, routinely passaged at a 1/6 dilution, then photographed 3 days later. MEFs shown were 10 days postinfection (2–3 days after puromycin selection). Including this representative result, this result was observed 5 times: 4 were technical replicates using the same uninfected *Sod1*$^{fl/fl}$ MEFs, but the infection protocol was performed at different days. The last replicate used *Sod1*$^{fl/fl}$ MEFs isolated from another embryo and was therefore the second biological replicate. Each replicate had 2 repeats: from the same infection protocol, *Sod1*$^{fl/fl}$ MEFs were passaged to 4 wells, then 2 wells were infected with pBABE-puro retroviruses, and 2 wells were infected with pBABE-puro-Cre retroviruses.

To verify this, another experiment was performed to examine SOD1 levels in *Sod1*$^{fl/fl}$ MEFs infected with pBABE-puro-Cre retroviruses, but this time at multiple time points. 7 days postinfection (2 days after puromycin selection), *Sod1* expression was largely lost, but

already started to recover in the cell population (Figure 4). However, 18 days postinfection, *Sod1* expression was completely recovered and was reached levels similar to the wild-type controls (Figure 4). *Sod1*$^{\Delta/\Delta}$-Cre MEFs from this experiment likely also had a decreased survival or proliferation rate, which might explain why they were overtaken quickly by the incompletely recombined MEFs. Lastly, an additional uninfected control was added to verify if the infection itself influenced *Sod1* expression (Figure 4). As expected, this was not the case since the uninfected control had the same SOD1 levels as the *Sod1*$^{fl/fl}$ MEFs infected with pBABE-puro retroviruses.

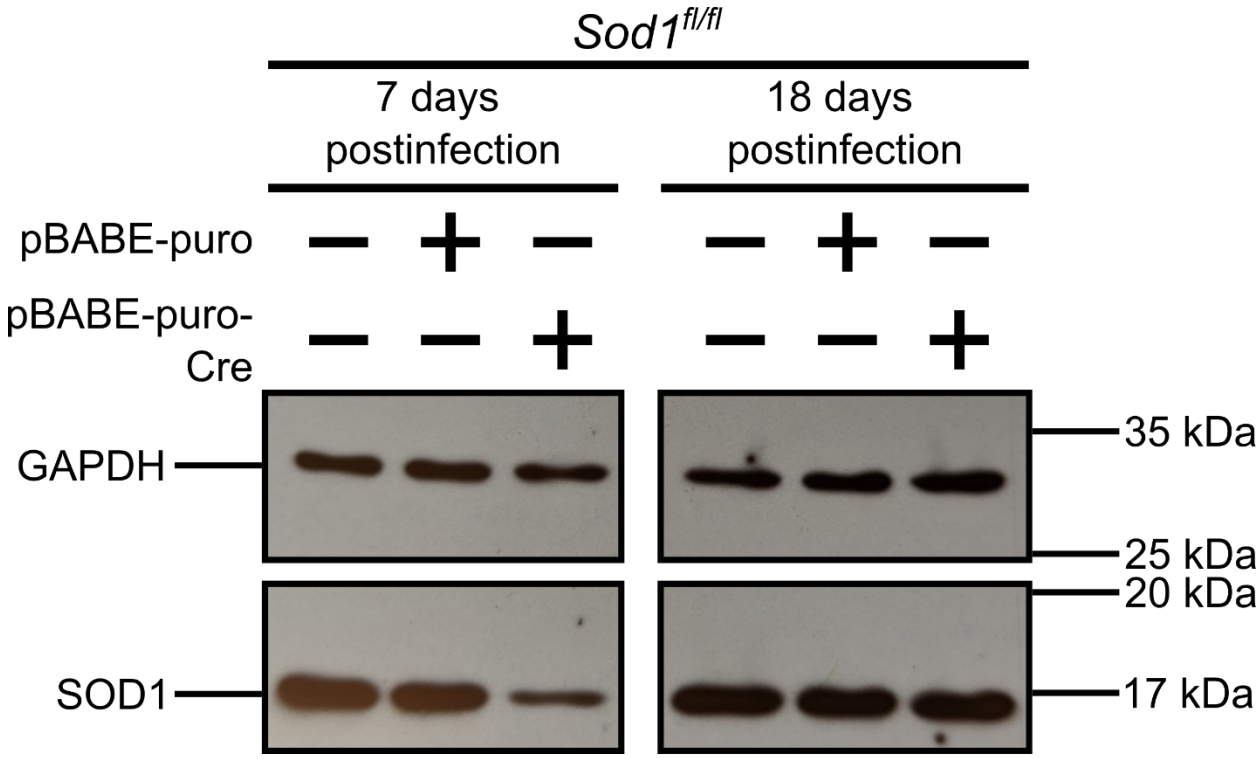

Figure 4. Recovery of *Sod1* expression over time after Cre-mediated *Sod1* KO in *Sod1*$^{fl/fl}$ MEFs. Immunoblot analysis of SOD1 at multiple time points in *Sod1*$^{fl/fl}$ MEFs infected with pBABE-puro or pBABE-puro-Cre retroviruses, or uninfected. MEFs were sampled 7 days postinfection (2 days after puromycin selection) and 18 days postinfection (13 days after puromycin selection). All *Sod1*$^{fl/fl}$ MEFs originated from the same embryo. Each lane was

loaded with 30 μg of the sample's total protein. Cytosolic protein GAPDH was used as a loading control. GAPDH primary antibody dilution: 1/3000. SOD1 primary antibody dilution: 1/750. Primary antibodies were incubated over 1 day. HRP-conjugated anti-rabbit secondary antibody dilution: 1/2000. Of note, SOD1 primary antibody's concentration was increased but incubated over one day only. This change was necessary since it was suspected that incubating primary antibodies over two days frequently caused high background staining on the films. The dilution was chosen based on previous experiments (data not shown). Including this representative result, this result was observed 3 times: 2 were technical replicates using the same uninfected *Sod1*$^{fl/fl}$ MEFs, but the infection protocol was performed at different days. The last result used *Sod1*$^{fl/fl}$ MEFs isolated from another embryo and was therefore the second biological replicate. Each replicate had 2 repeats: from the same infection protocol, *Sod1*$^{fl/fl}$ MEFs were passaged to 4 wells, then 2 wells were infected with pBABE-puro retroviruses, and 2 wells were infected with pBABE-puro-Cre retroviruses.

Taken together, these results suggest that acute loss of *Sod1 in vitro* leads to severely impaired cell proliferation and survival in MEFs. However, since *Sod1*$^{\Delta/\Delta}$-Cre MEFs were gradually being overtaken by the incompletely recombined MEFs, it would be challenging to maintain a highly pure *Sod1*$^{\Delta/\Delta}$-Cre cell population for a sufficient period of time to allow for proper testing of treatments and the observation of their effects on *Sod1* KO MEFs' phenotypes.

Vitamin C increased Cre-mediated *Sod1* KO MEFs' survival, but not L-NAME

Previous work from our lab has found that vitamin C improved the growth and survival of *Sod1*$^{-/-}$ MEFs (unpublished data). Therefore, in this thesis, vitamin C was also tested to see its effects on *Sod1*$^{\Delta/\Delta}$-Cre MEFs. Despite the flaws of the Cre-*loxP* recombination method, *Sod1*$^{\Delta/\Delta}$-Cre MEFs were still used for this experiment to observe the treatments' effects on these cells, before replacing this method with a better alternative. Treatments were

performed by adding vitamin C directly to cell culture media for a final concentration of 400 μM. Treatments were renewed every 1–2 days by renewing cell culture media and adding treatments at the same final concentration. *Sod1*$^{\Delta/\Delta}$-Cre MEFs treated with vitamin C (400 μM) had a visibly increased confluence compared to untreated *Sod1*$^{\Delta/\Delta}$-Cre MEFs (Figure 5).

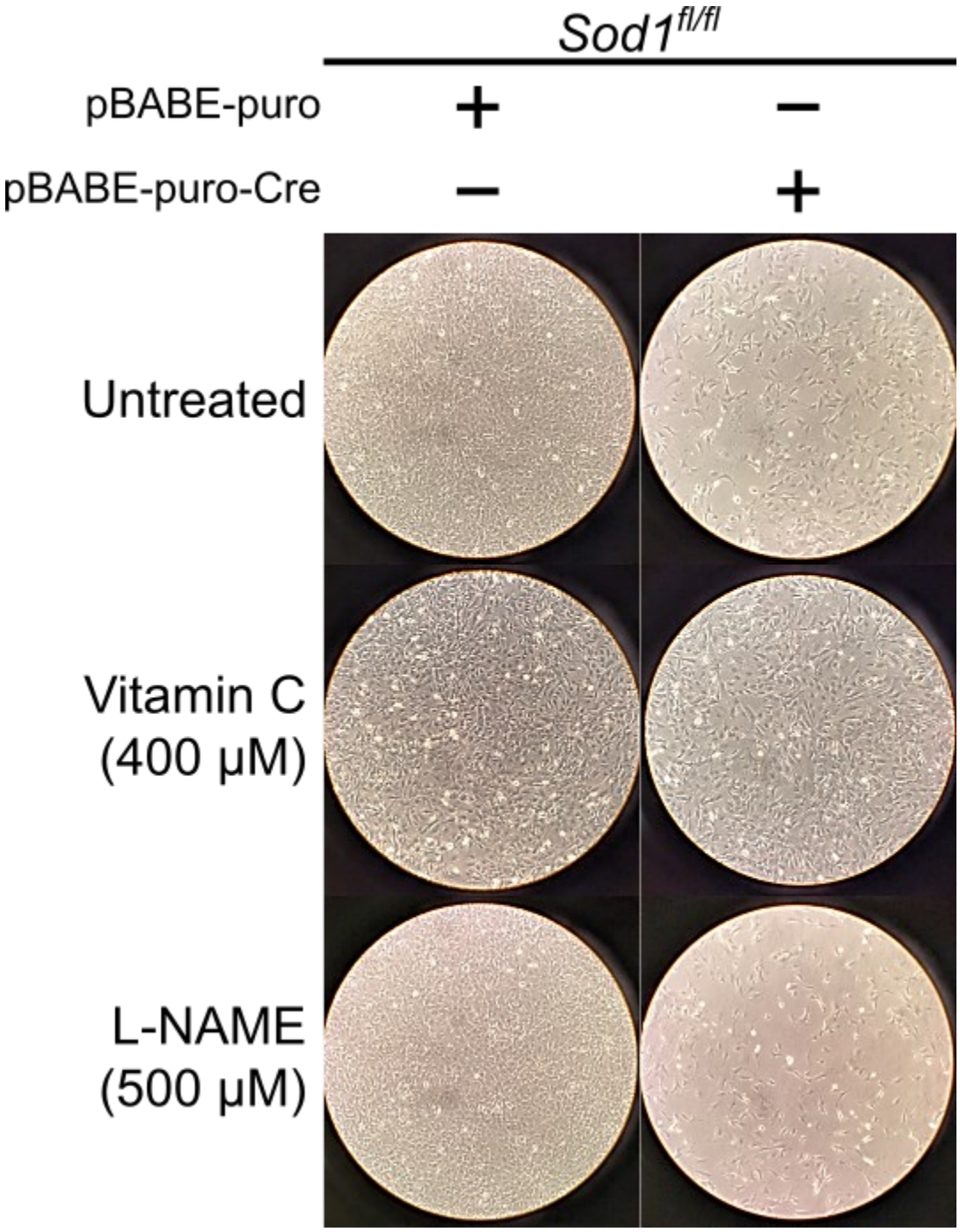

Figure 5. Increased confluence of *Sod1*$^{\Delta/\Delta}$-Cre MEFs after vitamin C treatment, but not L-NAME. Microscopy pictures of *Sod1*$^{fl/fl}$ MEFs infected with pBABE-puro or pBABE-puro-Cre retroviruses, and treated with vitamin C (400 μM) or L-NAME (500 μM) or untreated. 10 days postinfection (5 days after puromycin selection), MEFs were fully confluent, were routinely passaged at a 1/8 dilution, then photographed 4 days later. MEFs shown were 14 days postinfection (9 days after puromycin selection). PBS wash and the renewal of cell culture media and treatments were performed every 1–2 days. Including this representative result, this result was observed 2 times: 2 were technical replicates using the same uninfected *Sod1*$^{fl/fl}$ MEFs, but the infection protocol was performed at different days. Each replicate had 2 repeats: from the same infection protocol, *Sod1*$^{fl/fl}$ MEFs were passaged to 4 wells, then 2 wells were infected with pBABE-puro retroviruses, and 2 wells were infected with pBABE-puro-Cre retroviruses.

There is a possibility that part of the toxicity induced by the loss of *Sod1* is caused by increased peroxynitrite ($ONOO^-$) production, resulting from the reaction of nitric oxide ($^\bullet NO$) with the increased levels of superoxide ($O_2^{\bullet-}$) caused by the lack of SOD1. Therefore, L-NG-nitroarginine methyl ester (L-NAME) was another treatment chosen to test its ability in improving the survival of *Sod1*$^{\Delta/\Delta}$-Cre MEFs. L-NAME inhibits all isoforms of nitric oxide synthase (NOS) and consequently reduces $^\bullet NO$ production. Therefore, it should protect against excessive $ONOO^-$ production by lowering the quantity of available $^\bullet NO$ that can react with $O_2^{\bullet-}$. However, no obvious difference in confluence was found between 500 μM L-NAME–treated *Sod1*$^{\Delta/\Delta}$-Cre MEFs and wild-type MEFs (Figure 5). Similar results were obtained with L-NAME at 250 μM (data not shown). Therefore, excessive $ONOO^-$ is unlikely to be the main contributor of the slow proliferation and poor survival of *Sod1*$^{\Delta/\Delta}$-Cre MEFs *in vitro*.

Vitamin C increased germline *Sod1* KO MEFs' survival for a few weeks

Due to the difficulty in maintaining a cell population of pure *Sod1*$^{\Delta/\Delta}$-Cre MEFs generated by the Cre-*loxP* system (Figure 4), an alternative way to inactivate SOD1 was chosen. *Sod1* KO MEFs were instead isolated from the embryos of germline *Sod1* KO mice (*Sod1*$^{-/-}$). To identify the genotype of embryos derived from heterozygous crosses, the embryos' heads were used for genotyping. *Sod1*$^{-/-}$ MEFs were identified by the detection of their shorter, mutant *Sod1* sequence, and the undetectable wild-type *Sod1* sequence (Figure 6).

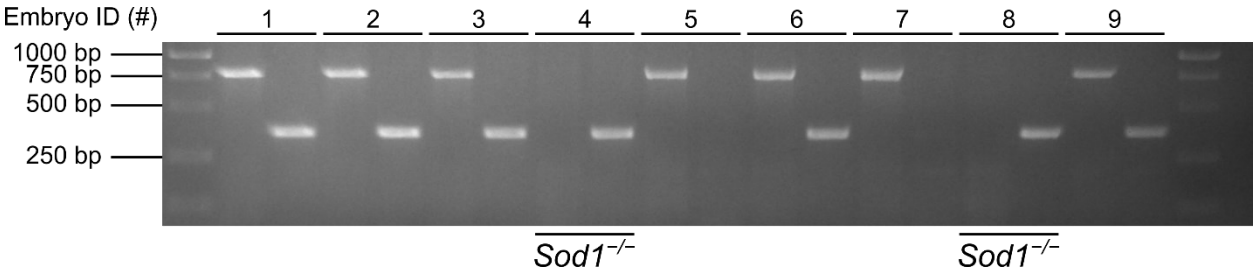

Figure 6. Representative genotyping image using PCR and agarose gel electrophoresis to identify *Sod1*$^{-/-}$ MEFs. For each embryo's DNA, PCR products were amplified using primers specific for wild-type *Sod1* (left lane) and mutant *Sod1* sequences (right lane). Each embryo was identified by a number from 1 to 9. Wild-type *Sod1*'s sequence length is 786 bp. Mutant *Sod1*'s sequence length is 350 bp.

Consistent with previously published work and the previous work of our lab, untreated *Sod1*$^{-/-}$ MEFs displayed growth failure and eventual death after only a few days in cell culture (Figure 7). To determine the rescue effect of vitamin C on *Sod1*$^{-/-}$ MEFs, different concentrations of vitamin C were tested, up to 400 μM. Similarly to what was observed in previous studies, vitamin C visibly increased *Sod1*$^{-/-}$ MEFs' survival (Figure 7). Vitamin C started to have a beneficial effect on *Sod1*$^{-/-}$ MEFs' survival at 25 μM and was most effective at 200 μM. At 400 μM, vitamin C was not as beneficial to *Sod1*$^{-/-}$ MEFs' survival compared to

vitamin C at 200 µM. Alongside the *Sod1*$^{-/-}$ experiment, the same experiment was performed with *Sod1*$^{+/+}$ MEFs instead, but no visible difference was observed between untreated and vitamin C–treated *Sod1*$^{+/+}$ wells (data not shown). One well of *Sod1*$^{+/+}$ MEFs was displayed for comparison.

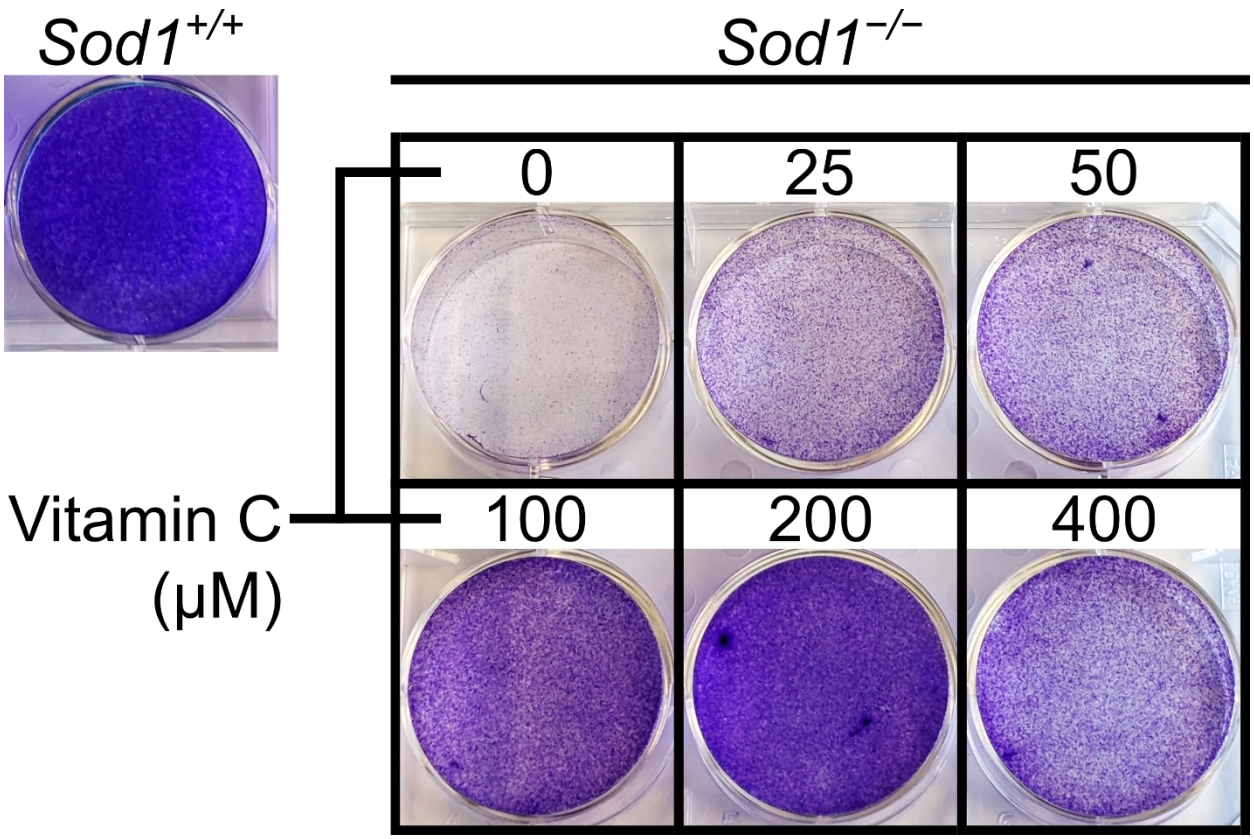

Figure 7. Increased survival of *Sod1*$^{-/-}$ MEFs after vitamin C treatment at 25 µM or higher. Crystal violet staining of *Sod1*$^{-/-}$ MEFs treated with vitamin C at different concentrations. 8 days after MEFs' isolation (4 days since the start of vitamin C treatment), MEFs were fully confluent and routinely passaged at a 1/10 dilution. 4 days later, crystal violet staining was performed since cell confluence properly represented what was observed consistently. Stained MEFs shown were 12 days after MEFs' isolation (8 days since the start of vitamin C treatment). PBS wash and the renewal of cell culture media and treatments were performed every day. Including this representative result, this result was observed 3 times: 3 were biological replicates. For *Sod1*$^{+/+}$ MEFs, only one replicate was done.

Although optimal vitamin C concentration drastically rescued *Sod1*$^{-/-}$ MEFs' survival and proliferation, vitamin C–treated *Sod1*$^{-/-}$ MEFs eventually stopped proliferating after ~39 treatment days (Figure 8). On treatment day 39, vitamin C–treated *Sod1*$^{-/-}$ MEFs were clearly enlarged and flattened, which is reminiscent of the senescent phenotype in MEFs. On treatment day 48, vitamin C–treated *Sod1*$^{-/-}$ MEFs were extremely enlarged and flattened. In contrast, wild-type MEFs were still able to proliferate normally (Figure 8). Therefore, vitamin C can extend *Sod1*$^{-/-}$ MEFs' survival and proliferation for a few weeks *in vitro* but it cannot rescue their long-term survival and proliferation. Of note, since untreated *Sod1*$^{-/-}$ MEFs quickly died without vitamin C, 200 μM vitamin C–treated *Sod1*$^{-/-}$ MEFs were used to replace them after every cell passage, but the untreated wells did not receive vitamin C afterwards. This untreated control was useful to demonstrate that *Sod1*$^{-/-}$ MEFs cannot survive without vitamin C, but also to ensure that the improved confluence of vitamin C–treated *Sod1*$^{-/-}$ MEFs was not caused by contamination from the growth of wild-type MEFs.

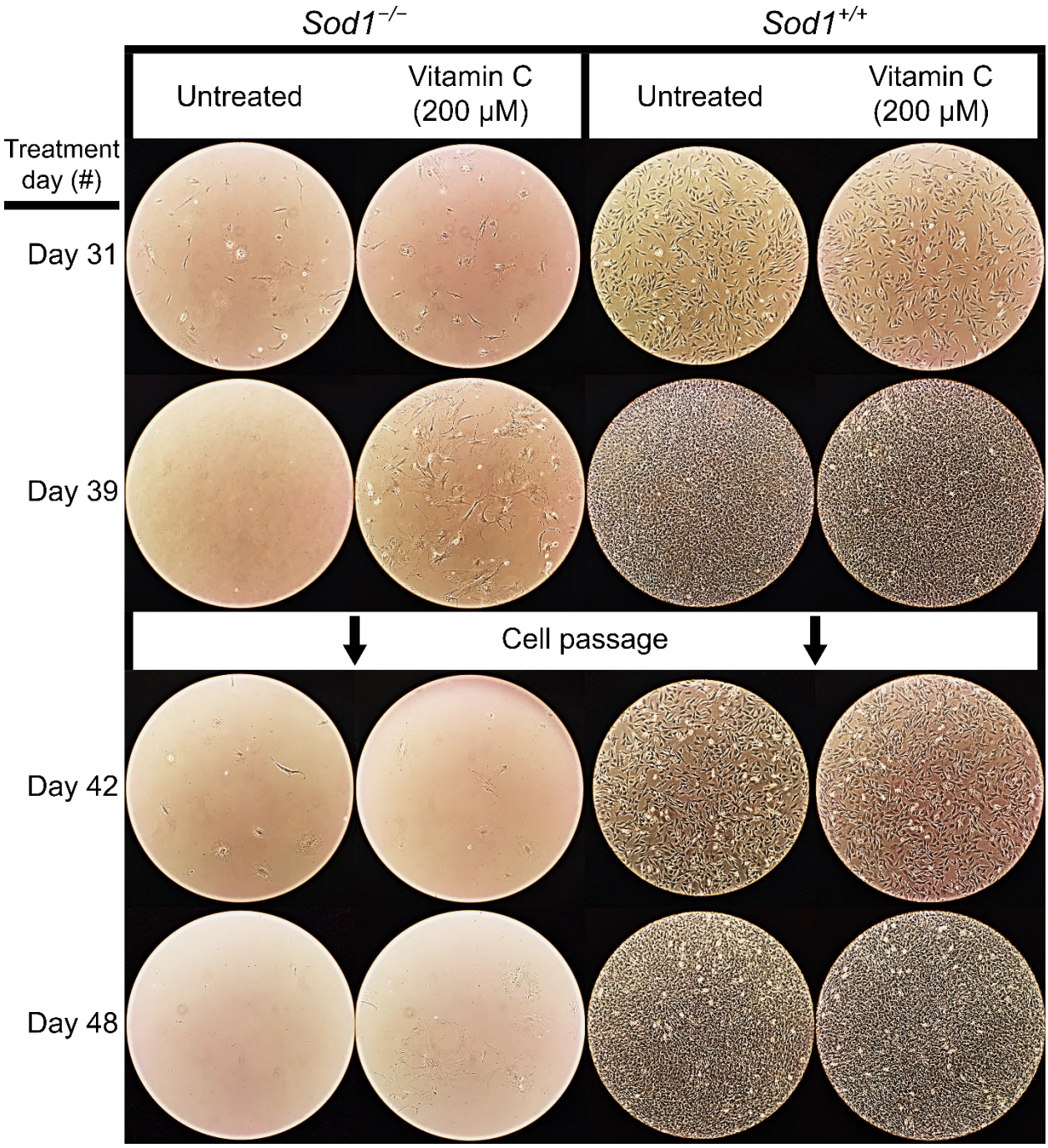

Figure 8. Proliferation arrest in vitamin C–treated *Sod1*$^{-/-}$ MEFs. Microscopy pictures of *Sod1*$^{-/-}$ MEFs between treatment days 31 and 48. Treatment day 0 (4 days after MEFs' isolation) started when vitamin C was first added to *Sod1*$^{-/-}$ and *Sod1*$^{+/+}$ MEFs. On treatment day 30 (34 days after MEFs' isolation), vitamin C–treated MEFs were fully confluent and routinely passaged at a 3/20 dilution (~1/7) to the untreated and vitamin C–treated wells.

Cells were photographed on treatment day 31 and every 2 days afterwards. On treatment day 41 (45 days after MEFs' isolation), cells were passaged again, as indicated in the figure. PBS wash and the renewal of cell culture media and treatments were performed every 2 days. Including this representative result, this result was observed 2 times: 2 were biological replicates. For *Sod1*$^{+/+}$ MEFs, only one replicate was done.

Compound library screening identified BHT as a possible vitamin C potentiator

Previous work from our lab screened the SCREEN-WELL® REDOX library for the identification of compounds that can improve *Sod1*$^{-/-}$ MEFs' survival *in vitro*. The library contains 84 compounds with defined prooxidant or antioxidant activity. None of the library's compounds were found to mitigate *Sod1*$^{-/-}$ MEFs' poor survival, except for vitamin C. In this thesis, the same library was screened but in combination with vitamin C in order to identify compounds that can further improve vitamin C–treated *Sod1*$^{-/-}$ MEFs' survival, compared to treating with vitamin C alone. The primary screening identified one potential hit: 2,6-di-tert-butyl-4-methylphenol, also known as BHT (Figure 9). Despite the low amounts of vitamin C during the first four days, combined treatments of vitamin C (100 μM) and BHT (10 μM) were still able to clearly have a positive effect on *Sod1*$^{-/-}$ MEFs' confluence, compared to *Sod1*$^{-/-}$ MEFs treated with vitamin C alone (Figure 9). This observation persisted even after the next cell passage. As an additional control, untreated *Sod1*$^{-/-}$ MEFs were also prepared, but MEFs from these wells died after only a few days (data not shown).

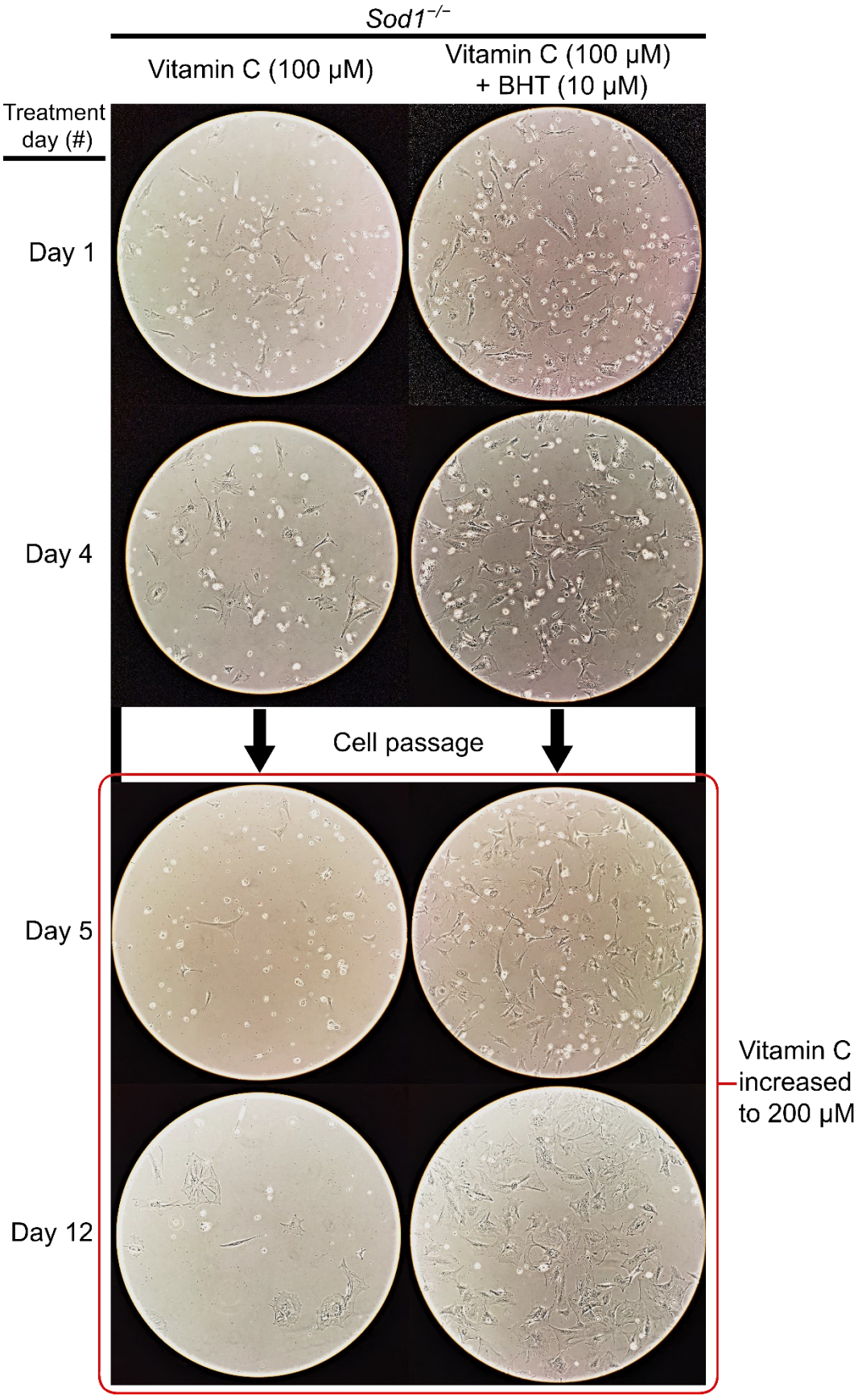
Sod1−/−
Vitamin C (100 μM)
Vitamin C (100 μM) + BHT (10 μM)
Treatment day (#)
Day 1
Day 4
Cell passage
Day 5
Day 12
Vitamin C increased to 200 μM

Figure 9. Increased confluence of *Sod1*$^{-/-}$ MEFs after the combined treatment of vitamin C and BHT. Microscopy pictures of *Sod1*$^{-/-}$ MEFs treated with vitamin C alone (100 μM) or vitamin C (100 μM) combined with BHT (10 μM). On treatment day 0 (4 days after MEFs' isolation), MEFs were fully confluent, passaged at a 1:4 dilution to a 12-well plate, then the treatments were added. On treatment day 1 and every day afterwards, cells were photographed. Cells were routinely passaged on treatment day 4 (8 days after MEFs' isolation). Starting on treatment day 5, vitamin C concentration was increased from 100 μM to 200 μM and renewed every 4 days. Since this was an initial screening experiment, this was only performed once.

BHT did not enhance vitamin C–treated germline *Sod1* KO MEFs' survival

To confirm BHT's ability in enhancing vitamin C–treated *Sod1*$^{-/-}$ MEFs' survival, treatments were performed again but with additional controls. This time, *Sod1*$^{-/-}$ MEFs were treated with BHT alone or in combination with vitamin C. Various concentrations of BHT were first tested in wild-type MEFs and no obvious toxicity was observed until 75 μM (data not shown). Therefore, concentrations of 50 μM and 75 μM were chosen. Once more, since untreated *Sod1*$^{-/-}$ MEFs died early after isolation, fully confluent 200 μM vitamin C–treated MEFs were necessary to replace them after every cell passage. The same thing was done for *Sod1*$^{-/-}$ MEFs treated with BHT alone, since BHT alone could not rescue *Sod1*$^{-/-}$ MEFs' survival at all (Figure 10). Unfortunately, BHT could not improve vitamin C–treated *Sod1*$^{-/-}$ MEFs' survival more than what was already observed with vitamin C alone (Figure 10). This was unlike what was previously observed in the compound library screen (Figure 9). BHT at 75 μM appeared to be slightly detrimental to vitamin C–treated *Sod1*$^{-/-}$ MEFs (Figure 10), just like what was previously observed with wild-type MEFs treated with BHT at 75 μM. Alongside the *Sod1*$^{-/-}$ experiment, the same experiment was performed with *Sod1*$^{+/+}$ MEFs instead, but no visible

difference was observed between treated and untreated *Sod1*$^{+/+}$ cells (data not shown). One well of *Sod1*$^{+/+}$ MEFs was displayed for comparison.

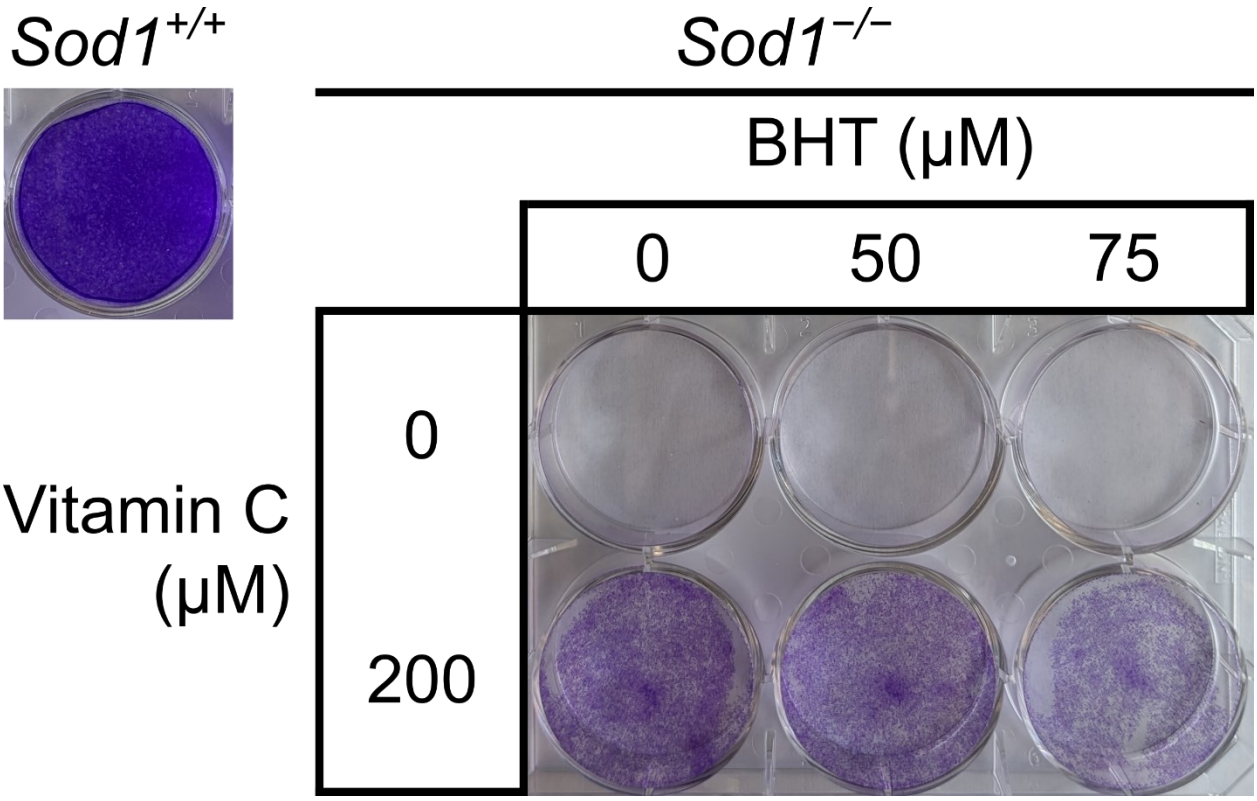

Figure 10. BHT at 50 or 75 μM did not further enhance vitamin C–treated *Sod1*$^{-/-}$ MEFs' survival. Crystal violet staining of *Sod1*$^{-/-}$ MEFs treated with vitamin C and BHT at different concentrations. 53 days after MEFs' isolation (49 days since the start of treatments), MEFs treated with vitamin C alone (200 μM) were fully confluent, routinely passaged at a 3/20 dilution (~1/7) to each well, then treatments were routinely performed at the indicated concentrations. After 9 more days, crystal violet staining was performed since the confluences properly represented what was observed consistently. Stained MEFs shown were 62 days after MEFs' isolation (58 days since the start of treatments). PBS wash and the renewal of cell culture media and treatments were performed every 2 days. Including this representative result, this result was observed 3 times: 3 were biological replicates. For *Sod1*$^{+/+}$ MEFs, only one replicate was done.

One possible reason as to why combined treatments of vitamin C and BHT did not further enhance *Sod1*$^{-/-}$ MEFs' survival unlike what was previously observed (Figure 9) is the difference in concentration. BHT at 50 µM was determined to not be toxic, but that does not necessarily mean 50 µM was the optimal concentration that could improve *Sod1*$^{-/-}$ MEFs' survival. In the compound library screen where an improvement of vitamin C–treated *Sod1*$^{-/-}$ MEFs' survival was observed, 10 µM BHT was used (Figure 9) and this could be the optimal concentration. Therefore, the same experiment was repeated, but with BHT at 10 and 20 µM instead. However, even at these lower concentrations, BHT still had no beneficial effects on the survival of *Sod1*$^{-/-}$ MEFs, with or without vitamin C (Figure 11).

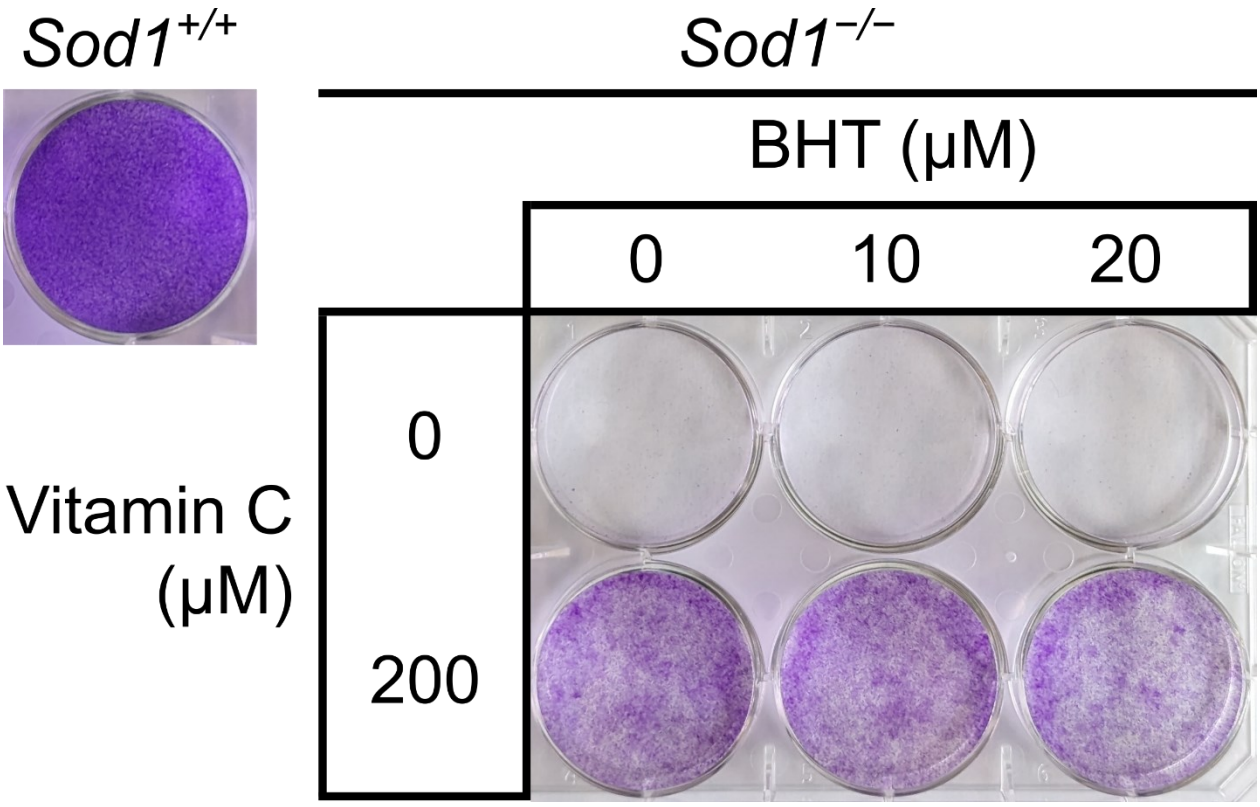

Figure 11. BHT at 10 or 20 µM did not further enhance vitamin C–treated *Sod1*$^{-/-}$ MEFs' survival. Crystal violet staining of *Sod1*$^{-/-}$ MEFs treated with vitamin C and BHT at different concentrations. 15 days after MEFs' isolation (13 days since the start of treatments), MEFs

treated with vitamin C alone (200 μM) were fully confluent and routinely passaged at a 3/20 dilution (~1/7) to each well, then treatments were routinely performed at the indicated concentrations. After 6 more days, crystal violet staining was performed since the confluences properly represented what was observed consistently. Stained MEFs shown were 21 days after MEFs' isolation (19 days since the start of treatments). PBS wash and the renewal of cell culture media and treatments were performed every 2 days. Including this representative result, this result was observed 2 times using 2 technical replicates: two 6-well plates were initially seeded with *Sod1*$^{-/-}$ MEFs and two 6-well plates were initially seeded with *Sod1*$^{+/+}$ MEFs. They were then treated at the concentrations shown in the figure.

Discussion

The use of the Cre-*loxP* system for *Sod1* KO

The aim of my project was to use the Cre-*loxP* system to acutely delete *Sod1* in *Sod1*$^{fl/fl}$ MEFs, observe the consequences of SOD1 loss *in vitro*, and subsequently search for treatments that can rescue the poor survival induced by the deletion of SOD1. Previous studies have found that *Sod1*$^{-/-}$ MEFs grew poorly under normal cell culture conditions (Huang et al., 1997; Tsunoda et al., 2013). Previous studies have also used Cre-*loxP* system to successfully perform *Sod2* KO in specific tissues, since *Sod2*$^{-/-}$ mice die within days or weeks after birth (Bhaskaran et al., 2023; Ikegami et al., 2002; Lustgarten et al., 2009; Marecki et al., 2014; Nojiri et al., 2006; Oh et al., 2012; Parajuli et al., 2011; Sasaki et al., 2011; Treiber et al., 2011). In our study, the Cre-*loxP* system was mainly used to avoid possible compensatory developmental responses that might have arisen in *Sod1*$^{-/-}$ embryos, since these could have influenced the phenotypes of *Sod1*$^{-/-}$ MEFs. But first, the Cre-*loxP* protocol had to be tested in order to observe its efficiency in deleting floxed alleles. For this purpose, *Mclk1*$^{fl/fl}$ MEFs were used. The human homolog is named *COQ7*. MCLK1/COQ7 is a mitochondrial enzyme required for the synthesis of ubiquinone, also known as Q. As mentioned in the literature review, Q acts as an electron carrier from complex I and II to complex III of the electron transport chain. *Mclk1*/*Coq7* KO MEFs do not synthesize coenzyme Q but are viable *in vitro* (Wang & Hekimi, 2013). However, the characteristic that is more experimentally relevant is their capacity to grow and proliferate at a rate comparable to that of unrecombined wild-type controls, under standard cell culture conditions. If the Cre-*loxP* system was first tested on *Sod1*$^{fl/fl}$ MEFs instead of *Mclk1*$^{fl/fl}$ MEFs, it would be difficult to determine if *Sod1*$^{\Delta/\Delta}$ MEFs'

poor growth is either caused by a toxic by-product from the Cre-mediated KO protocol, by the lack of *Sod1*, or another variable. By using *Mclk1*$^{fl/fl}$ MEFs instead, this allowed to clearly verify if the Cre-mediated KO protocol is inherently toxic to cells and if it performed acceptably or not. If not, then the protocol would have been amended until it performed acceptably. Using retroviruses containing pBABE-puro-Cre, *Mclk1*$^{fl/fl}$ MEFs were infected and this resulted in the successful and prolonged deletion of *Mclk1* for all *Mclk1*$^{fl/fl}$ MEFs (Figure 1). Since the Cre-*loxP* protocol was successful with *Mclk1*$^{fl/fl}$ MEFs, the experiments proceeded with *Sod1*$^{fl/fl}$ MEFs.

Consistent with published studies (Huang et al., 1997; Tsunoda et al., 2013) and work from our laboratory, acute loss of *Sod1* induced by the Cre-*loxP* system also led to rapid cell death and severely defective growth of *Sod1*$^{fl/fl}$ MEFs under standard cell culture conditions (Figure 3). To highlight how quickly *Sod1*$^{\Delta/\Delta}$-Cre MEFs died, confluence clearly decreased after only 2–3 days of puromycin selection (Figure 3). The study by Huang et al. (1997) observed the highest number of apoptotic *Sod1*$^{-/-}$ cells ~6 days after MEFs' isolation and nearly all *Sod1*$^{-/-}$ MEFs died 8 days after MEFs' isolation. Tsunoda et al. (2013) also observed a clear decrease in the confluence of *Sod1*$^{-/-}$ MEFs after only 1 day at 20% O_2 and all *Sod1*$^{-/-}$ MEFs were dead after 4 days at 20% O_2.

Despite a successful initial deletion of *Sod1* in practically all *Sod1*$^{fl/fl}$ MEFs after puromycin selection (Figure 2), *Sod1*$^{\Delta/\Delta}$-Cre MEFs were gradually being overtaken by the incompletely recombined *Sod1*$^{fl/fl}$-Cre or *Sod1*$^{fl/\Delta}$-Cre MEFs, sometimes starting after only 2 days of puromycin selection (Figure 4). As mentioned previously, this likely happened due to the significant proliferative advantage of the incompletely recombined MEFs over *Sod1*$^{\Delta/\Delta}$-Cre MEFs' proliferation. One possible reason why these incompletely recombined MEFs

survived puromycin selection is that the Cre infection incorporated enough puromycin resistance in some *Sod1*$^{fl/fl}$ MEFs, but not enough Cre expression to delete *Sod1* completely. This posed a significant challenge in identifying potential treatments that could rescue cell death triggered by the loss of *Sod1 in vitro*, since a treatment's rescue effect could be confused with the growth of those incompletely recombined MEFs. Additionally, certain experiments required many weeks of treatments, just like what was done to observe vitamin C–treated MEFs' eventual proliferation arrest (Figure 8). Therefore, MEFs isolated from germline *Sod1* KO mice (*Sod1*$^{-/-}$) had to be used instead. In retrospect, another reason explaining the reappearance of SOD1 is possibly due to an insufficient time used for puromycin selection. For example, a study that successfully used the Cre-*loxP* system performed a *Sp2* KO in immortalized MEFs, resulting in a strongly decreased proliferation in *Sp2* KO MEFs (Baur et al., 2010). This observation is similar to MEFs after a *Sod1* KO. However, they performed puromycin selection over seven days, which is much longer than the two days of puromycin selection we used.

Using mouse embryos from heterozygous crosses, the embryos' genotype has been confirmed through PCR and agarose gel electrophoresis (Figure 6). As for possible compensatory mechanisms, a previous study by Tsunoda et al. (2013) has shown that in *Sod1*$^{-/-}$ MEFs, there were no increases in the levels of a selection of antioxidant enzymes such as SOD2, PRDX1, and PRDX2. Additionally, a study on primary dermal fibroblasts also reported no compensatory expression of SOD2, GPX1, and catalase (Watanabe et al., 2013). However, Tsunoda et al. (2013) reported decreased levels of catalase and increased levels of hyperoxidized PRDX in *Sod1*$^{-/-}$ MEFs. In another study, the increased levels of hyperoxidized PRDX was also detected in *Sod1*$^{-/-}$ mice and this hyperoxidation inactivated PRDX, likely due

to excessive ROS from the lack of SOD1 (Homma et al., 2015). Although it does not seem like there are compensatory mechanisms that increase these specific antioxidant enzymes, the decreased levels of catalase highlight the main downside of using *Sod1*$^{-/-}$ MEFs: unpredictable changes in gene expression, which can potentially create confounding variables influencing *Sod1*$^{-/-}$ MEFs' phenotype in unexpected ways.

Lastly, it is worth noting that unlike what was shown previously where a complete loss of SOD1 was observed in samples collected 9 days postinfection (Figure 2), low levels of SOD1 were visible in the generated *Sod1*$^{\Delta/\Delta}$-Cre MEFs as early as 7 days postinfection (Figure 4), suggesting a lower recombination efficiency this time. To elaborate on this, if the recombination efficiency was lower and the time used for puromycin selection was insufficient, then more unrecombined MEFs would be left alive after puromycin selection. A higher number of unrecombined MEFs would overgrow the recombined MEFs even more quickly. It could also be due to different proliferation rates, since MEFs from both experiments originated from different *Sod1*$^{fl/fl}$ embryos. Although, the exact reason for the lower rate of recombination is unknown.

The rescue of *Sod1* KO MEFs' survival with treatments

Vitamin C treatment successfully increased *Sod1*$^{\Delta/\Delta}$-Cre MEFs' survival (Figure 5). As mentioned previously, *Sod1*$^{\Delta/\Delta}$-Cre MEFs were still used for this experiment to at least observe the treatments' effects on these cells, before replacing this method with a better alternative. Initially, vitamin C treatment at 100 μM for one day did not induce any obvious phenotypic changes (data not shown), therefore the concentration was increased to 400 μM and treatments were maintained every 1–2 days by renewing cell culture media. *Sod1*$^{\Delta/\Delta}$-Cre

MEFs treated with vitamin C (400 μM) had an increased confluence compared to the untreated control (Figure 5). Vitamin C was chosen as a treatment because previous work from our lab has found that vitamin C can improve the growth and survival of *Sod1*$^{-/-}$ MEFs. Multiple published studies have also shown that vitamin C derivative APPS improved *Sod1*$^{-/-}$ primary dermal fibroblasts' survival (Murakami et al., 2009; Shibuya et al., 2012; Shibuya et al., 2014; Watanabe et al., 2013). APPS' rescue effect was primarily attributed to the suppression of the increased levels of intracellular $O_2^{\bullet-}$ which led to the reduction of p53's expression back to wild-type levels and suppressed p53-mediated $O_2^{\bullet-}$ production (Murakami et al., 2009; Shibuya et al., 2012; Shibuya et al., 2014; Watanabe et al., 2013). Therefore, the rescue effect of vitamin C is likely also due to its strong antioxidant activity. As one of the hydrophilic antioxidants that accumulate in the aqueous phase of the cell, the basic biological function of vitamin C is to protect cell components against free radicals (Shen et al., 2021). Vitamin C diminishes the toxicity of $HO^{\bullet}$, $HOO^{\bullet}$, and $O_2^{\bullet-}$ by transferring the radical to vitamin C, resulting in the formation of the ascorbate radical, which is comparatively unreactive (Padayatty & Levine, 2016; Shen et al., 2021). Vitamin C also has other important properties. These include its ability to act as a cofactor or cosubstrate for many enzymes such as the three prolyl 4-hydroxylase isoenzymes involved in the hydroxylation of collagen by catalyzing enzymatic posttranslational modifications of procollagen (Peterkofsky, 1991). Vitamin C also acts as a cofactor in another set of prolyl-4-hydroxylase isoenzymes which are necessary for the hydroxylation of proline residues in hypoxia-inducible factor-1 alpha, an important transcription factor for oxygen sensing in multicellular animals (Myllyharju, 2008). After testing multiple concentrations of vitamin C on *Sod1*$^{-/-}$ MEFs, it was determined that proliferation was optimal at 200 μM, but not 400 μM (Figure 7). Knowing that ROS

concentrations within a physiological range is necessary for growth and proliferation (Reczek & Chandel, 2015; Sies & Jones, 2020), excessively increasing the level of intracellular antioxidants likely disrupts normal ROS homeostasis, leading to decreased cell growth and proliferation. For example, it has been shown that excessively increasing concentrations of antioxidants, such as NAC, inhibits G1 MEFs' entry into S phase (Menon et al., 2003).

While vitamin C successfully increased *Sod1*$^{\Delta/\Delta}$-Cre MEFs' survival, L-NAME did not (Figure 5). The loss of SOD1 increases $O_2^{\bullet-}$ levels and this increases the number of available $O_2^{\bullet-}$ that can react with the highly diffusible $^{\bullet}NO$ (Huie & Padmaja, 1993), leading to the overproduction of $ONOO^-$ and decreased levels of $^{\bullet}NO$. $ONOO^-$ is potentially toxic due to its ability to oxidize or nitrosylate lipids, proteins, and nucleic acids (Abalenikhina et al., 2020; Pacher et al., 2007). Additionally, $ONOO^-$ is a much more powerful oxidant, can cross cell membranes, and induces damage far from its initial site of formation (Murphy et al., 1998; Szabó et al., 2007). It was shown that L-NAME treatment was able to rescue the death of PC12 rat pheochromocytoma cells induced by the addition of antisense oligonucleotides downregulating *Sod1* (Troy et al., 1996). L-NAME is an inhibitor of all isoforms of NOS, an enzyme that catalyzes the production of $^{\bullet}NO$ from L-arginine (Palmer & Moncada, 1989; Rees et al., 1990). Inhibition of $^{\bullet}NO$ production by L-NAME could potentially decrease $ONOO^-$ formation by lowering the amount of available $^{\bullet}NO$ that can react with $O_2^{\bullet-}$. Therefore, L-NAME was used to test whether part of the toxicity induced by the loss of SOD1 is due to increased $ONOO^-$ production. *Sod1*$^{\Delta/\Delta}$-Cre MEFs treated with L-NAME (500 μM) had no obvious effect on cell confluence compared to the untreated *Sod1*$^{\Delta/\Delta}$-Cre MEFs (Figure 5). Similar results were obtained with L-NAME at 250 μM (data not shown). Therefore, the lack of SOD1 leading to increased and toxic levels of $ONOO^-$ is an unlikely explanation for the poor

survival and proliferation of *Sod1*$^{\Delta/\Delta}$-Cre MEFs *in vitro*. Due to this, L-NAME was not retested on *Sod1*$^{-/-}$ MEFs. However, it is possible that due to the increased formation of $ONOO^-$ from $O_2^{\bullet-}$ and $^{\bullet}NO$, decreased levels of $^{\bullet}NO$ is the culprit instead, since $^{\bullet}NO$ is an important signaling molecule (Valko et al., 2007). Additionally, it is worth noting that the actual effects of L-NAME on intracellular $^{\bullet}NO$ and $ONOO^-$ levels were not measured in this experiment. Therefore, it is still uncertain if L-NAME decreased $^{\bullet}NO$ levels and subsequently diminished the excessive production of $ONOO^-$.

Despite seemingly observing the improved survival of *Sod1*$^{-/-}$ MEFs after treating them with vitamin C, *Sod1*$^{-/-}$ MEFs stopped proliferating after ~39 treatment days (43 days after MEFs' isolation), in contrast to *Sod1*$^{+/+}$ MEFs (Figure 8). Therefore, the SCREEN-WELL® REDOX library was screened in order to find another compound that could complement the rescue of *Sod1*$^{-/-}$ MEFs by vitamin C. This library contains 84 compounds with defined prooxidant and antioxidant properties. Each library compound was tested at a concentration of 10 μM, in combination with vitamin C at 100 μM. The initial screen identified BHT as a potential hit, since the combined treatments of BHT and vitamin C clearly had a positive effect on *Sod1*$^{-/-}$ MEFs' confluence, compared to the vitamin C alone (Figure 9). BHT is widely used as an antioxidant in food, cosmetics, pharmaceuticals, oil, petroleum and rubber industries (Yehye et al., 2015). It is believed to act as a synthetic analog of vitamin E by inhibiting lipid peroxidation (Reische et al., 2002). Vitamin E scavenges peroxyl radicals ($ROO^{\bullet}$) efficiently, but not other radicals such as $HO^{\bullet}$, alkoxyl radical ($RO^{\bullet}$), thiyl radical ($RS^{\bullet}$), or $^{\bullet}NO_2$ (Niki, 2014). Vitamin E and vitamin C have a synergistic effect since vitamin C can reduce the vitamin E radical, regenerating vitamin E (Niki, 2014).

To confirm BHT's ability to further enhance vitamin C–treated *Sod1*$^{-/-}$ MEFs' survival and proliferation, the experiment was repeated. However, BHT did not further enhance the survival or proliferation of vitamin C–treated *Sod1*$^{-/-}$ MEFs' (Figure 10 and Figure 11). Therefore, lipid peroxidation does not seem to be a major contributor to the poor survival of *Sod1*$^{-/-}$ MEFs *in vitro*. Results of the combined treatment of BHT and vitamin C (Figure 10 and Figure 11) contradict results from the initial screening of the compound library (Figure 9). The main explanation for this contradiction were difficulties in homogenizing vitamin C–treated MEFs from the use of a low concentration of trypsin, at 0.05%. While vitamin C–treated *Sod1*$^{-/-}$ MEFs could easily detach from the cell culture plate itself, the cells could not separate from each other very easily and were united like a tissue. This is likely due to vitamin C's role as a cofactor or cosubstrate for the three prolyl 4-hydroxylase isoenzymes involved in the hydroxylation of collagen (Peterkofsky, 1991). However, the production of collagen in vitamin C–treated *Sod1*$^{-/-}$ MEFs remains to be investigated. For the experiment in figure 9, cells were treated for 3 minutes using ¼ of the total medium volume as 0.05% trypsin. This method normally allowed the homogenization of *Sod1*$^{-/-}$ MEFs but not for vitamin C–treated *Sod1*$^{-/-}$ MEFs. Due to this, it is possible that certain wells received more cells than they should have, increasing the variability in confluence between wells. The methodology was improved later (Figure 10 and Figure 11) by increasing trypsin's concentration (0.05% to 0.25%), the incubation time (3 minutes to 20 minutes), and the temperature during trypsin dissociation (~25°C to 37°C). This would normally be too harsh for *Sod1*$^{-/-}$ MEFs, but not for vitamin C–treated *Sod1*$^{-/-}$ MEFs.

To understand why cells were passaged despite not being close to full confluence in figure 9, this is because treatments were only renewed after passaging cells to a new plate

due to limited quantities of the library's compounds. Therefore, cells had to be passaged every 3 or 4 days in order to renew treatments. This is why a cell passage was performed on treatment day 4, despite cells not reaching full confluence (Figure 9). However, this method was clearly too harsh since even *Sod1*$^{-/-}$ MEFs treated with vitamin C alone could not reach full confluence due to the low frequency of vitamin C renewal. Therefore, starting at treatment day 5, vitamin C's concentration was increased from 100 to 200 µM and renewed every 4 days for all MEFs, except the untreated MEFs. Despite this, cells were still unable to reach full confluence after the first passage. Excluding the initial seeding of MEFs onto plates, this experiment only passaged the cells one time in total, on treatment day 4. The library's compounds were still only renewed after passaging cells due to limited quantities of compounds. Therefore, the addition of the library's compounds was only done two times: once during the initial seeding of MEFs and once on treatment day 4.

Lastly, unlike what was previously shown where vitamin C–treated MEFs stopped proliferating after ~39 days of treatment (Figure 8), vitamin C–treated MEFs used in figure 10 were still able to proliferate after 49 days of treatment (Figure 10). However, according to microscopy photographs taken before crystal violet staining was performed in figure 10, cells' proliferation has largely slowed down, were enlarged, and flattened morphologically (data not shown). The slowed proliferation is also displayed in figure 10, considering that even after 9 days since the last cell passage, vitamin C–treated MEFs were still unable to grow to the same full confluence reached by *Sod1*$^{+/+}$ MEFs. The variation in the number of days before cells stop proliferating is most likely due to genetic variations since *Sod1*$^{-/-}$ MEFs used in both experiments originated from different embryos.

SOD1's subcellular localization and the poor survival of *Sod1*$^{-/-}$ MEFs

Despite not finding any treatments other than vitamin C that could have a role in the rescue of *Sod1*$^{-/-}$ MEFs, an explanation will be attempted in order to elucidate the contradiction between the viability of *Sod1*$^{-/-}$ mice but not of *Sod1*$^{-/-}$ MEFs. First, the poor survival of *Sod1*$^{-/-}$ MEFs will be addressed. SOD1 is one of the most abundant proteins in cells, representing 1–2% of total detergent-soluble proteins in certain cells (Pardo et al., 1995). Among the three mammalian SOD isoforms, SOD1 is considered the cytoplasmic isoform. While it is true SOD1 is mostly localized to the cytosol, it has also been identified in the nucleus, mitochondrial intermembrane space, lysosomes, and peroxisomes (Chang et al., 1988; Crapo et al., 1992; Geller & Winge, 1982; Keller et al., 1991; Kira et al., 2002; Liou et al., 1993; Okado-Matsumoto & Fridovich, 2001; Sturtz et al., 2001). The poor survival of *Sod1*$^{-/-}$ MEFs is likely explained by the lack of SOD1 disrupting the ROS homeostasis in one or more of these subcellular locations.

Mitochondria are generally assumed to be the main source of $O_2^{\bullet-}$ and the third most abundant location of SOD1 is found in the mitochondrial intermembrane space (Chang et al., 1988). The mitochondrial electron transport chain generates $O_2^{\bullet-}$ in the mitochondrial matrix but also in the mitochondrial intermembrane space, where it becomes a substrate for SOD1 (Balaban et al., 2005; Hernansanz-Agustín & Enríquez, 2021; Murphy, 2008; Nolfi-Donegan et al., 2020; Valko et al., 2004). Thus, the lack of SOD1 likely leads to an excessive increase in the concentration of $O_2^{\bullet-}$ in the mitochondrial intermembrane space, disrupting mitochondrial ROS homeostasis and leading to mitochondrial dysfunction and cell death. This is supported by observations where *Sod1*$^{-/-}$ primary dermal fibroblasts had a 4-fold increase in mitochondrial $O_2^{\bullet-}$ compared to the wild type, a 2.2-fold increase in the number

of low–membrane potential mitochondria, and increased apoptotic cell death (Watanabe et al., 2013). As for *Sod2*$^{-/-}$ MEFs, they also have an impaired cell growth *in vitro* (Huang et al., 1997; Samper et al., 2003; Zhang et al., 2010). As mentioned in the literature review, SOD2 is exclusively located in mitochondria, mainly in the matrix and the inner membrane (Okado-Matsumoto & Fridovich, 2001). However, if mitochondrial dysfunction due to increased mitochondrial $O_2^{\bullet-}$ was the main reason causing the complete death of *Sod1*$^{-/-}$ MEFs *in vitro*, the complete death of *Sod2*$^{-/-}$ MEFs should also be observed *in vitro*, but *Sod2*$^{-/-}$ MEFs are still viable *in vitro* and are even able to immortalize (Huang et al., 1997; Samper et al., 2003; Zhang et al., 2010). Therefore, while it might partly exacerbate the poor survival of *Sod1*$^{-/-}$ MEFs, mitochondrial dysfunction is unlikely to be the main reason causing the poor survival of *Sod1*$^{-/-}$ MEFs.

Peroxisomes are also interesting organelles to consider. As mentioned in the literature review, the presence of both XO and NOS in peroxisomes is potentially damaging since they produce $O_2^{\bullet-}$ and $^{\bullet}NO$ respectively (Antonenkov et al., 2010; Di Meo et al., 2016; Frederiks & Vreeling-Sindelárová, 2002; Snezhkina et al., 2019). $O_2^{\bullet-}$ and $^{\bullet}NO$ react together to form $ONOO^-$, a highly reactive oxidant and a strong inducer of cytotoxicity (Abalenikhina et al., 2020; Huie & Padmaja, 1993). To regulate ROS levels, peroxisomes contain many antioxidant enzymes. Catalase is the main peroxisomal antioxidant, but SOD1 is also present to catalyze the dismutation of $O_2^{\bullet-}$ (Antonenkov et al., 2010). Therefore, another possibility explaining why *Sod1*$^{-/-}$ MEFs die quickly *in vitro* could be the increase in peroxisomal $O_2^{\bullet-}$ leading to excessive and toxic $ONOO^-$ accumulation. While this may occur in *Sod1*$^{-/-}$ MEFs, this is unlikely to be the main reason causing the death of *Sod1*$^{-/-}$ MEFs considering that less than 1% of SOD1 is localized in peroxisomes (Chang et al., 1988; Keller et al., 1991). Additionally,

previous studies have shown that the mutation or inhibition of XO did not improve aging-like pathologies in *Sod1*$^{-/-}$ mice (Shibuya et al., 2021).

The nucleus is the second most abundant location of SOD1 (Chang et al., 1988) and SOD1 localizes in the nucleus under both normal and pathological conditions (Xu et al., 2022). If only SOD1's main function in detoxifying $O_2^{\bullet-}$ is considered, it does not seem beneficial to localize SOD1 in the nucleus since $O_2^{\bullet-}$ is not produced in the nucleus and $O_2^{\bullet-}$ does not readily permeate through membranes such as the nuclear membrane. In reality, the nuclear localization of SOD1 is due to its conserved role as a transcription factor in response to increased intracellular oxidative stress (Tsang et al., 2014). In response to elevated endogenous or exogenous ROS, SOD1 has been shown to rapidly relocate into the nucleus where it binds to DNA promoters and promotes the expression of oxidative resistance and DNA repair genes, which are important to limit oxidative DNA damage, but also oxidative damage in general. Tsang et al. (2014) also demonstrated that nuclear SOD1 was essential to protect against oxidative DNA damage, not cytoplasmic SOD1. Additionally, in chicken DT40 cells, it was previously shown that nuclear SOD1 was important for the viability of cells by reducing DNA lesions, not cytoplasmic SOD1 (Inoue et al., 2010). To highlight the importance of SOD1 in preventing DNA damage, FACS analyses by Tsunoda et al. (2013) found that at 2% O_2, ~50% of *Sod1*$^{-/-}$ MEFs were tetraploid and they clearly had an enlarged, flat and vacuolated morphology under microscopy. Tetraploid cells were most likely a result of the senescence of MEFs due to acute and severe DNA damage, resulting in G2 exit and growth arrest at the G1 phase (Aylon & Oren, 2011; Margolis et al., 2003; Roger et al., 2021). The appearance of these *Sod1*$^{-/-}$ MEFs also looked very similar to senescent MEFs where a DNA damage response is activated, displaying an enlarged, flat and vacuolated morphology (Di

Micco et al., 2008). This is also supported by additional observations from Tsunoda et al. (2013) where at 20% O_2, ~37.5% of *Sod1*$^{-/-}$ MEFs were aneuploid, which corresponds to dead cells, and ~12.5% of *Sod1*$^{-/-}$ MEFs were tetraploid. The aneuploid cells were most likely dead cells from excessive oxidative stress, leading to p53 upregulation and apoptosis (Kang et al., 2013; Macip et al., 2003; Vurusaner et al., 2012). Additionally, SOD1 stabilizes the PeBoW complex necessary for the production of 60S ribosome subunits, and nuclear SOD1 was shown to be essential in suppressing the growth defect induced by *Sod1* KO in KRAS mutant NSCLC cells, not cytoplasmic SOD1 (Wang et al., 2021). This is also perhaps the main reason why *Sod2*$^{-/-}$ MEFs can survive *in vitro* since SOD1 is still functional. Taking everything into consideration, I speculate that the loss of SOD1 in the nucleus might largely contribute to the poor survival of *Sod1*$^{-/-}$ MEFs. Thus, besides its ability to scavenge $O_2^{\bullet-}$, SOD1's role as a transcriptional factor is likely essential for genomic stability and the protection of DNA from oxidative damage.

SOD1's most abundant location is in the cytosol (Chang et al., 1988). To explain SOD1's localization in the cytosol, it can be explained by its main function in detoxifying cytosolic $O_2^{\bullet-}$ anions that can sometimes be generated by various intracellular sources such as NOX and XOR (Bedard & Krause, 2007; Berry & Hare, 2004). Additionally, SOD1 has a role in regulating $O_2^{\bullet-}$ and H_2O_2 levels (Harraz et al., 2008). H_2O_2 is a major redox signalling molecule and maintaining H_2O_2 within a physiological range is important for cellular differentiation and proliferation (Reczek & Chandel, 2015; Sies & Jones, 2020). Therefore, as a counterargument, it is possible that the lack of SOD1 leads to unregulated cytosolic $O_2^{\bullet-}$ and H_2O_2 levels, disrupting ROS signalling, increasing cytosolic $ONOO^-$ production, and damaging various parts of the cell. While this may contribute to a certain degree to *Sod1*$^{-/-}$ MEFs'

phenotype, this is an unlikely explanation for the poor survival of *Sod1*$^{-/-}$ MEFs since, as mentioned previously, Tsang et al. (2014) demonstrated that nuclear SOD1 was essential to protect against oxidative DNA damage, not cytoplasmic SOD1. Another study has previously shown that nuclear SOD1 was essential for the viability of chicken DT40 cells by reducing DNA lesions, not cytoplasmic SOD1 (Inoue et al., 2010). Additionally, after *Sod1* KO, nuclear SOD1 was essential for the survival and proliferation of KRAS mutant NSCLC cells, not cytoplasmic SOD1 (Wang et al., 2021). Although, since these are cancer cells that typically engage in hyperactive ribosome biogenesis, this might be more related to SOD1's role in stabilizing the PeBoW complex for the production of 60S ribosome subunits (Wang et al., 2021). Lastly, although SOD1 is highly concentrated in lysosomes (Chang et al., 1988), lysosomal SOD1 was not discussed because they were most likely inactive and being degraded (Geller & Winge, 1982).

The viability of *Sod1*$^{-/-}$ mice

To explain the contradiction between the viability of *Sod1*$^{-/-}$ mice but not of *Sod1*$^{-/-}$ MEFs, certain authors have speculated that this is because the ~20% O_2 concentration *in vitro* is much higher than what is found in tissues *in vivo*, which is ~3–5% O_2 instead (Inoue et al., 2010; Tsunoda et al., 2013). Because of the high concentrations of O_2 *in vitro*, ROS generation is increased beyond what is normally encountered in those cells, which is especially detrimental for *Sod1*$^{-/-}$ MEFs since they lack SOD1. Tsunoda et al. (2013) have confirmed that levels of ROS and lipid peroxidation products were indeed significantly higher in *Sod1*$^{-/-}$ MEFs than in wild-type MEFs. Therefore, the lack of SOD1 prevents MEFs from adapting to the increased oxidative stress induced by ambient O_2 levels during *in vitro* culture, leading to

rapid cell death. While *Sod1*$^{-/-}$ MEFs were alive after decreasing oxygen levels to 2% O_2, they were senescent (Tsunoda et al., 2013). As observed previously, vitamin C mostly rescued *Sod1*$^{-/-}$ MEFs (Figure 5 and 7). Inoue et al. (2010) proposed that the liver of *Sod1*$^{-/-}$ mice might be able to produce vitamin C in sufficient quantities to maintain the viability of these mice. Combined with the low ~3–5% O_2 concentration *in vivo*, this is likely to be the main explanation. However, while *Sod1*$^{-/-}$ mice are viable, these two factors cannot completely revert the other phenotypic abnormalities experienced by *Sod1*$^{-/-}$ mice (Busuttil et al., 2005; Dasgupta et al., 2009; Elchuri et al., 2005; Fischer et al., 2012; Hashizume et al., 2008; Ho et al., 1998; Huang et al., 1999; Imamura et al., 2006; Iuchi et al., 2007; Matzuk et al., 1998; Morikawa et al., 2013; Muller et al., 2006; Nojiri et al., 2011; Shibuya et al., 2012; Uchiyama et al., 2006).

Conclusion and Summary

This work attempted to understand the causes of the poor survival of *Sod1* KO MEFs by testing different treatments *in vitro*. While vitamin C was able to partially rescue the survival and proliferation of MEFs lacking SOD1, it did not rescue their long-term survival and proliferation. These findings suggest that their poor viability is in part linked to an alteration in redox metabolism. However, the literature suggests other non-redox or non-enzymatic functions of SOD1 might be involved as well. L-NAME, a non-selective NOS inhibitor, was ineffective at suppressing the death of *Sod1* KO MEFs, suggesting $ONOO^-$ overproduction is unlikely to play an essential role in the poor viability of *Sod1* KO MEFs *in vitro*. A small redox compound library was screened to search for possible compounds that could have a synergistic effect with vitamin C and possibly completely rescue the survival and proliferation of *Sod1*$^{-/-}$ MEFs. However, this yielded no confirmed hits. Screening against larger libraries will be needed in future studies to identify other treatments that can completely rescue defects in cell survival and proliferation induced by the loss of *Sod1 in vitro*, which might provide further insights into the causes of *Sod1* KO MEFs' inability to survive *in vitro* and possibly other cellular roles involving SOD1.

References

Abalenikhina, Y. V., Kosmachevskaya, O. V., & Topunov, A. F. (2020). Peroxynitrite: Toxic Agent and Signaling Molecule (Review). *Applied Biochemistry and Microbiology*, *56*(6), 611-623. https://doi.org/10.1134/S0003683820060022

Abel, O., Powell, J. F., Andersen, P. M., & Al-Chalabi, A. (2012). ALSoD: A user-friendly online bioinformatics tool for amyotrophic lateral sclerosis genetics. *Human Mutation*, *33*(9), 1345-1351. https://doi.org/10.1002/humu.22157

Andersen, P. M. (2006). Amyotrophic lateral sclerosis associated with mutations in the CuZn superoxide dismutase gene. *Current Neurology and Neuroscience Reports*, *6*(1), 37-46. https://doi.org/10.1007/s11910-996-0008-9

Andrés, C. M. C., Pérez de la Lastra, J. M., Juan, C. A., Plou, F. J., & Pérez-Lebeña, E. (2022). Chemistry of Hydrogen Peroxide Formation and Elimination in Mammalian Cells, and Its Role in Various Pathologies. *Stresses*, *2*(3), 256-274. https://doi.org/10.3390/stresses2030019

Angermüller, S., Bruder, G., Völkl, A., Wesch, H., & Fahimi, H. D. (1987). Localization of xanthine oxidase in crystalline cores of peroxisomes. A cytochemical and biochemical study. *European journal of cell biology*, *45*(1), 137-144.

Antonenkov, V. D., Grunau, S., Ohlmeier, S., & Hiltunen, J. K. (2010). Peroxisomes Are Oxidative Organelles. *Antioxidants & Redox Signaling*, *13*(4), 525-537. https://doi.org/10.1089/ars.2009.2996

Arai, K., Kanaseki, T., & Ohkuma, S. (1991). Isolation of Highly Purified Lysosomes from Rat Liver: Identification of Electron Carrier Components on Lysosomal Membranes1.

The Journal of Biochemistry, *110*(4), 541-547. https://doi.org/10.1093/oxfordjournals.jbchem.a123616

Ayala, A., Muñoz, M. F., & Argüelles, S. (2014). Lipid Peroxidation: Production, Metabolism, and Signaling Mechanisms of Malondialdehyde and 4-Hydroxy-2-Nonenal. *Oxidative Medicine and Cellular Longevity*, *2014*, 360438. https://doi.org/10.1155/2014/360438

Aylon, Y., & Oren, M. (2011). p53: Guardian of ploidy. *Molecular Oncology*, *5*(4), 315-323. https://doi.org/10.1016/j.molonc.2011.07.007

Balaban, R. S., Nemoto, S., & Finkel, T. (2005). Mitochondria, Oxidants, and Aging. *Cell*, *120*(4), 483-495. https://doi.org/10.1016/j.cell.2005.02.001

Başaran, R., & Can Eke, B. (2017). Flavin Containing Monooxygenases and Metabolism of Xenobiotics [Article]. *Turkish Journal of Pharmaceutical Sciences*, *14*(1), 90-94. https://doi.org/10.4274/tjps.30592

Baur, F., Nau, K., Sadic, D., Allweiss, L., Elsässer, H.-P., Gillemans, N., Wit, T. d., Krüger, I., Vollmer, M., Philipsen, S., & Suske, G. (2010). Specificity Protein 2 (Sp2) Is Essential for Mouse Development and Autonomous Proliferation of Mouse Embryonic Fibroblasts. *PLOS ONE*, *5*(3), e9587. https://doi.org/10.1371/journal.pone.0009587

Bedard, K., & Krause, K.-H. (2007). The NOX Family of ROS-Generating NADPH Oxidases: Physiology and Pathophysiology. *Physiological Reviews*, *87*(1), 245-313. https://doi.org/10.1152/physrev.00044.2005

Berry, C. E., & Hare, J. M. (2004). Xanthine oxidoreductase and cardiovascular disease: molecular mechanisms and pathophysiological implications. *The Journal of Physiology*, *555*(3), 589-606. https://doi.org/10.1113/jphysiol.2003.055913

Bhaskaran, S., Kumar, G., Thadathil, N., Piekarz, K. M., Mohammed, S., Lopez, S. D., Qaisar, R., Walton, D., Brown, J. L., Murphy, A., Smith, N., Saunders, D., Beckstead, M. J., Plafker, S., Lewis, T. L., Towner, R., Deepa, S. S., Richardson, A., Axtell, R. C., & Van Remmen, H. (2023). Neuronal deletion of MnSOD in mice leads to demyelination, inflammation and progressive paralysis that mimics phenotypes associated with progressive multiple sclerosis. *Redox Biology*, *59*, 102550. https://doi.org/10.1016/j.redox.2022.102550

Blagosklonny, M. V. (2012). Cell cycle arrest is not yet senescence, which is not just cell cycle arrest: terminology for TOR-driven aging. *Aging (Albany NY)*, *4*(3), 159-165.

Boyd, S. D., Ullrich, M. S., Calvo, J. S., Behnia, F., Meloni, G., & Winkler, D. D. (2020). Mutations in Superoxide Dismutase 1 (Sod1) Linked to Familial Amyotrophic Lateral Sclerosis Can Disrupt High-Affinity Zinc-Binding Promoted by the Copper Chaperone for Sod1 (Ccs). *Molecules*, *25*(5), 1086. https://doi.org/10.3390/molecules25051086

Bozkurt, A. S. (2021). Publication Status of Mouse Embryonic Fibroblast Cells in Scientific Journals. *European Journal of Therapeutics*, *27*(2), 135-141. https://doi.org/10.5152/eurjther.2021.20111

Brenner, C., & Moulin, M. (2012). Physiological Roles of the Permeability Transition Pore. *Circulation Research*, *111*(9), 1237-1247. https://doi.org/10.1161/CIRCRESAHA.112.265942

Breyer, V., Weigel, I., Huang, T.-T., & Pischetsrieder, M. (2012). Endogenous mitochondrial oxidative stress in MnSOD-deficient mouse embryonic fibroblasts promotes mitochondrial DNA glycation. *Free Radical Biology and Medicine*, *52*(9), 1744-1749. https://doi.org/10.1016/j.freeradbiomed.2012.02.021

Broom, H. R., Rumfeldt, J. A. O., & Meiering, E. M. (2014). Many roads lead to Rome? Multiple modes of Cu,Zn superoxide dismutase destabilization, misfolding and aggregation in amyotrophic lateral sclerosis. *Essays in biochemistry*, *56*, 149-165. https://doi.org/10.1042/bse0560149

Brown, G. C., & Borutaite, V. (2012). There is no evidence that mitochondria are the main source of reactive oxygen species in mammalian cells. *Mitochondrion*, *12*(1), 1-4. https://doi.org/10.1016/j.mito.2011.02.001

Brown, R. H., & Al-Chalabi, A. (2017). Amyotrophic Lateral Sclerosis. *The New England Journal of Medicine*, *377*(2), 162-172. https://doi.org/10.1056/NEJMra1603471

Brugarolas, J., Chandrasekaran, C., Gordon, J. I., Beach, D., Jacks, T., & Hannon, G. J. (1995). Radiation-induced cell cycle arrest compromised by p21 deficiency. *Nature*, *377*(6549), 552-557. https://doi.org/10.1038/377552a0

Bruijn, L. I., Houseweart, M. K., Kato, S., Anderson, K. L., Anderson, S. D., Ohama, E., Reaume, A. G., Scott, R. W., & Cleveland, D. W. (1998). Aggregation and Motor Neuron Toxicity of an ALS-Linked SOD1 Mutant Independent from Wild-Type SOD1. *Science*, *281*(5384), 1851-1854. https://doi.org/doi:10.1126/science.281.5384.1851

Busuttil, R. A., Garcia, A. M., Cabrera, C., Rodriguez, A., Suh, Y., Kim, W. H., Huang, T.-T., & Vijg, J. (2005). Organ-specific increase in mutation accumulation and apoptosis rate in CuZn-superoxide dismutase-deficient mice. *Cancer Research*, *65*(24), 11271-11275. https://doi.org/10.1158/0008-5472.CAN-05-2980

Cao, S. S., & Kaufman, R. J. (2014). Endoplasmic reticulum stress and oxidative stress in cell fate decision and human disease. *Antioxid Redox Signal*, *21*(3), 396-413. https://doi.org/10.1089/ars.2014.5851

Carlsson, L. M., Jonsson, J., Edlund, T., & Marklund, S. L. (1995). Mice lacking extracellular superoxide dismutase are more sensitive to hyperoxia. *Proceedings of the National Academy of Sciences of the United States of America*, *92*(14), 6264-6268. https://doi.org/10.1073/pnas.92.14.6264

Carroll, M. C., Girouard, J. B., Ulloa, J. L., Subramaniam, J. R., Wong, P. C., Valentine, J. S., & Culotta, V. C. (2004). Mechanisms for activating Cu- and Zn-containing superoxide dismutase in the absence of the CCS Cu chaperone. *Proc Natl Acad Sci U S A*, *101*(16), 5964-5969. https://doi.org/10.1073/pnas.0308298101

Casareno, R. L. B., Waggoner, D., & Gitlin, J. D. (1998). The Copper Chaperone CCS Directly Interacts with Copper/Zinc Superoxide Dismutase *. *Journal of Biological Chemistry*, *273*(37), 23625-23628. https://doi.org/10.1074/jbc.273.37.23625

Chan, F. K., Zhang, J., Cheng, L., Shapiro, D. N., & Winoto, A. (1995). Identification of human and mouse p19, a novel CDK4 and CDK6 inhibitor with homology to p16ink4. *Mol Cell Biol*, *15*(5), 2682-2688. https://doi.org/10.1128/mcb.15.5.2682

Chang, L. Y., Slot, J. W., Geuze, H. J., & Crapo, J. D. (1988). Molecular immunocytochemistry of the CuZn superoxide dismutase in rat hepatocytes. *The Journal of Cell Biology*, *107*(6 Pt 1), 2169-2179. https://doi.org/10.1083/jcb.107.6.2169

Colavitti, R., Pani, G., Bedogni, B., Anzevino, R., Borrello, S., Waltenberger, J., & Galeotti, T. (2002). Reactive oxygen species as downstream mediators of angiogenic signaling by vascular endothelial growth factor receptor-2/KDR. *The Journal of Biological Chemistry*, *277*(5), 3101-3108. https://doi.org/10.1074/jbc.M107711200

Cox, A. G., Winterbourn, C. C., & Hampton, M. B. (2009). Mitochondrial peroxiredoxin involvement in antioxidant defence and redox signalling. *The Biochemical Journal*, *425*(2), 313-325. https://doi.org/10.1042/BJ20091541

Crapo, J. D., Oury, T., Rabouille, C., Slot, J. W., & Chang, L. Y. (1992). Copper,zinc superoxide dismutase is primarily a cytosolic protein in human cells. *Proceedings of the National Academy of Sciences*, *89*(21), 10405-10409. https://doi.org/10.1073/pnas.89.21.10405

Culotta, V. C., Klomp, L. W. J., Strain, J., Casareno, R. L. B., Krems, B., & Gitlin, J. D. (1997). The Copper Chaperone for Superoxide Dismutase*. *Journal of Biological Chemistry*, *272*(38), 23469-23472. https://doi.org/10.1074/jbc.272.38.23469

D'Autréaux, B., & Toledano, M. B. (2007). ROS as signalling molecules: mechanisms that generate specificity in ROS homeostasis. *Nature Reviews Molecular Cell Biology*, *8*(10), 813-824. https://doi.org/10.1038/nrm2256

Dasgupta, J., Kar, S., Remmen, H. V., & Melendez, J. A. (2009). Age-dependent increases in interstitial collagenase and MAP Kinase levels are exacerbated by superoxide dismutase deficiencies. *Experimental Gerontology*, *44*(8), 503-510. https://doi.org/10.1016/j.exger.2009.04.005

Datar, S. A., Jacobs, H. W., de la Cruz, A. F., Lehner, C. F., & Edgar, B. A. (2000). The Drosophila cyclin D-Cdk4 complex promotes cellular growth. *Embo j*, *19*(17), 4543-4554. https://doi.org/10.1093/emboj/19.17.4543

Davydov, D. R. (2011). Microsomal monooxygenase as a multienzyme system: the role of P450-P450 interactions. *Expert opinion on drug metabolism & toxicology*, *7*(5), 543-558. https://doi.org/10.1517/17425255.2011.562194

Davydov, D. R. (2016). Molecular organization of the microsomal oxidative system: a new connotation for an old term. *Biochemistry (Moscow) Supplement Series B: Biomedical Chemistry*, *10*(1), 10-21. https://doi.org/10.1134/S1990750816010042

Deepa, S. S., Van Remmen, H., Brooks, S. V., Faulkner, J. A., Larkin, L., McArdle, A., Jackson, M. J., Vasilaki, A., & Richardson, A. (2019). Accelerated sarcopenia in Cu/Zn superoxide dismutase knockout mice. *Free Radical Biology and Medicine*, *132*, 19-23. https://doi.org/10.1016/j.freeradbiomed.2018.06.032

Demidenko, Z. N., Zubova, S. G., Bukreeva, E. I., Pospelov, V. A., Pospelova, T. V., & Blagosklonny, M. V. (2009). Rapamycin decelerates cellular senescence. *Cell Cycle (Georgetown, Tex.)*, *8*(12), 1888-1895. https://doi.org/10.4161/cc.8.12.8606

Dhar, S. K., & St. Clair, D. K. (2012). Manganese superoxide dismutase regulation and cancer. *Free Radical Biology and Medicine*, *52*(11), 2209-2222. https://doi.org/10.1016/j.freeradbiomed.2012.03.009

Di Meo, S., Reed, T. T., Venditti, P., & Victor, V. M. (2016). Role of ROS and RNS Sources in Physiological and Pathological Conditions. *Oxidative Medicine and Cellular Longevity*, *2016*, 1245049. https://doi.org/10.1155/2016/1245049

Di Micco, R., Cicalese, A., Fumagalli, M., Dobreva, M., Verrecchia, A., Pelicci, P. G., & di Fagagna, F. d. A. (2008). DNA damage response activation in mouse embryonic fibroblasts undergoing replicative senescence and following spontaneous immortalization. *Cell Cycle*, *7*(22), 3601–3606. https://doi.org/10.4161/cc.7.22.7152

Donaghy, L., Hong, H.-K., Jauzein, C., & Choi, K.-S. (2015). The known and unknown sources of reactive oxygen and nitrogen species in haemocytes of marine bivalve molluscs. *Fish & Shellfish Immunology*, *42*(1), 91-97. https://doi.org/10.1016/j.fsi.2014.10.030

Elchuri, S., Oberley, T. D., Qi, W., Eisenstein, R. S., Jackson Roberts, L., Van Remmen, H., Epstein, C. J., & Huang, T.-T. (2005). CuZnSOD deficiency leads to persistent and widespread oxidative damage and hepatocarcinogenesis later in life. *Oncogene*, *24*(3), 367-380. https://doi.org/10.1038/sj.onc.1208207

Fang, Y., Yu, H., Liang, X., Xu, J., & Cai, X. (2014). Chk1-induced CCNB1 overexpression promotes cell proliferation and tumor growth in human colorectal cancer. *Cancer Biology & Therapy*, *15*(9), 1268–1279. https://doi.org/10.4161/cbt.29691

Fattman, C. L., Tan, R. J., Tobolewski, J. M., & Oury, T. D. (2006). Increased sensitivity to asbestos-induced lung injury in mice lacking extracellular superoxide dismutase. *Free Radical Biology & Medicine*, *40*(4), 601-607. https://doi.org/10.1016/j.freeradbiomed.2005.09.030

Field, L. S., Furukawa, Y., O'Halloran, T. V., & Culotta, V. C. (2003). Factors Controlling the Uptake of Yeast Copper/Zinc Superoxide Dismutase into Mitochondria*. *Journal of Biological Chemistry*, *278*(30), 28052-28059. https://doi.org/10.1074/jbc.M304296200

Fischer, L. R., Li, Y., Asress, S. A., Jones, D. P., & Glass, J. D. (2012). Absence of SOD1 leads to oxidative stress in peripheral nerve and causes a progressive distal motor axonopathy. *Experimental Neurology*, *233*(1), 163-171. https://doi.org/10.1016/j.expneurol.2011.09.020

Fisher, A. B. (2009). Redox signaling across cell membranes. *Antioxid Redox Signal*, *11*(6), 1349-1356. https://doi.org/10.1089/ars.2008.2378

Fleming, A. M., & Burrows, C. J. (2020). On the Irrelevancy of Hydroxyl Radical to DNA Damage from Oxidative Stress and Implications for Epigenetics. *Chemical Society reviews*, *49*(18), 6524-6528. https://doi.org/10.1039/d0cs00579g

Forman, H. J., & Fridovich, I. (1973). On the stability of bovine superoxide dismutase. The effects of metals. *The Journal of Biological Chemistry*, *248*(8), 2645-2649.

Frederiks, W. M., & Vreeling-Sindelárová, H. (2002). Ultrastructural localization of xanthine oxidoreductase activity in isolated rat liver cells. *Acta Histochemica*, *104*(1), 29-37. https://doi.org/10.1078/0065-1281-00629

Fridovich, I. (1995). SUPEROXIDE RADICAL AND SUPEROXIDE DISMUTASES. *Annual Review of Biochemistry*, *64*(Volume 64, 1995), 97-112. https://doi.org/10.1146/annurev.bi.64.070195.000525

Fukai, T., & Ushio-Fukai, M. (2011). Superoxide Dismutases: Role in Redox Signaling, Vascular Function, and Diseases. *Antioxidants & Redox Signaling*, *15*(6), 1583-1606. https://doi.org/10.1089/ars.2011.3999

Furukawa, Y. (2022). A pathological link between dysregulated copper binding in Cu/Zn-superoxide dismutase and amyotrophic lateral sclerosis. *Journal of Clinical Biochemistry and Nutrition*, *71*(2), 73-77. https://doi.org/10.3164/jcbn.22-42

Garfield, A. S. (2010). Derivation of Primary Mouse Embryonic Fibroblast (PMEF) Cultures. In A. Ward & D. Tosh (Eds.), *Mouse Cell Culture: Methods and Protocols* (pp. 19-27). Humana Press.

Gaschler, M. M., & Stockwell, B. R. (2017). Lipid peroxidation in cell death. *Biochemical and Biophysical Research Communications*, *482*(3), 419-425. https://doi.org/10.1016/j.bbrc.2016.10.086

Ge, Y., Wang, L., Li, D., Zhao, C., Li, J., & Liu, T. (2019). Exploring the Extended Biological Functions of the Human Copper Chaperone of Superoxide Dismutase 1. *The Protein Journal*, *38*(4), 463-471. https://doi.org/10.1007/s10930-019-09824-9

Geller, B. L., & Winge, D. R. (1982). Rat liver Cu,Zn-superoxide dismutase. Subcellular location in lysosomes. *Journal of Biological Chemistry*, *257*(15), 8945-8952. https://doi.org/10.1016/S0021-9258(18)34224-8

Gille, L., & Nohl, H. (2000). The Existence of a Lysosomal Redox Chain and the Role of Ubiquinone. *Archives of Biochemistry and Biophysics*, *375*(2), 347-354. https://doi.org/10.1006/abbi.1999.1649

Goldberg, A. L., & St. John, A. C. (1976). Intracellular Protein Degradation in Mammalian and Bacterial Cells: Part 2. *Annual Review of Biochemistry*, *45*(Volume 45, 1976), 747-804. https://doi.org/https://doi.org/10.1146/annurev.bi.45.070176.003531

Görlach, A., Klappa, P., & Kietzmann, D. T. (2006). The Endoplasmic Reticulum: Folding, Calcium Homeostasis, Signaling, and Redox Control. *Antioxidants & Redox Signaling*, *8*(9-10), 1391-1418. https://doi.org/10.1089/ars.2006.8.1391

Gurney, M. E., Pu, H., Chiu, A. Y., Dal Canto, M. C., Polchow, C. Y., Alexander, D. D., Caliendo, J., Hentati, A., Kwon, Y. W., Deng, H.-X., Chen, W., Zhai, P., Sufit, R. L., & Siddique, T. (1994). Motor Neuron Degeneration in Mice that Express a Human Cu,Zn Superoxide Dismutase Mutation. *Science*, *264*(5166), 1772-1775. https://doi.org/10.1126/science.8209258

Hansen, J. M., & Piorczynski, T. B. (2019). Use of Primary Mouse Embryonic Fibroblasts in Developmental Toxicity Assessments. In J. M. Hansen & L. M. Winn (Eds.), *Developmental Toxicology: Methods and Protocols* (pp. 7-17). Springer.

Harraz, M. M., Marden, J. J., Zhou, W., Zhang, Y., Williams, A., Sharov, V. S., Nelson, K., Luo, M., Paulson, H., Schöneich, C., & Engelhardt, J. F. (2008). SOD1 mutations disrupt redox-sensitive Rac regulation of NADPH oxidase in a familial ALS model. *The Journal of Clinical Investigation*, *118*(2), 659-670. https://doi.org/10.1172/JCI34060

Hashizume, K., Hirasawa, M., Imamura, Y., Noda, S., Shimizu, T., Shinoda, K., Kurihara, T., Noda, K., Ozawa, Y., Ishida, S., Miyake, Y., Shirasawa, T., & Tsubota, K. (2008). Retinal Dysfunction and Progressive Retinal Cell Death in SOD1-Deficient Mice. *The American Journal of Pathology*, *172*(5), 1325-1331. https://doi.org/10.2353/ajpath.2008.070730

Hernansanz-Agustín, P., & Enríquez, J. A. (2021). Generation of Reactive Oxygen Species by Mitochondria. *Antioxidants*, *10*(3), 415. https://www.mdpi.com/2076-3921/10/3/415

Ho, Y.-S., Gargano, M., Cao, J., Bronson, R. T., Heimler, I., & Hutz, R. J. (1998). Reduced Fertility in Female Mice Lacking Copper-Zinc Superoxide Dismutase*. *Journal of Biological Chemistry*, *273*(13), 7765-7769. https://doi.org/10.1074/jbc.273.13.7765

Hölzel, M., Rohrmoser, M., Schlee, M., Grimm, T., Harasim, T., Malamoussi, A., Gruber-Eber, A., Kremmer, E., Hiddemann, W., Bornkamm, G. W., & Eick, D. (2005). Mammalian WDR12 is a novel member of the Pes1–Bop1 complex and is required for ribosome biogenesis and cell proliferation. *The Journal of Cell Biology*, *170*(3), 367-378. https://doi.org/10.1083/jcb.200501141

Homma, T., Okano, S., Lee, J., Ito, J., Otsuki, N., Kurahashi, T., Kang, E. S., Nakajima, O., & Fujii, J. (2015). SOD1 deficiency induces the systemic hyperoxidation of peroxiredoxin in the mouse. *Biochemical and Biophysical Research Communications*, *463*(4), 1040-1046. https://doi.org/https://doi.org/10.1016/j.bbrc.2015.06.055

Hrycay, E. G., & Bandiera, S. M. (2012). The monooxygenase, peroxidase, and peroxygenase properties of cytochrome P450. *Archives of Biochemistry and Biophysics*, *522*(2), 71-89. https://doi.org/https://doi.org/10.1016/j.abb.2012.01.003

Hrycay, E. G., & Bandiera, S. M. (2015). Monooxygenase, Peroxidase and Peroxygenase Properties and Reaction Mechanisms of Cytochrome P450 Enzymes. In E. G. Hrycay & S. M. Bandiera (Eds.), *Monooxygenase, Peroxidase and Peroxygenase Properties and Mechanisms of Cytochrome P450* (pp. 1-61). Springer International Publishing. https://doi.org/10.1007/978-3-319-16009-2_1

Huang, T.-T., Carlson, E. J., Kozy, H. M., Mantha, S., Goodman, S. I., Ursell, P. C., & Epstein, C. J. (2001). Genetic modification of prenatal lethality and dilated cardiomyopathy in Mn superoxide dismutase mutant mice. *Free Radical Biology and Medicine*, *31*(9), 1101-1110. https://doi.org/10.1016/S0891-5849(01)00694-3

Huang, T.-T., Yasunami, M., Carlson, E. J., Gillespie, A. M., Reaume, A. G., Hoffman, E. K., Chan, P. H., Scott, R. W., & Epstein, C. J. (1997). Superoxide-Mediated Cytotoxicity in Superoxide Dismutase-Deficient Fetal Fibroblasts. *Archives of Biochemistry and Biophysics*, *344*(2), 424-432. https://doi.org/10.1006/abbi.1997.0237

Huang, T. T., Carlson, E. J., Raineri, I., Gillespie, A. M., Kozy, H., & Epstein, C. J. (1999). The use of transgenic and mutant mice to study oxygen free radical metabolism. *Annals of the*

New York Academy of Sciences, *893*, 95-112. https://doi.org/10.1111/j.1749-6632.1999.tb07820.x

Huie, R. E., & Padmaja, S. (1993). The Reaction of no With Superoxide. *Free Radical Research Communications*, *18*(4), 195-199. https://doi.org/10.3109/10715769309145868

Ichikawa, M., Nishino, T., Nishino, T., & Ichikawa, A. (1992). Subcellular localization of xanthine oxidase in rat hepatocytes: high-resolution immunoelectron microscopic study combined with biochemical analysis. *The Journal of Histochemistry and Cytochemistry: Official Journal of the Histochemistry Society*, *40*(8), 1097-1103. https://doi.org/10.1177/40.8.1619276

Ikegami, T., Suzuki, Y.-i., Shimizu, T., Isono, K.-i., Koseki, H., & Shirasawa, T. (2002). Model mice for tissue-specific deletion of the manganese superoxide dismutase (MnSOD) gene. *Biochemical and Biophysical Research Communications*, *296*(3), 729-736. https://doi.org/10.1016/S0006-291X(02)00933-6

Illés, E., Mizrahi, A., Marks, V., & Meyerstein, D. (2019). Carbonate-radical-anions, and not hydroxyl radicals, are the products of the Fenton reaction in neutral solutions containing bicarbonate. *Free Radical Biology & Medicine*, *131*, 1-6. https://doi.org/10.1016/j.freeradbiomed.2018.11.015

Illés, E., Patra, S. G., Marks, V., Mizrahi, A., & Meyerstein, D. (2020). The FeII(citrate) Fenton reaction under physiological conditions. *Journal of Inorganic Biochemistry*, *206*, 111018. https://doi.org/https://doi.org/10.1016/j.jinorgbio.2020.111018

Imamura, Y., Noda, S., Hashizume, K., Shinoda, K., Yamaguchi, M., Uchiyama, S., Shimizu, T., Mizushima, Y., Shirasawa, T., & Tsubota, K. (2006). Drusen, choroidal neovascularization, and retinal pigment epithelium dysfunction in SOD1-deficient

mice: A model of age-related macular degeneration. *Proceedings of the National Academy of Sciences*, *103*(30), 11282-11287. https://doi.org/10.1073/pnas.0602131103

Inoue, E., Tano, K., Yoshii, H., Nakamura, J., Tada, S., Watanabe, M., Seki, M., & Enomoto, T. (2010). SOD1 Is Essential for the Viability of DT40 Cells and Nuclear SOD1 Functions as a Guardian of Genomic DNA. *Journal of Nucleic Acids*, *2010*, 795946. https://doi.org/10.4061/2010/795946

Islinger, M., Li, K. W., Seitz, J., Völkl, A., & Lüers, G. H. (2009). Hitchhiking of Cu/Zn Superoxide Dismutase to Peroxisomes – Evidence for a Natural Piggyback Import Mechanism in Mammals. *Traffic*, *10*(11), 1711-1721. https://doi.org/https://doi.org/10.1111/j.1600-0854.2009.00966.x

Iuchi, Y., Kibe, N., Tsunoda, S., Okada, F., Bannai, S., Sato, H., & Fujii, J. (2008). Deficiency of the cystine-transporter gene, xCT, does not exacerbate the deleterious phenotypic consequences of SOD1 knockout in mice. *Molecular and Cellular Biochemistry*, *319*(1), 125-132. https://doi.org/10.1007/s11010-008-9885-3

Iuchi, Y., Okada, F., Onuma, K., Onoda, T., Asao, H., Kobayashi, M., & Fujii, J. (2007). Elevated oxidative stress in erythrocytes due to a SOD1 deficiency causes anaemia and triggers autoantibody production. *Biochemical Journal*, *402*(2), 219-227. https://doi.org/10.1042/BJ20061386

Jirawatnotai, S., Hu, Y., Livingston, D. M., & Sicinski, P. (2012). Proteomic Identification of a Direct Role for Cyclin D1 in DNA Damage Repair. *Cancer Research*, *72*(17), 4289-4293. https://doi.org/10.1158/0008-5472.CAN-11-3549

Jomova, K., Raptova, R., Alomar, S. Y., Alwasel, S. H., Nepovimova, E., Kuca, K., & Valko, M. (2023). Reactive oxygen species, toxicity, oxidative stress, and antioxidants: chronic diseases and aging. *Archives of Toxicology*, *97*(10), 2499-2574. https://doi.org/10.1007/s00204-023-03562-9

Kanakkanthara, A., Jeganathan, K. B., Limzerwala, J. F., Baker, D. J., Hamada, M., Nam, H.-J., van Deursen, W. H., Hamada, N., Naylor, R. M., Becker, N. A., Davies, B. A., van Ree, J. H., Mer, G., Shapiro, V. S., Maher, L. J., Katzmann, D. J., & van Deursen, J. M. (2016). Cyclin A2 is an RNA binding protein that controls Mre11 mRNA translation. *Science*, *353*(6307), 1549-1552. https://doi.org/10.1126/science.aaf7463

Kang, M. Y., Kim, H.-B., Piao, C., Lee, K. H., Hyun, J. W., Chang, I.-Y., & You, H. J. (2013). The critical role of catalase in prooxidant and antioxidant function of p53. *Cell Death & Differentiation*, *20*(1), 117-129. https://doi.org/10.1038/cdd.2012.102

Kausar, S., Wang, F., & Cui, H. (2018). The Role of Mitochondria in Reactive Oxygen Species Generation and Its Implications for Neurodegenerative Diseases. *Cells*, *7*(12), 274. https://doi.org/10.3390/cells7120274

Kawamata, H., & Manfredi, G. (2010). Import, Maturation, and Function of SOD1 and Its Copper Chaperone CCS in the Mitochondrial Intermembrane Space. *Antioxidants & Redox Signaling*, *13*(9), 1375-1384. https://doi.org/10.1089/ars.2010.3212

Keller, G. A., Warner, T. G., Steimer, K. S., & Hallewell, R. A. (1991). Cu,Zn superoxide dismutase is a peroxisomal enzyme in human fibroblasts and hepatoma cells. *Proceedings of the National Academy of Sciences of the United States of America*, *88*(16), 7381-7385. https://doi.org/10.1073/pnas.88.16.7381

Kikuchi, H., Almer, G., Yamashita, S., Guégan, C., Nagai, M., Xu, Z., Sosunov, A. A., McKhann, G. M., & Przedborski, S. (2006). Spinal cord endoplasmic reticulum stress associated with a microsomal accumulation of mutant superoxide dismutase-1 in an ALS model. *Proceedings of the National Academy of Sciences*, *103*(15), 6025-6030. https://doi.org/10.1073/pnas.0509227103

Kim, H. W., Lin, A., Guldberg, R. E., Ushio-Fukai, M., & Fukai, T. (2007). Essential Role of Extracellular SOD in Reparative Neovascularization Induced by Hindlimb Ischemia. *Circulation Research*, *101*(4), 409-419. https://doi.org/10.1161/CIRCRESAHA.107.153791

Kira, Y., Sato, E. F., & Inoue, M. (2002). Association of Cu,Zn-Type Superoxide Dismutase with Mitochondria and Peroxisomes. *Archives of Biochemistry and Biophysics*, *399*(1), 96-102. https://doi.org/10.1006/abbi.2001.2738

Kornweitz, H., Burg, A., & Meyerstein, D. (2015). Plausible Mechanisms of the Fenton-Like Reactions, M = Fe(II) and Co(II), in the Presence of RCO2– Substrates: Are OH• Radicals Formed in the Process? *The Journal of Physical Chemistry A*, *119*(18), 4200-4206. https://doi.org/10.1021/jp512826f

Lebovitz, R. M., Zhang, H., Vogel, H., Cartwright, J., Dionne, L., Lu, N., Huang, S., & Matzuk, M. M. (1996). Neurodegeneration, myocardial injury, and perinatal death in mitochondrial superoxide dismutase-deficient mice. *Proceedings of the National Academy of Sciences of the United States of America*, *93*(18), 9782-9787.

Leitch, J. M., Yick, P. J., & Culotta, V. C. (2009). The right to choose: multiple pathways for activating copper,zinc superoxide dismutase. *J Biol Chem*, *284*(37), 24679-24683. https://doi.org/10.1074/jbc.R109.040410

Leontieva, O. V., Lenzo, F., Demidenko, Z. N., & Blagosklonny, M. V. (2012). Hyper-mitogenic drive coexists with mitotic incompetence in senescent cells. *Cell Cycle*, *11*(24), 4642–4649. https://doi.org/10.4161/cc.22937

Levanon, D., Lieman-Hurwitz, J., Dafni, N., Wigderson, M., Sherman, L., Bernstein, Y., Laver-Rudich, Z., Danciger, E., Stein, O., & Groner, Y. (1985). Architecture and anatomy of the chromosomal locus in human chromosome 21 encoding the Cu/Zn superoxide dismutase. *The EMBO Journal*, *4*(1), 77-84. https://doi.org/10.1002/j.1460-2075.1985.tb02320.x

Lewandowski, Ł., Kepinska, M., & Milnerowicz, H. (2019). The copper-zinc superoxide dismutase activity in selected diseases. *European Journal of Clinical Investigation*, *49*(1), e13036. https://doi.org/10.1111/eci.13036

Li, Y., Huang, T. T., Carlson, E. J., Melov, S., Ursell, P. C., Olson, J. L., Noble, L. J., Yoshimura, M. P., Berger, C., Chan, P. H., Wallace, D. C., & Epstein, C. J. (1995). Dilated cardiomyopathy and neonatal lethality in mutant mice lacking manganese superoxide dismutase. *Nature Genetics*, *11*(4), 376-381. https://doi.org/10.1038/ng1295-376

Liochev, S. I., & Fridovich, I. (2004). Bicarbonate-enhanced peroxidase activity of Cu,Zn SOD: is the distal oxidant bound or diffusible? *Archives of Biochemistry and Biophysics*, *421*(2), 255-259. https://doi.org/10.1016/j.abb.2003.11.015

Liou, W., Chang, L.-Y., Geuze, H. J., Strous, G. J., Crapo, J. D., & Slot, J. W. (1993). Distribution of CuZn superoxide dismutase in rat liver. *Free Radical Biology and Medicine*, *14*(2), 201-207. https://doi.org/10.1016/0891-5849(93)90011-I

Lustgarten, M. S., Jang, Y. C., Liu, Y., Muller, F. L., Qi, W., Steinhelper, M., Brooks, S. V., Larkin, L., Shimizu, T., Shirasawa, T., McManus, L. M., Bhattacharya, A., Richardson, A., & Van

Remmen, H. (2009). Conditional knockout of Mn-SOD targeted to type IIB skeletal muscle fibers increases oxidative stress and is sufficient to alter aerobic exercise capacity. *American Journal of Physiology-Cell Physiology*, *297*(6), C1520-C1532. https://doi.org/10.1152/ajpcell.00372.2009

Lutz, C. (2018). Mouse models of ALS: Past, present and future. *Brain Research*, *1693*, 1-10. https://doi.org/10.1016/j.brainres.2018.03.024

Macip, S., Igarashi, M., Berggren, P., Yu, J., Lee, S. W., & Aaronson, S. A. (2003). Influence of Induced Reactive Oxygen Species in p53-Mediated Cell Fate Decisions. *Molecular and Cellular Biology*, *23*(23), 8576–8585. https://doi.org/10.1128/MCB.23.23.8576-8585.2003

Malhotra, J. D., & Kaufman, R. J. (2007). Endoplasmic Reticulum Stress and Oxidative Stress: A Vicious Cycle or a Double-Edged Sword? *Antioxidants & Redox Signaling*, *9*(12), 2277-2294. https://doi.org/10.1089/ars.2007.1782

Marecki, J. C., Parajuli, N., Crow, J. P., & MacMillan-Crow, L. A. (2014). The Use of the Cre/loxP System to Study Oxidative Stress in Tissue-Specific Manganese Superoxide Dismutase Knockout Models. *Antioxidants & Redox Signaling*, *20*(10), 1655-1670. https://doi.org/10.1089/ars.2013.5293

Margolis, R. L., Lohez, O. D., & Andreassen, P. R. (2003). G1 tetraploidy checkpoint and the suppression of tumorigenesis. *Journal of Cellular Biochemistry*, *88*(4), 673-683. https://doi.org/10.1002/jcb.10411

Marin, E. P., Derakhshan, B., Lam, T. T., Davalos, A., & Sessa, W. C. (2012). Endothelial cell palmitoylproteomic identifies novel lipid-modified targets and potential substrates

for protein acyl transferases. *Circ Res*, *110*(10), 1336-1344. https://doi.org/10.1161/circresaha.112.269514

Marklund, S. L. (1982). Human copper-containing superoxide dismutase of high molecular weight. *Proceedings of the National Academy of Sciences of the United States of America*, *79*(24), 7634-7638. https://doi.org/10.1073/pnas.79.24.7634

Markossian, K. A., & Kurganov, B. I. (2003). Copper Chaperones, Intracellular Copper Trafficking Proteins. Function, Structure, and Mechanism of Action. *Biochemistry (Moscow)*, *68*(8), 827-837. https://doi.org/10.1023/A:1025740228888

Martínez-Alonso, D., & Malumbres, M. (2020). Mammalian cell cycle cyclins. *Seminars in Cell & Developmental Biology*, *107*, 28-35. https://doi.org/10.1016/j.semcdb.2020.03.009

Matzuk, M. M., Dionne, L., Guo, Q., Kumar, T. R., & Lebovitz, R. M. (1998). Ovarian function in superoxide dismutase 1 and 2 knockout mice. *Endocrinology*, *139*(9), 4008-4011. https://doi.org/10.1210/endo.139.9.6289

McCord, J. M., & Fridovich, I. (1969). Superoxide dismutase. An enzymic function for erythrocuprein (hemocuprein). *The Journal of Biological Chemistry*, *244*(22), 6049-6055.

Melov, S., Coskun, P., Patel, M., Tuinstra, R., Cottrell, B., Jun, A. S., Zastawny, T. H., Dizdaroglu, M., Goodman, S. I., Huang, T.-T., Miziorko, H., Epstein, C. J., & Wallace, D. C. (1999). Mitochondrial disease in superoxide dismutase 2 mutant mice. *Proceedings of the National Academy of Sciences of the United States of America*, *96*(3), 846-851.

Melov, S., Doctrow, S. R., Schneider, J. A., Haberson, J., Patel, M., Coskun, P. E., Huffman, K., Wallace, D. C., & Malfroy, B. (2001). Lifespan Extension and Rescue of Spongiform

Encephalopathy in Superoxide Dismutase 2 Nullizygous Mice Treated with Superoxide Dismutase–Catalase Mimetics. *The Journal of Neuroscience*, *21*(21), 8348-8353. https://doi.org/10.1523/JNEUROSCI.21-21-08348.2001

Melov, S., Schneider, J. A., Day, B. J., Hinerfeld, D., Coskun, P., Mirra, S. S., Crapo, J. D., & Wallace, D. C. (1998). A novel neurological phenotype in mice lacking mitochondrial manganese superoxide dismutase. *Nature Genetics*, *18*(2), 159-163. https://doi.org/10.1038/ng0298-159

Menon, S. G., Sarsour, E. H., Spitz, D. R., Higashikubo, R., Sturm, M., Zhang, H., & Goswami, P. C. (2003). Redox regulation of the G1 to S phase transition in the mouse embryo fibroblast cell cycle. *Cancer Research*, *63*(9), 2109-2117.

Miao, L., & St. Clair, D. K. (2009). Regulation of superoxide dismutase genes: Implications in disease. *Free Radical Biology and Medicine*, *47*(4), 344-356. https://doi.org/10.1016/j.freeradbiomed.2009.05.018

Milani, P., Gagliardi, S., Cova, E., & Cereda, C. (2011). SOD1 Transcriptional and Posttranscriptional Regulation and Its Potential Implications in ALS. *Neurol Res Int*, *2011*, 458427. https://doi.org/10.1155/2011/458427

Mondola, P., Damiano, S., Sasso, A., & Santillo, M. (2016). The Cu, Zn Superoxide Dismutase: Not Only a Dismutase Enzyme. *Frontiers in Physiology*, *7*. https://doi.org/10.3389/fphys.2016.00594

Montanaro, L., Treré, D., & Derenzini, M. (2008). Nucleolus, Ribosomes, and Cancer. *The American Journal of Pathology*, *173*(2), 301-310. https://doi.org/10.2353/ajpath.2008.070752

Morikawa, D., Nojiri, H., Saita, Y., Kobayashi, K., Watanabe, K., Ozawa, Y., Koike, M., Asou, Y., Takaku, T., Kaneko, K., & Shimizu, T. (2013). Cytoplasmic reactive oxygen species and SOD1 regulate bone mass during mechanical unloading. *Journal of Bone and Mineral Research*, *28*(11), 2368-2380. https://doi.org/10.1002/jbmr.1981

Muller, F. L., Song, W., Liu, Y., Chaudhuri, A., Pieke-Dahl, S., Strong, R., Huang, T.-T., Epstein, C. J., Roberts, L. J., Csete, M., Faulkner, J. A., & Van Remmen, H. (2006). Absence of CuZn superoxide dismutase leads to elevated oxidative stress and acceleration of age-dependent skeletal muscle atrophy. *Free Radical Biology and Medicine*, *40*(11), 1993-2004. https://doi.org/10.1016/j.freeradbiomed.2006.01.036

Murakami, K., Inagaki, J., Saito, M., Ikeda, Y., Tsuda, C., Noda, Y., Kawakami, S., Shirasawa, T., & Shimizu, T. (2009). Skin atrophy in cytoplasmic SOD-deficient mice and its complete recovery using a vitamin C derivative. *Biochemical and Biophysical Research Communications*, *382*(2), 457-461. https://doi.org/10.1016/j.bbrc.2009.03.053

Murphy, Michael P. (2008). How mitochondria produce reactive oxygen species. *Biochemical Journal*, *417*(1), 1-13. https://doi.org/10.1042/BJ20081386

Murphy, M. P., Packer, M. A., Scarlett, J. L., & Martin, S. W. (1998). Peroxynitrite: A Biologically Significant Oxidant. *General Pharmacology: The Vascular System*, *31*(2), 179-186. https://doi.org/10.1016/S0306-3623(97)00418-7

Müssnich, P., Raverot, G., Jaffrain-Rea, M.-L., Fraggetta, F., Wierinckx, A., Trouillas, J., Fusco, A., & D'Angelo, D. (2015). Downregulation of miR-410 targeting the cyclin B1 gene plays a role in pituitary gonadotroph tumors. *Cell Cycle*, *14*(16), 2590–2597. https://doi.org/10.1080/15384101.2015.1064207

Myllyharju, J. (2008). Prolyl 4-hydroxylases, key enzymes in the synthesis of collagens and regulation of the response to hypoxia, and their roles as treatment targets. *Annals of Medicine*, *40*(6), 402-417. https://doi.org/10.1080/07853890801986594

Nelsen, C. J., Rickheim, D. G., Tucker, M. M., Hansen, L. K., & Albrecht, J. H. (2003). Evidence That Cyclin D1 Mediates Both Growth and Proliferation Downstream of TOR in Hepatocytes *. *Journal of Biological Chemistry*, *278*(6), 3656-3663. https://doi.org/10.1074/jbc.M209374200

Niki, E. (2014). Role of vitamin E as a lipid-soluble peroxyl radical scavenger: in vitro and in vivo evidence. *Free Radical Biology and Medicine*, *66*, 3-12. https://doi.org/10.1016/j.freeradbiomed.2013.03.022

Nishino, T., Okamoto, K., Eger, B. T., Pai, E. F., & Nishino, T. (2008). Mammalian xanthine oxidoreductase – mechanism of transition from xanthine dehydrogenase to xanthine oxidase. *The FEBS Journal*, *275*(13), 3278-3289. https://doi.org/10.1111/j.1742-4658.2008.06489.x

Noë, A. (2021, 2021). *Thesis | Critical function of superoxide dismutase 1 (SOD1) in relation to nitric oxide in mouse skeletal muscles | ID: ht24wp90q | eScholarship@McGill*.

Nojiri, H., Saita, Y., Morikawa, D., Kobayashi, K., Tsuda, C., Miyazaki, T., Saito, M., Marumo, K., Yonezawa, I., Kaneko, K., Shirasawa, T., & Shimizu, T. (2011). Cytoplasmic superoxide causes bone fragility owing to low-turnover osteoporosis and impaired collagen cross-linking. *Journal of Bone and Mineral Research*, *26*(11), 2682-2694. https://doi.org/10.1002/jbmr.489

Nojiri, H., Shimizu, T., Funakoshi, M., Yamaguchi, O., Zhou, H., Kawakami, S., Ohta, Y., Sami, M., Tachibana, T., Ishikawa, H., Kurosawa, H., Kahn, R. C., Otsu, K., & Shirasawa, T. (2006).

Oxidative stress causes heart failure with impaired mitochondrial respiration. *J Biol Chem*, *281*(44), 33789-33801. https://doi.org/10.1074/jbc.M602118200

Nolfi-Donegan, D., Braganza, A., & Shiva, S. (2020). Mitochondrial electron transport chain: Oxidative phosphorylation, oxidant production, and methods of measurement. *Redox Biology*, *37*, 101674. https://doi.org/10.1016/j.redox.2020.101674

Oh, S. S., Sullivan, K. A., Wilkinson, J. E., Backus, C., Hayes, J. M., Sakowski, S. A., & Feldman, E. L. (2012). Neurodegeneration and early lethality in superoxide dismutase 2-deficient mice: a comprehensive analysis of the central and peripheral nervous systems. *Neuroscience*, *212*, 201-213. https://doi.org/10.1016/j.neuroscience.2012.03.026

Okado-Matsumoto, A., & Fridovich, I. (2001). Subcellular Distribution of Superoxide Dismutases (SOD) in Rat Liver: Cu,Zn-SOD IN MITOCHONDRIA *. *Journal of Biological Chemistry*, *276*(42), 38388-38393. https://doi.org/10.1074/jbc.M105395200

Pacher, P., Beckman, J. S., & Liaudet, L. (2007). Nitric Oxide and Peroxynitrite in Health and Disease. *Physiological Reviews*, *87*(1), 315-424. https://doi.org/10.1152/physrev.00029.2006

Padayatty, S., & Levine, M. (2016). Vitamin C: the known and the unknown and Goldilocks. *Oral Diseases*, *22*(6), 463-493. https://doi.org/10.1111/odi.12446

Palmer, R. M. J., & Moncada, S. (1989). A novel citrulline-forming enzyme implicated in the formation of nitric oxide by vascular endothelial cells. *Biochemical and Biophysical Research Communications*, *158*(1), 348-352. https://doi.org/10.1016/S0006-291X(89)80219-0

Parajuli, N., Marine, A., Simmons, S., Saba, H., Mitchell, T., Shimizu, T., Shirasawa, T., & MacMillan-Crow, L. A. (2011). Generation and characterization of a novel kidney-specific manganese superoxide dismutase knockout mouse. *Free Radical Biology and Medicine*, *51*(2), 406-416. https://doi.org/10.1016/j.freeradbiomed.2011.04.024

Pardo, C. A., Xu, Z., Borchelt, D. R., Price, D. L., Sisodia, S. S., & Cleveland, D. W. (1995). Superoxide dismutase is an abundant component in cell bodies, dendrites, and axons of motor neurons and in a subset of other neurons. *Proceedings of the National Academy of Sciences*, *92*(4), 954-958. https://doi.org/doi:10.1073/pnas.92.4.954

Park, J. W., Qi, W.-N., Cai, Y., Zelko, I., Liu, J. Q., Chen, L.-E., Urbaniak, J. R., & Folz, R. J. (2005). Skeletal muscle reperfusion injury is enhanced in extracellular superoxide dismutase knockout mouse. *American Journal of Physiology-Heart and Circulatory Physiology*, *289*(1), H181-H187. https://doi.org/10.1152/ajpheart.00458.2004

Pérez, V. I., Bokov, A., Remmen, H. V., Mele, J., Ran, Q., Ikeno, Y., & Richardson, A. (2009). Is the oxidative stress theory of aging dead? *Biochimica et Biophysica Acta (BBA) - General Subjects*, *1790*(10), 1005-1014. https://doi.org/10.1016/j.bbagen.2009.06.003

Peterkofsky, B. (1991). Ascorbate requirement for hydroxylation and secretion of procollagen: relationship to inhibition of collagen synthesis in scurvy. *The American Journal of Clinical Nutrition*, *54*(6), 1135S-1140S. https://doi.org/10.1093/ajcn/54.6.1135s

Polticelli, F., Battistoni, A., O'Neill, P., Rotilio, G., & Desideri, A. (1998). Role of the electrostatic loop charged residues in Cu,Zn superoxide dismutase. *Protein Science: A*

Publication of the Protein Society, *7*(11), 2354-2358. https://doi.org/10.1002/pro.5560071112

Pope, C. R., De Feo, C. J., & Unger, V. M. (2013). Cellular distribution of copper to superoxide dismutase involves scaffolding by membranes. *Proc Natl Acad Sci U S A*, *110*(51), 20491-20496. https://doi.org/10.1073/pnas.1309820110

Pouyet, L., & Carrier, A. (2010). Mutant mouse models of oxidative stress. *Transgenic Research*, *19*(2), 155-164. https://doi.org/10.1007/s11248-009-9308-6

Quinlan, C. L., Orr, A. L., Perevoshchikova, I. V., Treberg, J. R., Ackrell, B. A., & Brand, M. D. (2012). Mitochondrial complex II can generate reactive oxygen species at high rates in both the forward and reverse reactions. *The Journal of Biological Chemistry*, *287*(32), 27255-27264. https://doi.org/10.1074/jbc.M112.374629

Quinlan, C. L., Perevoshchikova, I. V., Hey-Mogensen, M., Orr, A. L., & Brand, M. D. (2013). Sites of reactive oxygen species generation by mitochondria oxidizing different substrates. *Redox Biology*, *1*(1), 304-312. https://doi.org/10.1016/j.redox.2013.04.005

Reaume, A. G., Elliott, J. L., Hoffman, E. K., Kowall, N. W., Ferrante, R. J., Siwek, D. R., Wilcox, H. M., Flood, D. G., Beal, M. F., Brown, R. H., Scott, R. W., & Snider, W. D. (1996). Motor neurons in Cu/Zn superoxide dismutase-deficient mice develop normally but exhibit enhanced cell death after axonal injury. *Nature Genetics*, *13*(1), 43-47. https://doi.org/10.1038/ng0596-43

Reczek, C. R., & Chandel, N. S. (2015). ROS-dependent signal transduction. *Current opinion in cell biology*, *33*, 8-13. https://doi.org/10.1016/j.ceb.2014.09.010

Rees, D. D., Palmer, R. M., Schulz, R., Hodson, H. F., & Moncada, S. (1990). Characterization of three inhibitors of endothelial nitric oxide synthase in vitro and in vivo. *British Journal of Pharmacology*, *101*(3), 746-752. https://doi.org/10.1111/j.1476-5381.1990.tb14151.x

Reische, D. W., Lillard, D. A., & Eitenmiller, R. R. (2002). Antioxidants. In *Food Lipids* (2 ed.). CRC Press.

Roger, L., Tomas, F., & Gire, V. (2021). Mechanisms and Regulation of Cellular Senescence. *International Journal of Molecular Sciences*, *22*(23), 13173. https://doi.org/10.3390/ijms222313173

Rokhlenko, Y., Geacintov, N. E., & Shafirovich, V. (2012). Lifetimes and Reaction Pathways of Guanine Radical Cations and Neutral Guanine Radicals in an Oligonucleotide in Aqueous Solutions. *Journal of the American Chemical Society*, *134*(10), 4955-4962. https://doi.org/10.1021/ja212186w

Rosen, D. R., Siddique, T., Patterson, D., Figlewicz, D. A., Sapp, P., Hentati, A., Donaldson, D., Goto, J., O'Regan, J. P., Deng, H.-X., Rahmani, Z., Krizus, A., McKenna-Yasek, D., Cayabyab, A., Gaston, S. M., Berger, R., Tanzi, R. E., Halperin, J. J., Herzfeldt, B., . . . Brown, R. H. (1993). Mutations in Cu/Zn superoxide dismutase gene are associated with familial amyotrophic lateral sclerosis. *Nature*, *362*(6415), 59-62. https://doi.org/10.1038/362059a0

Rufini, A., Tucci, P., Celardo, I., & Melino, G. (2013). Senescence and aging: the critical roles of p53. *Oncogene*, *32*(43), 5129-5143. https://doi.org/10.1038/onc.2012.640

Saito, T., & Nishino, T. (1989). Differences in redox and kinetic properties between NAD-dependent and O2-dependent types of rat liver xanthine dehydrogenase. *J Biol Chem*, *264*(17), 10015-10022.

Salmon, A. B., Richardson, A., & Pérez, V. I. (2010). Update on the oxidative stress theory of aging: Does oxidative stress play a role in aging or healthy aging? *Free Radical Biology and Medicine*, *48*(5), 642-655. https://doi.org/10.1016/j.freeradbiomed.2009.12.015

Samper, E., Nicholls, D. G., & Melov, S. (2003). Mitochondrial oxidative stress causes chromosomal instability of mouse embryonic fibroblasts. *Aging Cell*, *2*(5), 277-285. https://doi.org/10.1046/j.1474-9728.2003.00062.x

Sasaki, T., Shimizu, T., Koyama, T., Sakai, M., Uchiyama, S., Kawakami, S., Noda, Y., Shirasawa, T., & Kojima, S. (2011). Superoxide dismutase deficiency enhances superoxide levels in brain tissues during oxygenation and hypoxia-reoxygenation. *J Neurosci Res*, *89*(4), 601-610. https://doi.org/10.1002/jnr.22581

Schwarz, D. S., & Blower, M. D. (2015). The endoplasmic reticulum: structure, function and response to cellular signaling. *Cellular and Molecular Life Sciences: CMLS*, *73*(1), 79-94. https://doi.org/10.1007/s00018-015-2052-6

Sentman, M.-L., Granström, M., Jakobson, H., Reaume, A., Basu, S., & Marklund, S. L. (2006). Phenotypes of Mice Lacking Extracellular Superoxide Dismutase and Copper- and Zinc-containing Superoxide Dismutase*. *Journal of Biological Chemistry*, *281*(11), 6904-6909. https://doi.org/10.1074/jbc.M510764200

Shen, J., Griffiths, P. T., Campbell, S. J., Utinger, B., Kalberer, M., & Paulson, S. E. (2021). Ascorbate oxidation by iron, copper and reactive oxygen species: review, model

development, and derivation of key rate constants. *Scientific Reports*, *11*(1), 7417. https://doi.org/10.1038/s41598-021-86477-8

Shibuya, S., Kinoshita, K., & Shimizu, T. (2012). Protective effects of vitamin C derivatives on skin atrophy caused by Sod1 deficiency. In *Handbook of diet, nutrition and the skin* (pp. 350-364). Wageningen Academic.

Shibuya, S., Ozawa, Y., Toda, T., Watanabe, K., Tometsuka, C., Ogura, T., Koyama, Y.-i., & Shimizu, T. (2014). Collagen peptide and vitamin C additively attenuate age-related skin atrophy in Sod1-deficient mice. *Bioscience, Biotechnology, and Biochemistry*, *78*(7), 1212-1220. https://doi.org/10.1080/09168451.2014.915728

Shibuya, S., Watanabe, K., Ozawa, Y., & Shimizu, T. (2021). Xanthine Oxidoreductase-Mediated Superoxide Production Is Not Involved in the Age-Related Pathologies in Sod1-Deficient Mice. *International Journal of Molecular Sciences*, *22*(7), 3542. https://doi.org/10.3390/ijms22073542

Sies, H., & Jones, D. P. (2020). Reactive oxygen species (ROS) as pleiotropic physiological signalling agents. *Nature Reviews Molecular Cell Biology*, *21*(7), 363-383. https://doi.org/10.1038/s41580-020-0230-3

Singhal, P. K., Sassi, S., Lan, L., Au, P., Halvorsen, S. C., Fukumura, D., Jain, R. K., & Seed, B. (2016). Mouse embryonic fibroblasts exhibit extensive developmental and phenotypic diversity. *Proceedings of the National Academy of Sciences*, *113*(1), 122-127. https://doi.org/10.1073/pnas.1522401112

Skopp, A., Boyd, S. D., Ullrich, M. S., Liu, L., & Winkler, D. D. (2019). Copper–zinc superoxide dismutase (Sod1) activation terminates interaction between its copper chaperone

(Ccs) and the cytosolic metal-binding domain of the copper importer Ctr1. *BioMetals*, *32*(4), 695-705. https://doi.org/10.1007/s10534-019-00206-3

Slot, J. W., Geuze, H. J., Freeman, B. A., & Crapo, J. D. (1986). Intracellular localization of the copper-zinc and manganese superoxide dismutases in rat liver parenchymal cells. *Laboratory Investigation; a Journal of Technical Methods and Pathology*, *55*(3), 363-371.

Snezhkina, A. V., Kudryavtseva, A. V., Kardymon, O. L., Savvateeva, M. V., Melnikova, N. V., Krasnov, G. S., & Dmitriev, A. A. (2019). ROS Generation and Antioxidant Defense Systems in Normal and Malignant Cells. *Oxidative Medicine and Cellular Longevity*, *2019*, 6175804. https://doi.org/10.1155/2019/6175804

Sturtz, L. A., Diekert, K., Jensen, L. T., Lill, R., & Culotta, V. C. (2001). A Fraction of Yeast Cu,Zn-Superoxide Dismutase and Its Metallochaperone, CCS, Localize to the Intermembrane Space of Mitochondria: A PHYSIOLOGICAL ROLE FOR SOD1 IN GUARDING AGAINST MITOCHONDRIAL OXIDATIVE DAMAGE *. *Journal of Biological Chemistry*, *276*(41), 38084-38089. https://doi.org/10.1074/jbc.M105296200

Sun, Y., & Oberley, L. W. (1996). Redox regulation of transcriptional activators. *Free Radical Biology and Medicine*, *21*(3), 335-348. https://doi.org/10.1016/0891-5849(96)00109-8

Sundaresan, M., Yu, Z. X., Ferrans, V. J., Irani, K., & Finkel, T. (1995). Requirement for generation of H2O2 for platelet-derived growth factor signal transduction. *Science (New York, N.Y.)*, *270*(5234), 296-299. https://doi.org/10.1126/science.270.5234.296

Szabó, C., Ischiropoulos, H., & Radi, R. (2007). Peroxynitrite: biochemistry, pathophysiology and development of therapeutics. *Nature Reviews Drug Discovery*, *6*(8), 662-680. https://doi.org/10.1038/nrd2222

Tan, Y. S., & Lei, Y. L. (2019). Generation and Culture of Mouse Embryonic Fibroblasts. *Methods in Molecular Biology (Clifton, N.J.)*, *1960*, 85-91. https://doi.org/10.1007/978-1-4939-9167-9_7

Treiber, N., Maity, P., Singh, K., Kohn, M., Keist, A. F., Ferchiu, F., Sante, L., Frese, S., Bloch, W., Kreppel, F., Kochanek, S., Sindrilaru, A., Iben, S., Högel, J., Ohnmacht, M., Claes, L. E., Ignatius, A., Chung, J. H., Lee, M. J., . . . Scharffetter-Kochanek, K. (2011). Accelerated aging phenotype in mice with conditional deficiency for mitochondrial superoxide dismutase in the connective tissue. *Aging Cell*, *10*(2), 239-254. https://doi.org/10.1111/j.1474-9726.2010.00658.x

Trist, B. G., Hilton, J. B., Hare, D. J., Crouch, P. J., & Double, K. L. (2021). Superoxide Dismutase 1 in Health and Disease: How a Frontline Antioxidant Becomes Neurotoxic. *Angewandte Chemie International Edition*, *60*(17), 9215-9246. https://doi.org/10.1002/anie.202000451

Troy, C. M., Derossi, D., Prochiantz, A., Greene, L. A., & Shelanski, M. L. (1996). Downregulation of Cu/Zn superoxide dismutase leads to cell death via the nitric oxide-peroxynitrite pathway. *Journal of Neuroscience*, *16*(1), 253-261. https://doi.org/10.1523/JNEUROSCI.16-01-00253.1996

Tsan, M. F. (2001). Superoxide dismutase and pulmonary oxygen toxicity: lessons from transgenic and knockout mice (Review). *International Journal of Molecular Medicine*, *7*(1), 13-19. https://doi.org/10.3892/ijmm.7.1.13

Tsang, C. K., Chen, M., Cheng, X., Qi, Y., Chen, Y., Das, I., Li, X., Vallat, B., Fu, L.-W., Qian, C.-N., Wang, H.-Y., White, E., Burley, S. K., & Zheng, X. F. S. (2018). SOD1 Phosphorylation by mTORC1 Couples Nutrient Sensing and Redox Regulation. *Molecular Cell*, *70*(3), 502-515.e508. https://doi.org/10.1016/j.molcel.2018.03.029

Tsang, C. K., Liu, Y., Thomas, J., Zhang, Y., & Zheng, X. F. S. (2014). Superoxide dismutase 1 acts as a nuclear transcription factor to regulate oxidative stress resistance. *Nature Communications*, *5*, 3446. https://doi.org/10.1038/ncomms4446

Tsunoda, S., Kibe, N., Kurahashi, T., & Fujii, J. (2013). Differential responses of SOD1-deficient mouse embryonic fibroblasts to oxygen concentrations. *Archives of Biochemistry and Biophysics*, *537*(1), 5-11. https://doi.org/10.1016/j.abb.2013.06.008

Tu, B. P., & Weissman, J. S. (2004). Oxidative protein folding in eukaryotes. *The Journal of Cell Biology*, *164*(3), 341-346. https://doi.org/10.1083/jcb.200311055

Uchiyama, S., Shimizu, T., & Shirasawa, T. (2006). CuZn-SOD Deficiency Causes ApoB Degradation and Induces Hepatic Lipid Accumulation by Impaired Lipoprotein Secretion in Mice *. *Journal of Biological Chemistry*, *281*(42), 31713-31719. https://doi.org/10.1016/S0021-9258(19)84085-1

Valentine, J. S., Doucette, P. A., & Zittin Potter, S. (2005). Copper-zinc superoxide dismutase and amyotrophic lateral sclerosis. *Annual Review of Biochemistry*, *74*(1), 563-593. https://doi.org/10.1146/annurev.biochem.72.121801.161647

Valko, M., Izakovic, M., Mazur, M., Rhodes, C. J., & Telser, J. (2004). Role of oxygen radicals in DNA damage and cancer incidence. *Molecular and Cellular Biochemistry*, *266*(1-2), 37-56. https://doi.org/10.1023/b:mcbi.0000049134.69131.89

Valko, M., Leibfritz, D., Moncol, J., Cronin, M. T. D., Mazur, M., & Telser, J. (2007). Free radicals and antioxidants in normal physiological functions and human disease. *The International Journal of Biochemistry & Cell Biology*, *39*(1), 44-84. https://doi.org/10.1016/j.biocel.2006.07.001

Valko, M., Morris, H., & Cronin, M. T. D. (2005). Metals, toxicity and oxidative stress. *Current Medicinal Chemistry*, *12*(10), 1161-1208. https://doi.org/10.2174/0929867053764635

Van Remmen, H., Ikeno, Y., Hamilton, M., Pahlavani, M., Wolf, N., Thorpe, S. R., Alderson, N. L., Baynes, J. W., Epstein, C. J., Huang, T.-T., Nelson, J., Strong, R., & Richardson, A. (2003). Life-long reduction in MnSOD activity results in increased DNA damage and higher incidence of cancer but does not accelerate aging. *Physiological Genomics*, *16*(1), 29-37. https://doi.org/10.1152/physiolgenomics.00122.2003

Vurusaner, B., Poli, G., & Basaga, H. (2012). Tumor suppressor genes and ROS: complex networks of interactions. *Free Radical Biology and Medicine*, *52*(1), 7-18. https://doi.org/10.1016/j.freeradbiomed.2011.09.035

Wang, X., Zhang, H., Sapio, R., Yang, J., Wong, J., Zhang, X., Guo, J. Y., Pine, S., Van Remmen, H., Li, H., White, E., Liu, C., Kiledjian, M., Pestov, D. G., & Steven Zheng, X. F. (2021). SOD1 regulates ribosome biogenesis in KRAS mutant non-small cell lung cancer. *Nature Communications*, *12*, 2259. https://doi.org/10.1038/s41467-021-22480-x

Wang, Y., Branicky, R., Noë, A., & Hekimi, S. (2018). Superoxide dismutases: Dual roles in controlling ROS damage and regulating ROS signaling. *Journal of Cell Biology*, *217*(6), 1915-1928. https://doi.org/10.1083/jcb.201708007

Wang, Y., & Hekimi, S. (2013). Mitochondrial respiration without ubiquinone biosynthesis. *Human Molecular Genetics*, *22*(23), 4768-4783. https://doi.org/10.1093/hmg/ddt330

Watanabe, K., Shibuya, S., Koyama, H., Ozawa, Y., Toda, T., Yokote, K., & Shimizu, T. (2013). Sod1 Loss Induces Intrinsic Superoxide Accumulation Leading to p53-Mediated Growth Arrest and Apoptosis. *International Journal of Molecular Sciences*, *14*(6), 10998-11010. https://doi.org/10.3390/ijms140610998

Watanabe, K., Shibuya, S., Ozawa, Y., Nojiri, H., Izuo, N., Yokote, K., & Shimizu, T. (2014). Superoxide Dismutase 1 Loss Disturbs Intracellular Redox Signaling, Resulting in Global Age-Related Pathological Changes. *BioMed Research International*, *2014*, 140165. https://doi.org/10.1155/2014/140165

Watanabe, K., Shibuya, S., Ozawa, Y., Toda, T., & Shimizu, T. (2021). Pathological Relationship between Intracellular Superoxide Metabolism and p53 Signaling in Mice. *International Journal of Molecular Sciences*, *22*(7), 3548. https://doi.org/10.3390/ijms22073548

Weisiger, R. A., & Fridovich, I. (1973). Mitochondrial Superoxide Dismutase: SITE OF SYNTHESIS AND INTRAMITOCHONDRIAL LOCALIZATION. *Journal of Biological Chemistry*, *248*(13), 4793-4796. https://doi.org/10.1016/S0021-9258(19)43735-6

Williams, M. D., Van Remmen, H., Conrad, C. C., Huang, T. T., Epstein, C. J., & Richardson, A. (1998). Increased Oxidative Damage Is Correlated to Altered Mitochondrial Function in Heterozygous Manganese Superoxide Dismutase Knockout Mice*. *Journal of Biological Chemistry*, *273*(43), 28510-28515. https://doi.org/10.1074/jbc.273.43.28510

Wong, P. C., Waggoner, D., Subramaniam, J. R., Tessarollo, L., Bartnikas, T. B., Culotta, V. C., Price, D. L., Rothstein, J., & Gitlin, J. D. (2000). Copper chaperone for superoxide dismutase is essential to activate mammalian Cu/Zn superoxide dismutase. *Proceedings of the National Academy of Sciences of the United States of America*, *97*(6), 2886-2891.

Xu, J., Su, X., Burley, S. K., & Zheng, X. F. S. (2022). Nuclear SOD1 in Growth Control, Oxidative Stress Response, Amyotrophic Lateral Sclerosis, and Cancer. *Antioxidants*, *11*(2), 427. https://doi.org/10.3390/antiox11020427

Yamanobe, T., Okada, F., Iuchi, Y., Onuma, K., Tomita, Y., & Fujii, J. (2007). Deterioration of ischemia/reperfusion-induced acute renal failure in SOD1-deficient mice. *Free Radical Research*, *41*(2), 200–207. https://doi.org/10.1080/10715760601038791

Yehye, W. A., Rahman, N. A., Ariffin, A., Abd Hamid, S. B., Alhadi, A. A., Kadir, F. A., & Yaeghoobi, M. (2015). Understanding the chemistry behind the antioxidant activities of butylated hydroxytoluene (BHT): A review. *European Journal of Medicinal Chemistry*, *101*, 295-312. https://doi.org/10.1016/j.ejmech.2015.06.026

Yin, H., Xu, L., & Porter, N. A. (2011). Free Radical Lipid Peroxidation: Mechanisms and Analysis. *Chemical Reviews*, *111*(10), 5944-5972. https://doi.org/10.1021/cr200084z

Yusuf, B., Gopurappilly, R., Dadheech, N., Gupta, S., Bhonde, R., & Pal, R. (2013). Embryonic fibroblasts represent a connecting link between mesenchymal and embryonic stem cells. *Development, Growth & Differentiation*, *55*(3), 330-340. https://doi.org/10.1111/dgd.12043

Zeeshan, H. M. A., Lee, G. H., Kim, H.-R., & Chae, H.-J. (2016). Endoplasmic Reticulum Stress and Associated ROS. *International Journal of Molecular Sciences*, *17*(3), 327. https://www.mdpi.com/1422-0067/17/3/327

Zelko, I. N., Mariani, T. J., & Folz, R. J. (2002). Superoxide dismutase multigene family: a comparison of the CuZn-SOD (SOD1), Mn-SOD (SOD2), and EC-SOD (SOD3) gene structures, evolution, and expression. *Free Radical Biology and Medicine*, *33*(3), 337-349. https://doi.org/10.1016/S0891-5849(02)00905-X

Zhang, Y., Zhang, H.-M., Shi, Y., Lustgarten, M., Li, Y., Qi, W., Zhang, B.-X., & Van Remmen, H. (2010). Loss of manganese superoxide dismutase leads to abnormal growth and signal transduction in mouse embryonic fibroblasts. *Free Radical Biology and Medicine*, *49*(8), 1255-1262. https://doi.org/10.1016/j.freeradbiomed.2010.07.006

Zito, E., Chin, K. T., Blais, J., Harding, H. P., & Ron, D. (2010). ERO1-beta, a pancreas-specific disulfide oxidase, promotes insulin biogenesis and glucose homeostasis. *J Cell Biol*, *188*(6), 821-832. https://doi.org/10.1083/jcb.200911086